Hydrographic Observations
At the Woods Hole Oceanographic Institution
Hawaii Ocean Time-series Site: 2018 - 2019

Data Report #15

Fernando Carvalho Pacheco, Fernando Santiago-Mandujano, Kellen Rosburg, Andrew King, Ksenia Trifonova, Albert Plueddemann, Robert Weller, James Potemra, Roger Lukas, Jefrey Snyder, Daniel Fitzgerald, and Nan Galbraith

December 2020

SOEST Publication no. 11186

Hydrographic Observations at the Woods Hole Oceanographic Institution Hawaii Ocean Time-series Site: 2018-2019

by

Fernando Carvalho Pacheco[1], Fernando Santiago-Mandujano[1], Kellen Rosburg[1], Andrew King[1], Ksenia Trifonova[1], Albert Plueddemann[2], Robert Weller[2], James Potemra[1], Roger Lukas[1], Jefrey Snyder[1], Daniel Fitzgerald[1], and Nan Galbraith[2]

The University of Hawaii at Manoa
School of Ocean and Earth Science and Technology
1000 Pope Road
Honolulu, Hawaii 96822
U.S.A

December 2020

Data Report #15

Reproduction in whole or in part is permitted for any purpose of the United States Government. This data report should be cited as Pacheco F.C., et al., 2020, Hydrographic observations at the Woods Hole Oceanographic Institution Hawaii Ocean Time-Series Site: 2017-2018, Data Report #15, School of Ocean Science and Technology publication # 11186, University of Hawaii at Manoa, 115 pp. (http://www.soest.hawaii.edu/whots/WHOTS-15_datareport.pdf)

It is approved for public release, distribution unlimited.

1 The University of Hawaii (UH) at Manoa
2 Woods Hole Oceanographic Institution (WHOI)

Acknowledgments

Many people participated in the WHOTS mooring deployment/recovery cruises. They are listed in Table II-1 and Table II-4. We gratefully acknowledge their contributions and support. Thanks are due to all the personnel of the Upper Ocean Processes Group (UOP) at WHOI who prepared the WHOTS buoy's instrumentation and mooring; to Kelsey Maloney, Tully Rohrer, Svetlana Natarov, Noah Howins, Ryan Tabata, and Garret Hebert, for their technical assistance with the moored and shipboard instrumentation; to Kellie Terada for her excellent project support. We gratefully acknowledge the support from the colleagues at Sea-Bird to maintain the quality of the CTD data. We would also like to thank the captains and crew of the Ship *Hi'ialakai,* Ship *Oscar Sette,* and the University of Hawaii (UH) Marine Center staff for their efforts. The WHOTS mooring work is funded in part by the Ocean Observing and Monitoring Division, Climate Program Office (FundRef number 100007298), National Oceanic and Atmospheric Administration, U.S. Department of Commerce, under grant NA14OAR4320158 to the Woods Hole Oceanographic Institution. This work was also supported by the National Science Foundation grant OCE12-60164.

Table of Contents

I. INTRODUCTION 1

II. DESCRIPTION OF THE WHOTS-15 MOORING CRUISES 3

A. WHOTS-15 CRUISE: WHOTS-15 MOORING DEPLOYMENT 3
B. WHOTS-16 CRUISE: WHOTS-15 MOORING RECOVERY 5

III. DESCRIPTION OF WHOTS-15 MOORING 7

IV. WHOTS (15-16) CRUISE SHIPBOARD OBSERVATIONS 12

A. CONDUCTIVITY, TEMPERATURE, AND DEPTH (CTD) PROFILING 12
1. Data acquisition and processing 12
2. CTD sensor calibration and corrections 13
B. WATER SAMPLING AND ANALYSIS 14
C. THERMOSALINOGRAPH DATA ACQUISITION AND PROCESSING 15
1. WHOTS-15 Cruise 15
2. WHOTS-16 Cruise 17
D. SHIPBOARD ADCP 19
1. WHOTS-15 Deployment Cruise 19
2. WHOTS-16 Deployment Cruise 19

V. MOORED INSTRUMENT OBSERVATIONS 20

A. MICROCAT/SEACAT DATA PROCESSING PROCEDURES 20
1. Internal Clock Check and Missing Samples 21
2. Pressure Drift Correction and Pressure Variability 21
3. Temperature Sensor Stability 23
4. Conductivity Calibration 30
B. ACOUSTIC DOPPLER CURRENT PROFILER 41
1. Compass Calibrations 41
2. ADCP Configurations 44
3. ADCP data processing procedures 44
C. VECTOR MEASURING CURRENT METER (VMCM) 51
D. GLOBAL POSITIONING SYSTEM RECEIVER 57

VI. RESULTS 57

A. CTD PROFILING DATA 59
B. THERMOSALINOGRAPH DATA 71
C. MICROCAT DATA 74
D. MOORED ADCP DATA 93
E. MOORED AND SHIPBOARD ADCP COMPARISONS 97
F. NEXT GENERATION VECTOR MEASURING CURRENT METER DATA (VMCM) 104
G. GPS DATA 105
H. MOORING MOTION 106

VII. REFERENCES 108

VIII. APPENDICES 109

A. APPENDIX 1: WHOTS-15 300 KHZ - SERIAL 7637 109
B. APPENDIX 2: WHOTS-15 600 KHZ ADCP CONFIGURATION (SERIAL 13917) 110

List of Figures

Figure I-1.WHOTS-15 mooring design....2
Figure V-1. Linearly corrected pressures from MicroCATs between 7 and 155 m during WHOTS-15 deployment....22
Figure V-2. The temperature difference between MicroCAT SN 5994 at 1.5 m, and near-surface temperature sensors...24
Figure V-3. The temperature difference between the 7-m MicroCAT and the 10-m VMCM....26
Figure V-4. The temperature difference between the 25-m MicroCAT and the 30-m VMCM....27
Figure V-5. The temperature difference between the 45-m MicroCAT and the 47.5-m ADCP....28
Figure V-6. The temperature difference between the 120-m MicroCAT and the 125-m ADCP....29
Figure V-7. Temperature differences and salinity differences between MicroCATs #12246 and #12246....32
Figure V-8. Conductivity sensor corrections for MicroCATs from 2 to 15 meters during WHOTS-15....33
Figure V-9.Conductivity sensor corrections for MicroCATs from 25 to 40 meters during WHOTS-15....34
Figure V-10. Conductivity sensor corrections for MicroCATs from 45 to 55 meters during WHOTS-15....35
Figure V-11.Conductivity sensor corrections for MicroCATs from 65 to 85 meters during WHOTS-15....36
Figure V-12.Conductivity sensor corrections for MicroCATs from 95 to 120 meters during WHOTS-15....37
Figure V-13.Conductivity sensor corrections for MicroCATs from 134 to 136 meters during WHOTS-15....38
Figure V-14.Conductivity sensor corrections for MicroCATs at 154, 155 and 4658 meters during WHOTS-15....39
Figure V-15.Conductivity sensor correction for MicroCAT at 4658 meters during WHOTS-15....40
Figure V-16.Results of the post-cruise compass calibration, conducted October 29th, 2019, on ADCP SN 7637....43
Figure V-17.Results of the post-cruise compass calibration, conducted October 29th, 2019, on ADCP SN 13917....43
Figure V-18. Temperature record from the 300 kHz ADCP during WHOTS-15 mooring....46
Figure V-19. Same as Figure V-18, but for the 600 kHz ADCP....46
Figure V-20. Sound speed profile during the deployment of the WHOTS-15 mooring from 2 dbar CTD....47
Figure V-21. Eastward velocity component for the 300 kHz and the 600 kHz ADCPs....48
Figure V-22. Histogram of the vertical velocity of the 300 kHz ADCP....50
Figure V-23.Same as Figure V-22, but for 600kHz ADCP....50
Figure V-24. A comparison of 30 m VMCM and ADCP U velocity for WHOTS-15....53
Figure V-25. Same as in Figure V-24 but for the meridional (V) velocity component....54
Figure V-26. Same as in Figure V-24 but for the 10 m VMCM....55
Figure V-27. Same as Figure V-26, but for the meridional (V) velocity component....56
Figure VI-1. Profiles of CTD temperature, salinity, and potential density (Σ_{Θ}) as a function of pressure....60
Figure VI-2. Same as in Figure VI-1, but for station 50, cast 2. Same as Figure VI-1, but for station 50, cast 3....61
Figure VI-3. Same as in Figure VI-1, but for station 50, cast 4. Same as in Figure VI-1, but for station 50 cast 5....62
Figure VI-4. Same as in Figure VI-1, but for station 50, cast 6. Same as in Figure VI-1, but for station 52, cast 1....63
Figure VI-5. Same as in Figure VI-1, but for station 52, cast 2. Same as in Figure VI-1, but for station 52, cast 3....64
Figure VI-6. Same as in Figure VI-1, but for station 52, cast 4. Same as in Figure VI-1, but for station 52, cast 5....65
Figure VI-7. Profiles of CTD temperature, salinity, and potential density (ΣΘ) as a function of pressure....66
Figure VI-8. Same as in Figure VI-7 but for station 50, cast 2. Same as Figure VI-7., but for station 50 cast 3....67
Figure VI-9. Same as in Figure VI-7, but for station 50, cast 4. Same as in Figure VI-7, but for station 50 cast 5....68
Figure VI-10. Same as in Figure VI-7, but for station 52, cast 1. Same as in Figure VI-7 but for station 52, cast 2....69
Figure VI-11. Same as Figure VI-7 , but for station 52, cast 3. Same as Figure VI-7 but for station 52 cast 4....70
Figure VI-12. Final processed temperature, salinity, and potential density (ΣΘ) data from the continuous underway system onboard the R/V Hi'ialakai during the WHOTS-15 cruise....71
Figure VI-13. Timeseries of latitude, longitude, and ship's speed during the WHOTS-15 cruise....72
Figure VI-14. Final processed temperature , salinity, and potential density (ΣΘ) data from the continuous underway system onboard the R/V Oscar Sette during the WHOTS-16 cruise....73
Figure VI-15. Timeseries of latitude, longitude, and ship's speed during the WHOTS-16 cruise....74
Figure VI-16. Temperatures from MicroCATs during WHOTS-15 deployment at 1.5, 7, 15, and 25 m....75
Figure VI-17. Same as in Figure VI-16, but at 35, 40, 45, and 50 m....76
Figure VI-18. Same as in Figure VI-16, but at 55, 65, 75, and 85 m....77
Figure VI-19. Same as in Figure VI-16, but at 95, 105, 120, and 135 m....78
Figure VI-20. Same as inFigure VI-16, but at 155 m....79
Figure VI-21. Salinities from MicroCATs during WHOTS-15 deployment at 1.5, 7, 15, and 25 m....80
Figure VI-22. Same as in Figure VI-21, but at 35, 40, 45, and 50 m....81
Figure VI-23. Same as in Figure VI-21, but at 55, 65, 75, and 85 m....82

Figure VI-24. Same as in Figure VI-21, but at 95, 105, 120, and 135 m. 83
Figure VI-25. Same as in Figure VI-21, but at 155 m. 84
Figure VI-26. Potential densities (σθ) from MicroCATs during WHOTS-15 deployment at 1.5, 7, 15, and 25 m. 85
Figure VI-27. Same as in Figure VI-26, but at 35, 40, 45, and 50 m. 86
Figure VI-28. Same as in Figure VI-26, but at 55, 65, 75, and 85 m. 87
Figure VI-29. Same as in Figure VI-26, but at 95, 105, 120, and 135 m. 88
Figure VI-30. Same as in Figure VI-26, but at 155 m. 89
Figure VI-31. Contour plots of temperature and salinity versus depth from SeaCATs/ MicroCATs during WHOTS-1 through WHOTS-15 deployments. 90
Figure VI-32. Contour plots of potential density , versus depth, and of salinity versus from SeaCATs/MicroCATs 91
Figure VI-33. Potential temperature and salinity time-series from the ALOHA Cabled Observatory (ACO) 92
Figure VI-34. Contour plot of east velocity component (m s-1) versus depth and time from the moored ADCPs from the WHOTS-1 through -15 deployments. 93
Figure VI-35. Contour plot of north velocity component (m s-1) versus depth and time from the moored ADCPs from the WHOTS-1 through -15 deployments. 94
Figure VI-36. Contour plot of vertical velocity component (m s-1) versus depth and time from the moored ADCPs from the WHOTS-1 through -15 deployments. 94
Figure VI-37. Staggered time-series of east velocity component (m s-1) for each bin of the 600 kHz and 300 kHz (lower panel) moored ADCPs during WHOTS-15. 95
Figure VI-38. Same as Figure VI 38 but for north velocity component 96
Figure VI-39. Same as Figure VI 38, but for vertical velocity component. 96
Figure VI-40. The contour of zonal currents (m s-1) from the Ship Hi'ialakai's Ocean Surveyor narrowband 75 kHz shipboard ADCP , and the moored 300 kHz ADCP from the WHOTS-15 mooring 97
Figure VI-41. The contour of meridional currents (m s-1) from the Ship Hi'ialakai's Ocean Surveyor narrowband 75 kHz shipboard ADCP , and the moored 300 kHz ADCP from the WHOTS-15 moorin 98
Figure VI-42. The contour of zonal currents (m s-1) from the Ship Oscar Sette Ocean Surveyor narrowband 75 kHz shipboard ADCP , and the moored 300 kHz ADCP from the WHOTS-15 mooring 99
Figure VI-43. Contours of meridional currents (m s-1) from the Ship Oscar Sette Ocean Surveyor narrowband 75 kHz shipboard ADCP , and the moored 300 kHz ADCP from the WHOTS-15 mooring 100
Figure VI-44. Mean current profiles during shipboard ADCP versus moored 300 kHz ADCP intercomparisons from HOT-306 through HOT-315 and from WHOTS-15 and WHOTS-16 cruises. 102
Figure VI-45. Mean current profiles during shipboard ADCP versus moored 600 kHz ADCP intercomparisons from HOT-306. 103
Figure VI-46. Horizontal velocity data (m/s) during WHOTS-15 from the VMCMs at 10 m depth and at 30 m depth ...104
Figure VI-47. GPS Latitude and longitude time series from the WHOTS-15 deployment 105
Figure VI-48. The power spectrum of latitude and longitude for the WHOTS-15. The variables f, K1, and K2 represent the inertial period, solar-diurnal and solar-semidiurnal constituents. 106
Figure VI-49. Scatter plots of ADCP tilt and distance of the buoy to its anchor for the 300 kHz and the 600 kHz ADCP deployments. 107

List of Tables

Table II-1.Scientific personnel on Ship Hi'ialakai during the WHOTS-15 deployment cruise. 3
Table II-2. CTD stations occupied during the WHOTS-15 cruise 4
Table II-3.Configuration of the Ocean Surveyor 75kHz ADCP on board the Ship Hi'ialakai during the WHOTS-15 cruise. 5
Table II-4.Scientific personnel on Ship Oscar Sette during the WHOTS-16 cruise (WHOTS-15 mooring recovery).....5
Table II-5.CTD stations during the WHOTS-16 cruise (WHOTS-15 mooring recovery). 6
Table II-6.Configuration of the Ocean Surveyor 75kHz ADCP on board the Ship Oscar Sette during the WHOTS-16 7
Table III-1.WHOTS-15 mooring subsurface instrument deployment information. All times are in UTC. 9
Table III-2. WHOTS-15 MicroCAT and SBE-56 Temperature Sensor Information. All times stated are in UTC. 9
Table III-3. WHOTS-15 mooring ADCP deployment and configuration information. All times are in UTC. 10
Table III-4. WHOTS-15 MicroCAT recovery Information. All times stated are in UTC. 10
Table III-5.WHOTS-15 mooring ADCP recovery information. All times are in UTC.....11
Table IV-1.The precision of salinity measurements of secondary lab standards. 14
Table IV-2.ADCP record times (UTC) for the Narrow Band 75 kHz ADCP during the WHOTS-15cruise 19
Table IV-3. ADCP record times (UTC) for the 75 kHz ADCP during the WHOTS-16 cruise. 19
Table V-1. WHOTS-15 MicroCAT temperature sensor calibration dates and sensor drift during deployments.....20
Table V-2. Pressure bias of MicroCATs with pressure sensors. 21
Table V-3. Specifications of the ADCP's used for the WHOTS-15 mooring. 41
Table V-4. Results from the WHOTS-15 pre-deployment 300 kHz ADCP compass field calibration procedure. 41
Table V-5. Results from the WHOTS-15 pre-deployment 600 kHz ADCP compass field calibration procedure. 42
Table V-6. Results from the WHOTS-15 post-deployment 300kHz ADCP compass field calibration procedure.....42
Table V-7. Results from the WHOTS-15 post-deployment 600kHz ADCP compass field calibration procedure. 42
Table V-8. ADCP record times (UTC) during WHOTS-15 deployment 44
Table V-9.Record times (UTC) for the VMCMs at 10 m and 30 m during the WHOTS-15 deployment 51
Table V-10. GPS record times (UTC) during WHOTS-15.....57

I. Introduction

In 2003, Robert Weller (Woods Hole Oceanographic Institution [WHOI]), Albert Plueddemann (WHOI), and Roger Lukas (the University of Hawaii [UH]) proposed to establish a long-term surface mooring at the Hawaii Ocean Time-series (HOT) Station ALOHA (22°45'N, 158°W) to provide sustained, high-quality air-sea fluxes and the associated upper ocean response as a coordinated part of the HOT program, and as an element of the global array of ocean reference stations supported by the National Oceanic and Atmospheric Administration's (NOAA) Office of Climate Observation.

With support from NOAA and the National Science Foundation (NSF), the WHOI HOT Site (WHOTS) surface mooring has been maintained at Station ALOHA since August 2004. This project aims to provide long-term, high-quality air-sea fluxes as a coordinated part of the HOT program and contribute to the goals of observing heat, freshwater, and chemical fluxes at a site representative of the oligotrophic North Pacific Ocean. The approach maintains a surface mooring outfitted for meteorological and oceanographic measurements at a site near Station ALOHA by successive mooring turnarounds. These observations are being used to investigate air-sea interaction processes related to climate variability and change.

The original mooring system is described in the mooring deployment/recovery cruise reports (Plueddemann *et al.*, 2006; Whelan *et al.*, 2007). Briefly, a Surlyn foam surface buoy is equipped with meteorological instrumentation including two complete Air-Sea Interaction Meteorological (ASIMET) systems (Hosom *et al.*, 1995; Colbo and Weller, 2009), measuring air and sea surface temperatures, relative humidity, barometric pressure, wind speed and direction, incoming shortwave and longwave radiation, and precipitation. Complete surface meteorological measurements are recorded every minute, as required to compute air-sea fluxes of heat, freshwater, and momentum. Each ASIMET system also transmits hourly averages of the surface meteorological variables via the Argos satellite system and iridium. The mooring line is instrumented to collect time series of upper ocean temperatures, salinities, and velocities with the surface forcing record. This mooring includes conductivity, salinity and temperature recorders, two Vector Measuring Current Meters (VMCMs), and two Acoustic Doppler current profilers (ADCPs). See the WHOTS-15 mooring diagram in Figure I-1.

The subsurface instrumentation is located vertically to resolve the temporal variations of shear and stratification in the upper pycnocline to support the study of mixed layer entrainment. Experience with moored profiler measurements near Hawaii suggests that Richardson's number estimates over 10 m scales are adequate. Salinity is crucial to water mass stratification, as salt-stratified barrier layers are observed at HOT and in the region (Kara *et al.*, 2000). Thus Sea-Bird MicroCATs with vertical separation ranging from 5-20 m were used to measure temperature and salinity. A Teledyne RD Instruments (TRDI) ADCP obtains current profiles across the entrainment zone and another in the mixed layer. Both ADCPs are in an upward-looking configuration, one is at 125 m, using 4 m bins, and the other is at 47.5 m using 2 m bins. To provide near-surface velocity (where the ADCP estimates are less reliable), we deploy two VMCMs. The simple mooring design is a balance between resolving extremes versus the typical annual cycling of the mixed layer (see Plueddemann *et al.*, 2006; Santiago-Mandujano *et al.*, 2007).

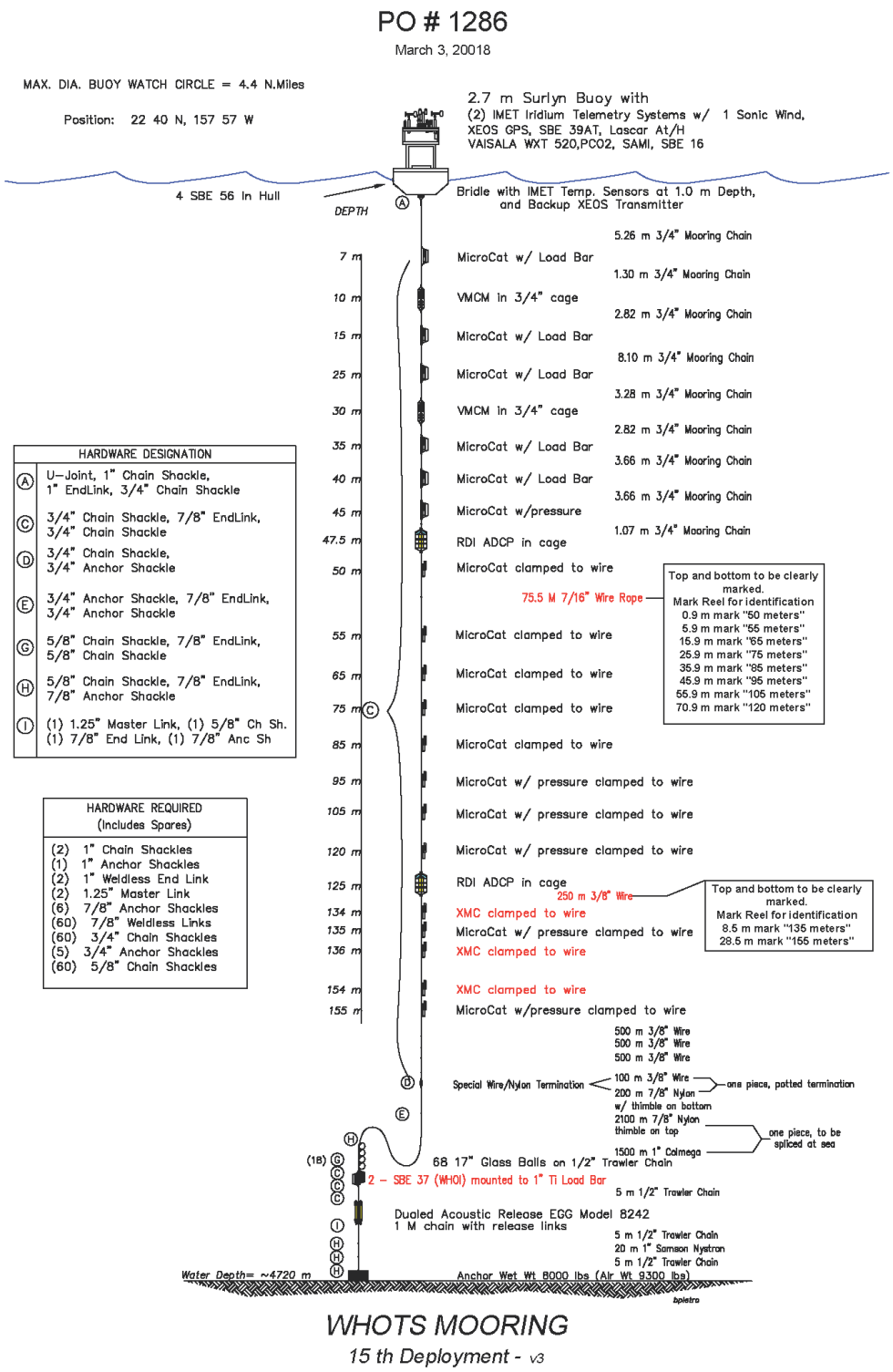

Figure I-1.WHOTS-15 mooring design

The fifteenth WHOTS mooring was deployed on September 23rd, 2018, during an eight-day cruise (WHOTS-15 cruise) and was recovered on October 8th, 2019, during a nine-day cruise (WHOTS-16 cruise). The cruises were aboard the NOAA Ship *Hi'ialakai* and *Oscar Sette*, respectively. A sixteenth mooring was deployed during the WHOTS-16 cruise; to be recovered in 2021.

This report documents and describes the oceanographic observations made on the 15th WHOTS mooring for nearly one year and from shipboard measurements during the two cruises when the mooring was deployed and recovered. Sections II and III include a detailed description of the cruises and the mooring, respectively. Sampling and processing procedures of the hydrographic casts, thermosalinograph, and shipboard ADCP data collected during these cruises are described in Section IV. Section V includes the processing procedures for the data collected by the moored instruments: SeaCATs, MicroCATs, VMCMs, and moored ADCPs. Plots of the resulting data and preliminary analysis are presented in Section VI.

II. Description of the WHOTS-15 Mooring Cruises

A. WHOTS-15 Cruise: WHOTS-15 Mooring Deployment

The Woods Hole Oceanographic Institution Upper Ocean Processes Group (WHOI/UOP), with the UH group's assistance, conducted the fifteenth deployment of the WHOTS mooring onboard the NOAA Ship *Hi'ialakai* during the WHOTS-15 cruise between September 21st and September 29th, 2018. The WHOTS-15 mooring was deployed at Station 50 on September 23rd, 2018, 01:17 UTC at 22° 45.94 'N, 157° 53.70 'W, and the WHOTS-14 mooring were recovered on September 27th. The scientific personnel that participated during the cruise are listed in Table II-1.

Table II-1.Scientific personnel on Ship Hi'ialakai during the WHOTS-15 deployment cruise.

Name	Title or function	Affiliation
Plueddeman, Albert	Chief Scientist	WHOI
Pietro, Ben	Senior Engineering Assistant	WHOI
Hasbrouck, Emerson	Engineering Assistant	WHOI
Greenwood, Ben	Research Associate	WHOI
Snyder, Jefrey	Marine Electronics Technician	UH
Santiago-Mandujano, Fernando	Research Associate	UH
Natarov, Svetlana	Research Associate	UH
Hebert, Garret	Undergraduate Volunteer	UH
Howins, Noah	Undergraduate Volunteer	UH
Maloney, Kelsey	Student Assistant	UH
Todd, James	Program Manager	CPO

The UH group conducted the shipboard oceanographic observations during the cruise.

A Sea-Bird CTD (conductivity, temperature, and depth) system was used to measure T, S, and O_2 profiles during CTD casts. The time, location, and maximum CTD pressure for each

profile are listed in Table II-2. Twelve CTD casts were conducted during the WHOTS-15 cruise. CTD profile data were collected at Station 52 (near the WHOTS-14 buoy) and Station 50 (near the WHOTS-15 buoy). A test cast was conducted at Station 20 (21°29.06'N 158°22.04'W) offshore of Makaha, HI, to an approximate depth of 1500 m to test three acoustic releases. Six CTD yo-yo casts were conducted to obtain profiles for comparison with subsurface instruments on the WHOTS-15 mooring after deployment, and five yo-yo casts were performed for comparison with the WHOTS-14 mooring before recovery. These casts were started less than 0.5 nm from the buoys with varying drift during each cast and consisted of 5 up-down cycles between near the surface and 200 m.

Table II-2. CTD stations occupied during the WHOTS-15 cruise

Station/cast	**Date**	**Time (UTC)**	**Location** ***(using NMEA data)***	**Maximum pressure (dbar)**
20 / 1	09/22/2018	03:19	21° 29.06´ N, 158° 22.04´ W	1518
52 / 1	09/23/2018	15:52	22° 41.69´ N, 157° 56.44´ W	202
52 / 2	09/23/2018	19:52	22° 41.62´ N, 157° 56.63´ W	204
52 / 3	09/23/2018	23:57	22° 41.73´ N, 157° 56.91´ W	204
52 / 4	09/24/2018	03:53	22° 41.87´ N, 157° 56.45´ W	204
52 / 5	09/24/2018	07:46	22° 41.65´ N, 157° 56.58´ W	204
50 / 1	09/25/2018	15:52	22° 47.28´ N, 157° 52.64´ W	202
50 / 2	09/25/2018	19:54	22° 47.59´ N, 157° 52.43´ W	204
50 / 3	09/25/2018	23:57	22° 47.28´ N, 157° 52.78´ W	204
50 / 4	09/26/2018	03:55	22° 47.37´ N, 157° 52.25´ W	204
50 / 5	09/26/2018	07:50	22° 47.25´ N, 157° 52.45´ W	204
50 / 6	09/28/2018	15:51	22° 44.21´ N, 157° 53.37´ W	214

Also, continuous ADCP and near-surface thermosalinograph data were obtained while underway.

The NOAA Ship *Hi'ialakai* was equipped with an RD Instruments Ocean Surveyor 75 kHz ADCP, set to function in broadband and narrowband configurations. The configuration information is shown in Table II-3. The ADCP used input from an S.G. Brown gyrometer and a Furuno GP 90 GPS receiver to establish the ship's heading and attitude. At the same time, an Applanix POSMV4 system archived attitude data for use in post-processing.

A complete description of these operations is available in the WHOTS-15 cruise report (Santiago-Mandujano *et al.*, 2019).

Table II-3.Configuration of the Ocean Surveyor 75kHz ADCP on board the Ship Hi'ialakai during the WHOTS-15 cruise.

	OS75BB	**OS75NB**
Sample interval (s)	300	300
Number of bins	80	60
Bin Length (m)	8	16
Pulse Length (m)	8	16
Transducer depth (m)	5	5
Blanking length (m)	8	8

Near-surface temperature and salinity data during the WHOTS-15 cruise were acquired from the thermosalinograph (TSG) system installed on the NOAA Ship Hi'ialakai. The sensors were sampling water from the continuous seawater system running through the ship. They were comprised of one thermosalinograph model SBE-21 (SN 3155) and a micro-thermosalinograph model SBE-45 (SN 4540403-0150), both with (internal) temperature and conductivity sensors located in the ship's wet lab, about 67 m from separate hull intakes; and an SBE-38 (SN 215) external temperature sensor located at the entrance to one of the water intakes. The SBE-21 recorded data every 6 seconds, and the other two instruments recorded data every second. The water intake for the SBE-21 and SBE-38 is located at the ship's bow, next to the starboard side bow thruster at a depth of 2 m. The intake for the SBE-45 is situated near the middle of the ship, also 2 m deep. The system has a pressure gauge showing a flow pressure of about ten psi during the cruise. Each thermosalinograph system had a debubbler.

Both thermosalinographs exhibited several conductivity and temperature glitches, especially the SBE-21. The temperature differences between the internal SBE-45 and SBE-21 were between 0.4 and 0.8 °C. However, the computed salinity differences between these two instruments were between -0.03 and 0.03 g/kg. A diurnal cycle is apparent in the temperature and conductivity.

B. WHOTS-16 Cruise: WHOTS-15 Mooring Recovery

The WHOI/UOP Group conducted the mooring turnaround operations during the WHOTS-16 cruise between October 4th and 12th, 2019. The WHOTS-16 mooring was deployed at Station 52 on October 6th, 2019, 02:12 UTC at 22° 40.096 'N, 157° 56.788 'W, and the WHOTS-15 mooring was recovered on October 8th, 2019. The scientific personnel that participated during the cruise are listed in Table II-4.

Table II-4.Scientific personnel on Ship Oscar Sette during the WHOTS-16 cruise (WHOTS-15 mooring recovery)

Name	**Title or function**	**Affiliation**
Plueddeman, Albert	Chief Scientist	WHOI
Pietro, Ben	Senior Engineering Assistant	WHOI
Graham, Raymond	Research Assistant	WHOI
Santiago-Mandujano, Fernando	Research Associate	UH
Maloney, Kelsey	Student Assistant	UH
Fitzgerald, Dan	Marine Technician	UH

Name	Title or function	Affiliation
Rohrer, Tully	Research Associate	UH
Tabata, Ryan	Research Oceanography Specialist	UH
Howins, Noah	Student	UH
Pezoa, Sergio	Scientist	ESRL
Gonzales, Sean	Student	HPU

The UH group conducted the shipboard oceanographic observations during the cruise. A complete description of these operations is available in the WHOTS-16 cruise report (see http://www.soest.hawaii.edu/whots/proc_reports/WHOTS-16_CruiseRpt.pdf) .

A Sea-Bird CTD system was used to measure T, S, and O_2 profiles during CTD casts. The time, location, and maximum CTD pressure for each profile are listed in Table II-5. Eleven CTD casts were conducted during the WHOTS-16 cruise, from September 21st through 28th, 2019. CTD profile data were collected at Station 20 (in transit to the WHOTS mooring), Station 50 (near the WHOTS-15 buoy), and Station 52 (near the WHOTS-16 buoy). The cast at Station 20 was 1500 m deep, and three acoustic releases (two to be used in the WHOTS-16 mooring and one backup) were attached to the rosette frame for function testing. Five CTD yoyo casts were conducted to obtain profiles for comparison with subsurface instruments on the WHOTS-16 mooring after deployment. Five yo-yo casts were performed for comparison with the WHOTS-15 mooring before recovery. These casts were started about 0.25 nm from the buoys with varying drift during each cast and consisted of 5 up-down cycles between near the surface and 204 to 218 m.

Water samples were taken from all casts; 3 to 4 samples for each of them. These samples were to be analyzed for salinity at UH and used to calibrate the CTD conductivity sensors.

Table II-5.CTD stations during the WHOTS-16 cruise (WHOTS-15 mooring recovery).

Station/cast	Date	Time (UTC)	Location *(using NMEA data)*	Maximum pressure (dbar)
20 / 1	10/5/2019	01:51	21° 28.164´ N, 158° 21.552´ W	1502
52 / 1	10/10/2019	16:38	22° 40.391´ N, 157° 58.744´ W	215
52 / 2	10/10/2019	19:55	22° 40.551´ N, 157° 58.679´ W	211
52 / 3	10/10/2019	23:58	22° 40.790´ N, 157° 58.635´ W	211
52 / 4	10/11/2019	04:05	22° 41.023´ N, 157° 58.256´ W	211
52 / 5	10/11/2019	07:55	22° 40.551´ N, 157° 58.323´ W	209
50 / 1	10/06/2019	16:10	22° 45.101´ N, 157° 55.049´ W	213
50 / 2	10/06/2019	20:03	22° 44.962´ N, 157° 54.839´ W	211
50 / 3	10/07/2019	00:04	22° 45.136´ N, 157° 55.144´ W	218
50 / 4	10/07/2019	04:08	22° 45.209´ N, 157° 55.006´ W	211
50 / 5	10/07/2019	07:56	22° 44.787´ N, 157° 55.066´ W	210

Also, continuous ADCP and near-surface thermosalinograph data were obtained while underway.

The NOAA Ship *Oscar Sette* was equipped with a TRDI Ocean Surveyor 75 kHz ADCP, set to function in broadband and narrowband configurations. The configuration information is shown in Table II-6. The ADCP used input from a SAMOS gyrometer and Furuno GP 150, a GPS receiver, to establish the ship's heading and attitude.

.

Table II-6.Configuration of the Ocean Surveyor 75kHz ADCP on board the Ship Oscar Sette during the WHOTS-16 cruise

	OS75BB	**OS75NB**
Sample interval (s)	300	300
Number of bins	80	55
Bin Length (m)	8	16
Pulse Length (m)	8	16
Transducer depth (m)	5	5
Blanking length (m)	8	8

Near-surface temperature and salinity data during the WHOTS-16 cruise were acquired from the thermosalinograph (TSG) system installed on the NOAA Ship *Oscar Sette.* The sensors were sampling water from the continuous seawater system running through the ship. They were comprised of one thermosalinograph model SBE-21 (SN 3168) and a micro-thermosalinograph model SBE-45 (SN 0290), both with (internal) temperature and conductivity sensors located in the ship's chemistry lab, about 70 m from the hull intake; and an SBE-38 (SN 266) external temperature sensor located at the entrance of the water intake. All instruments recorded data every second. The water intake is located at the ship's bow, forward from the starboard side bow thruster at a depth of 3 m. The system has a flow meter in the chemistry lab, showing a flow rate of about 1.1 liters/minute during the cruise. Only the SBE-45 has a debubbler. Salinity water samples were taken every 8 hours from the exhaust in the Chemistry lab using 0.25-liter glass bottles, to be measured in the UH lab to correct any drift in the thermosalinograph conductivities.

III. Description of WHOTS-15 Mooring

The WHOTS-15 mooring, deployed on September 23rd, 2018, from NOAA's Ship *Hi'ialakai*, was outfitted with two complete sets of ASIMET sensors on the buoy and underneath subsurface instruments from 7 to 155 m depth and near the bottom. See (Santiago-Mandujano *et al.*, 2019)for a complete description of the buoy. The WHOTS-15 recovery on October 8th, 2019, resulted in about 380 days on station.

The buoy tower also contains a radar reflector, two marine lanterns, and Iridium satellite transmission systems that provide continuous buoy position monitoring. A Xeos Melo Global Positioning System (GPS) receiver, an SBE-39 temperature sensor adapted to measure air temperature, and a Vaisala WXT-520 multi-variable (temperature, humidity, pressure, wind, and precipitation) were also mounted on the tower. A fourth positioning system (Xeos Sable transmitter) was mounted beneath the hull. Several other instruments were mounted on the buoy. A Battelle pCO_2 system, a pumped SBE-16 CTD, and a SAMI-2 pH sensor were mounted to the

buoy's underside. A Sea-Bird SBE-63 hosted a dissolved oxygen sensor. Three down-looking radiometers were mounted on the buoy. One hyperspectral sensor is mounted facing upward near the radiometers as a reference for the incoming spectral irradiance. A Wetlabs ECOFLNTUS chlorophyll fluorometer was also mounted on the buoy hull.

Five internally-logging Sea-Bird SBE-56 temperature sensors were bolted to the buoy hull's underside, measuring sea surface temperature (SST) and salinity. The SBE-56s measured SST once every 60 sec between 80-110 cm below the surface, and two SBE-37 MicroCATs were at 1.52 m (see Table III-2).

Instrumentation provided by UH for the WHOTS-15 mooring included 17 SBE-37 Microcats, and two TRDI Workhorse ADCPs, transmitting in 300 kHz and 600 kHz, respectively. The Microcats all measured temperature and conductivity, with eleven of them measuring pressure. All MicroCATs were deployed with antifoulant capsules. In addition to the buoy instrumentation, WHOI provided two Vector Measuring Current Meters (VMCMs), two deep Microcats (SBE-37) installed near the bottom of the mooring, and all required subsurface mooring hardware.

Table III-1 provides a listing of the WHOTS-15 subsurface instrumentation at their nominal depths on the mooring, along with serial numbers, sampling rates, and other pertinent information. A cold water spike was induced to the UH MicroCATs before deployment (Table III-1) and after recovery Table III-4 by placing an ice pack in contact with their temperature sensor to check for any drift in their internal clock. To produce a spike in the ADCP data, each instrument’s transducer was rubbed gently by hand for 20 seconds (Table III-3 Table III-5).

The RDI 300 kHz Workhorse Sentinel ADCP, SN 7637, was deployed at 125 m with transducers facing upwards with an additional external battery pack. This instrument was set to ping at 4-second intervals for 160 seconds every 10 minutes, and the burst sampling was designed to minimize aliasing by occasional large ocean swell orbital motions. The bin size was set for 4 m. The total number of ensemble records was 55,176. The first ensemble was on 09/22/2018 at 00:00:00Z, and the last was on 10/10/2019 at 03:49.59Z (see Table III-3, Table III-5, and Section VIII.A for more configuration). This instrument also measured temperature.

The RDI 600 kHz Workhorse Sentinel ADCP, SN 13917, was deployed at 47.5 m with transducers facing upwards with an additional external battery pack. The instrument was set to ping at 2-second intervals for 160 seconds every 10 minutes, and the burst sampling was designed to minimize aliasing by occasional large ocean swell orbital motions. The bin size was set for 2 m. The total number of ensemble records was 5,987. The first ensemble was on 09/22/2018 at 00:00:00Z, and the last was on 11/02/2018 at 13:39:59Z (see Table III-3, Table III-5, and Section 0 for more configuration). This instrument also measured temperature.

The two VMCMs, SN 009 and 010, were deployed at 10 m and 30 m depth. The instruments were prepared for deployment by the WHOI/UOP group and set to sample at 2-minutes and 1-minute intervals, respectively. These instruments also measured temperature.

Table III-1.WHOTS-15 mooring subsurface instrument deployment information. All times are in UTC.

SN:	Instrument	Depth (m)	Pressure SN	Sample Interval (sec)	Start Logging Data		Cold Spike begin		Cold Spike end		Time in Water	
6892	MicroCAT	7	2651324	75	9/18/18	00:00:00	9/21/18	22:15:00	9/21/18	22:45:00	9/22/18	19:28:00
009	VMCM	10	N/A	180	9/17/18	03:20:00	9/22/18	18:57:00 *	60	N/A	9/22/18	19:10:00
3382	MicroCAT	15	N/A	180	9/18/18	0:00:00	9/21/18	22:15:00	9/21/18	22:45:00	9/22/18	19:02:00
129877	Vemco 69khz Receiver	25	N/A	N/A	9/19/18	0:00:00	N/A	N/A	N/A	N/A	9/22/18	18:53:00
4663	MicroCAT	25	N/A	180	9/18/18	0:00:00	9/21/18	22:15:00	9/21/18	22:45:00	9/22/18	18:53:00
010	VMCM	30	N/A	60	9/22/18	02:00:00	9/22/18	18:43:00	N/A	N/A	9/22/18	18:52:00
3633	MicroCAT	35	N/A	180	9/18/18	0:00:00	9/21/18	22:15:00	9/21/18	22:45:00	9/22/18	18:48:00
3381	MicroCAT	40	N/A	180	9/18/18	0:00:00	9/21/18	22:15:00	9/21/18	22:45:00	9/22/18	18:42:00
3668	MicroCAT	45	5579	240	9/18/18	00:00:00	9/21/18	22:15:00	9/21/18	22:45:00	9/22/18	18:37:00
13917	600 kHz ADCP	47.5	N/A	600	9/22/18	0:00:00	N/A	Table III-3	N/A	Table III-3	9/22/18	19:45:00
3619	MicroCAT	50	N/A	180	9/18/18	0:00:00	9/21/18	22:15:00	9/21/18	22:45:00	9/22/18	19:47:00
3620	MicroCAT	55	N/A	180	9/18/18	0:00:00	9/21/18	22:15:00	9/21/18	22:45:00	9/22/18	19:47:00
3621	MicroCAT	65	N/A	180	9/18/18	0:00:00	9/21/18	22:15:00	9/21/18	22:45:00	9/22/18	19:48:00
3622	MicroCAT	75	N/A	180	9/18/18	0:00:00	9/21/18	22:15:00	9/21/18	22:45:00	9/22/18	19:49:00
4699	MicroCAT	85	10209	240	9/18/18	0:00:00	9/21/18	22:15:00	9/21/18	22:45:00	9/22/18	19:50:00
3791	MicroCAT	95	N/A	180	9/18/18	0:00:00	9/21/18	22:15:00	9/21/18	22:45:00	9/22/18	19:51:00
2769	MicroCAT	105	2949	240	9/18/18	0:00:00	9/21/18	22:15:00	9/21/18	22:45:00	9/22/18	19:52:00
4700	MicroCAT	120	2479944	240	9/18/18	0:00:00	9/21/18	22:15:00	9/21/18	22:45:00	9/22/18	19:54:00
7637	300 kHz ADCP	125	N/A	600	9/22/18	0:00:00	N/A	Table III-3	N/A	Table III-3	9/22/18	19:57:00
15729	XMC	134	N/A	3600	9/21/18	21:00:00	9/21/18	22:15:00	9/21/18	22:45:00	9/22/18	20:01:00
2965	MicroCAT	135	3021	240	9/18/18	0:00:00	9/21/18	22:15:00	9/21/18	22:45:00	9/22/18	20:01:00
15817	XMC	136	13427	3600	9/21/18	21:00:00	9/21/18	22:15:00	9/21/18	22:45:00	9/22/18	20:01:00
15818	XMC	154	13438	3600	9/21/18	21:00:00	9/21/18	22:15:00	9/21/18	22:45:00	9/22/18	20:03:00
4701	MicroCAT	155	10211	240	9/18/18	00:00:00	9/21/18	22:15:00	9/21/18	22:45:00	9/22/18	20:03:00
12247	MicroCAT	38m off bottom	2153129	300	9/18/18	01:00:00	9/22/18	05:01:00	9/22/18	05:42:00	9/23/18	01:07:00
12246	MicroCAT	38m off bottom	2153128	300	9/18/18	01:00:00	9/22/18	05:01:00	9/22/18	05:42:00	9/23/18	01:07:00

** VMCM Spin start times*

Table III-2. WHOTS-15 MicroCAT and SBE-56 Temperature Sensor Information. All times stated are in UTC.

Instrument	SN	Depth (m)	Sample Interval (sec)
SBE-56	6150	0.80	60
SBE-56	6239	0.90	60
SBE-56	6410	0.95	60
SBE-56	6412	1.10	60
SBE-56	7212	0.8	60
MicroCAT	5994	1.52	300
MicroCAT	5996	1.52	300

Table III-3. WHOTS-15 mooring ADCP deployment and configuration information. All times are in UTC.

	ADCP S/N 7637	ADCP S/N 13917
Frequency (kHz)	300	600
Number of Depth Cells	30	25
Depth Cell Size (m)	4 m	2 m
Pings per Ensemble	40	80
Time between Ensembles	10 min	10 min
Ping interval	4 sec	2 sec
Time of First Ping	09/22/18, 00:00:00	09/22/18, 00:00:00
Transducer 1 Spike Time	09/22/18, 01:15:00	09/22/18, 01:15:00
Transducer 2 Spike Time	09/22/18, 01:25:00	09/22/18, 01:25:00
Transducer 3 Spike Time	09/22/18, 01:35:00	09/22/18, 01:35:00
Transducer 4 Spike Time	09/22/18. 01:45:00	09/22/18. 01:45:00
Time in Water	09/22/18, 19:57:00	09/22/18, 19:57:00
Depth (m)	125 m	47.5 m

All WHOTS-15 instruments were successfully recovered; recovery information for the C-T instruments is shown in Table III-4. Most of the instruments had some degree of biofouling, with the most substantial fouling near the surface. The fouling extended down to the ADCP at 125 m, although it was minor at that level.

All MicroCATs were in good condition after recovery. MicroCAT 3382 (15 m) had a bent in its sensor guard. Instrument SN 4663 (25m) had barnacles blocking the top of its conductivity cell, and instruments SN 3668 (45m) and 3620 (55m) had barnacles attached at the bottom and top end of their conductivity cells, respectively, partially blocking the flow. The data from all instruments were downloaded onboard the ship, and all instruments returned full data records. A post-cruise evaluation showed no missing samples in all the MicroCATs and the 300 kHz ADCP, except for the 600 kHz ADCP that failed before the recovery. Table III-4 has an initial evaluation of the data quality; more details are in Section V.A, and Section VI.C.

Table III-4. WHOTS-15 MicroCAT recovery Information. All times stated are in UTC.

Depth (m)	Sea-Bird Serial #	Time out of water	Time of Spike	Time Logging Stopped	Samples Logged	Data Quality
7	SBE 37-6892	10/9/19 19:01:00	10/10/19 01:20:00	10/10/19 16:03:00	446595	Good
15	SBE 37-3382	10/9/19 19:12:00	10/10/19 01:20:00	10/10/19 03:46:03	186315	C-offset
25	SBE 37-4663	10/9/19 19:19:00	10/10/19 01:20:00	10/10/19 00:55:45	186258	Good
35	SBE 37-3663	10/9/19 19:28:00	10/10/19 01:20:00	10/10/19 18:51:00	186137	Good
40	SBE 37-3381	10/9/19 19:31:00	10/10/19 01:20:00	10/10/19 21:57:15	186199	Good
45	SBE 37-3668	10/9/19 17:35:00	10/10/19 01:20:00	10/11/19 02:00:10	139349	Good
47.5	ADCP-13917	10/9/19 17:30:00	N/A	10/11/19 04:14:00	5987	Failed 11/2/2018
50	SBE 37-3619	10/9/19 17:28:00	10/10/19 01:20:00	10/10/19 04:14:00	185805	Good
55	SBE 37-3620	10/9/19 17:27:00	10/10/19 01:20:00	10/10/19 02:17:55	185806	Good
65	SBE 37-3621	10/9/19 17:26:00	10/10/19 01:20:00	10/10/19 02:29:55	185810	Good

75	SBE 37-3632	10/9/19 17:25:00	10/10/19 01:20:00	10/11/19 02:37:30	186293	Good
85	SBE 37-4699	10/9/19 17:24:00	10/10/19 01:20:00	10/11/19 00:10:20	139682	Good
95	SBE 37-3791	10/9/19 17:23:00	10/10/19 01:20:00	10/10/19 21:19:00	186186	Good
105	SBE 37-2769	10/9/19 17:22:00	10/10/19 01:20:00	10/10/19 18:11:50	139593	C-offset
120	SBE 37-4700	10/9/19 17:20:00	10/10/19 01:20:00	10/10/19 15:30:45	139552	Good
125	ADCP-7637	10/9/19 17:15:00	N/A	10/11/19 04:12:24	55177	Good
134	SBE XMC-15729	10/9/19 17:14:00	10/10/19 01:20:00	10/10/19 08:17:30	9204	Good
135	SBE 37-2965	10/9/19 17:14:00	10/10/19 01:20:00	10/10/19 15:38:30	131174	Good
136	SBE XMC-15817	10/9/19 17:14:00	10/10/19 01:20:00	10/10/19 06:57:30	9202	Good
154	SBE 37-15818	10/9/19 17:12:00	10/10/19 01:20:00	10/10/19 17:33:30	9201	Good
155	SBE 37 -4701	10/9/19 17:11:00	10/10/19 01:20:00	10/10/19 02:18:20	139354	Good
36 mab	SBE 37-12246	10/9/19 00:38:00	10/10/19 01:20:00	10/09/19 06:36:00	111557	Good
36 mab	SBE 37-12247	10/9/19 00:38:00	10/10/19 01:20:00	10/09/19 04:27:30	111804	Good

The data from the upward-looking 300 kHz ADCP at 125m were considered good. The instrument was pinging upon recovery. There appeared to be no questionable data from this ADCP at this time, apart from near-surface side-lobe interference. On the other hand, the 600 kHz instrument was recovered with a depleted battery, and it was not pinging. No apparent flooding or rust was detected inside the instrument's cage. The data recorder indicated that it stopped functioning on November 2nd, 2018.

Table III-5.WHOTS-15 mooring ADCP recovery information. All times are in UTC.

	ADCP S/N 7637	**ADCP S/N 13917**
Transducer 1 Spike Time	10/10/19, 02:42:30	
Transducer 2 Spike Time	10/10/19, 02:42:45	
Transducer 3 Spike Time	10/10/19, 02:43:00	
Transducer 4 Spike Time	10/10/19, 02:43:15	
Time out of Water	10/9/19, 17:15:00	10/9/19 17:30:00

IV. WHOTS (15-16) cruise shipboard observations

The hydrographic profile observations made during the WHOTS cruises were obtained with a Sea-Bird CTD package with dual temperature, salinity, and oxygen sensors. This CTD was installed on a rosette-sampler with 5 L Niskin sampling bottles for calibration water samples. Furthermore, the *Hi'ialakai* and *Oscar Sette* came equipped with a thermosalinograph system that provided a continuous depiction of the near-surface layer's temperature and salinity. Horizontal currents over the depth range of 30-700 m were measured from the shipboard 75 kHz Ocean Surveyor (OS75) ADCP (narrowband) with a vertical resolution of 16m for the WHOTS-15 and WHOTS-16 cruises. Broadband mode for the OS75 provided additional current data over the range upper 200 m with a vertical resolution of 8m.

Data gaps occurred when the system was shut down temporarily during communications with the acoustic releases used for the moorings during both cruises. Periods of missing data between 300 and 450 m in the broadband ADCP were apparent due to the lack of scattering material in the water.

A. Conductivity, Temperature, and Depth (CTD) profiling

Continuous measurements of temperature, conductivity, dissolved oxygen, and pressure were made with the UH Sea-Bird SBE-9/11Plus CTD underwater unit #91361 (BETA), deck unit 112060 during WHOTS-15 and WHOTS-16 cruises. The CTD was equipped with an internal Digiquartz pressure sensor and pairs of external temperature, conductivity, and oxygen sensors.

Each temperature-conductivity sensor pair used a Sea-Bird TC duct, which circulated seawater through independent pump and plumbing installations. The CTD configuration also included two oxygen sensors, installed in the plumbing for each sensor set. In both cruises, the CTD was mounted in a vertical position in the lower part of a rosette sampler, with the sensors' water intakes located at the bottom of the rosette.

The package was deployed on a conducting cable, which allowed for real-time data acquisition and display. The deployment procedure consisted of lowering the package to approximately 10 dbar and waiting until the CTD pumps started operating. The CTD was then raised until the sensors were close to the surface to begin the CTD cast. The time and position of each cast were obtained via a GPS connection to the CTD deck box. Four salinity samples were taken on each cast for calibration of the conductivity sensors.

1. Data acquisition and processing

CTD data were acquired at the instrument's highest sampling rate of 24 samples per second. Digital data were stored on a laptop computer, and, for redundancy, the analog signal was recorded on VHS videotapes. Backups of CTD data were made onto USB storage cards.

The raw CTD data were quality controlled and screened for spikes described in the WHOTS Data Report 1 (Santiago-Mandujano *et al.*, 2007). Data alignment, averaging, correction, and reporting were done as described in Tupas *et al.* (1993). Spikes in the data occur when the CTD samples the disturbed water of its wake. Therefore, the downcast samples were rejected when the

CTD was moving upward or when its acceleration exceeded 0.5 m s^{-2} in magnitude. The data were subsequently averaged into 2-dbar pressure bins after calibrating the CTD conductivity with the bottle salinities.

The data were additionally screened by comparing the T-C sensor pairs. These differences permitted the identification of problems with the sensors. The data from only one T-C pair, whichever was deemed most reliable, is reported here. Only data from the downcast are reported, as wake effects from the rosette commonly contaminate upcast data.

Temperature is reported on the ITS-90 scale. Salinity and all derived units were calculated using the UNESCO (1981) routines; salinity is reported in the Practical Salinity(S_A) scale (PSS-78). Oxygen is reported in μmol kg^{-1}.

2. CTD sensor calibration and corrections

Pressure

The pressure calibration strategy for CTD pressure transducer SN 75434 used during WHOTS-15 and WHOTS-16 cruises employed a high-quality quartz pressure transducer as a transfer standard. Periodic recalibrations of this lab standard were performed with a primary pressure standard. The only corrections applied to the CTD pressures were a constant offset determined when the CTD first enters the water on each cast. Also, a span correction determined from bench tests on the sensor against the transfer standard was applied. These procedures and corrections are thoroughly documented in the HOT-2018 data report (Fukieki *et al.*, 2020).

Temperature/Conductivity

Sea-Bird SBE-3-Plus temperature and SBE 4C conductivity transducers were used during WHOTS-15 and -16 cruises. These sensors' history and performance have been monitored during HOT cruises, and calibrations and drift corrections applied during WHOTS cruises are thoroughly documented in the HOT-2018 data report (Fukieki *et al.*, 2020).

Dissolved Oxygen

Sea-Bird SBE-43 oxygen sensors were used during the WHOTS-15 and -16 cruises. The WHOTS-15 oxygen data were calibrated using calibration coefficients obtained during the HOT-305 cruise conducted on 9-13 September 2018, before the WHOTS-15 cruise, which used the same oxygen sensors. The CTD empirical calibration was performed using oxygen water samples and the procedure from Owens and Millard Jr (1985). See Tupas *et al.* (1996) for details on these calibrations procedures. Similarly, the oxygen data from WHOTS-16 were calibrated using calibration coefficients obtained during the HOT-315 cruise conducted on 3-7 September 2019, before the WHOTS-16 cruise, which used the same oxygen sensors.

B. Water sampling and analysis

Salinity

Salinity samples were collected by a rosette sampler during CTD casts at selected depths during WHOTS-15 and -16, and then sub-sampled in 250 ml glass bottles. The top of each bottle and thimble were thoroughly dried before being tightly capped to prevent water from being trapped between the cap or thimble and the bottle's mouth. It has been observed that residual water trapped in this way increases its salinity due to evaporation, and it can leak into the sample when the bottle is opened for measuring. Samples from each cruise were measured after the cruise in the UH laboratory using a Guildline Autosal 8400B (SN 70168). IAPSO[1] standard seawater samples were measured to standardize the Autosal, and samples from a large batch of "secondary standard" (substandard) seawater were measured after every 24-48 samples to detect drift in the Autosal. Standard deviations of the secondary standard measurements were less than ± 0.002 for WHOTS-15 and -16 cruises (Table IV-1).

The substandard water was collected by a rosette sampler from 1020 m at station ALOHA during HOT cruises and drained into a 50-liter Nalgene plastic carboy. In the laboratory, the water was then thoroughly mixed in a glass carboy for 20 minutes by manually shaking, rolling, and tilting the carboy vigorously, after which a 2-inch protective layer of white oil was added on top to deter evaporation. The substandard water was allowed to stand for approximately three days before it was used and was stored in the same temperature-controlled room as the Autosal, protecting it from the light with black plastic bags to inhibit biological growth. Substandard seawater batches #65, and #66 were prepared on October 23rd, 2018, and December 21st, 2018, respectively, and were used for WHOTS-15 and -16 samples, respectively.

Samples from the WHOTS-15 and WHOTS-16 cruises were measured during the same day as the HOT-306 and HOT-316 samples, respectively. Table IV-1 shows the precision measurements of the secondary sub-standards.

Table IV-1.The precision of salinity measurements of secondary lab standards.

Cruise	Mean Salinity +/- SD	# Samples	Substandard Batch #	IAPSO Batch #
WHOTS-15	34.4861 ± 0.0016	4	65	P160
WHOTS-16	34.4985 ± 0.0005	4	66	P163

[1] International Association for Physical Sciences of the Ocean

C. Thermosalinograph data acquisition and processing

1. WHOTS-15 Cruise

Near-surface temperature and salinity data during the WHOTS-15 cruise were acquired from the thermosalinograph (TSG) system installed on the NOAA Ship *Hi'ialakai*. The *Hi'ialakai* has a water intake depth of 2 m located at the ship's bow, next to the starboard side bow thruster. The sensors located in the ship's wet lab about 67 m from the intake were sampling water from the continuous seawater system running through the ship. They were comprised of one thermosalinograph model SBE-21 (SN 3155) and a micro-thermosalinograph model SBE-45 (SN 0150), both with (internal) temperature and conductivity sensors; and an SBE-38 (SN 0215) external temperature sensor located at the water intake. The SBE-21 recorded data every 5 seconds, and the other two instruments recorded data every second. The system had a pressure gauge showing a flow pressure between 10 to 15 psi when the water intake was open. Both thermosalinograph systems had a de-bubbler.

Temperature Calibration

External temperature data from the SBE-38 sensor (last calibrated at Sea-Bird on January 16th, 2018) were used to measure the seawater temperature. These data were compared to the data collected during CTD casts.

Nominal Conductivity Calibration

Data from the SBE-21 conductivity and temperature sensors were used to calculate the intake seawater salinity. These sensors were last calibrated at Sea-Bird on November 8th, 2017. All conductivity data from the thermosalinograph were nominally calibrated with coefficients from this calibration. However, all the final salinity data reported here were calibrated against bottle data, as explained below.

Data Processing

Daily files containing navigation data recorded every second were concatenated with the thermosalinograph data. The thermosalinograph data were then screened for gross errors, with upper and lower bounds of 18 °C and 35 °C for temperature and 3 and 6 Siemens m $^{-1}$ for conductivity. There were no points outside the valid temperature range and no points outside the valid conductivity range.

A 5-point running median filter was used to detect one- or two-point temperature and conductivity glitches in the thermosalinograph data. Glitches in temperature and conductivity detected by the 5-point median filter were immediately replaced by the median. Threshold values of 0.3 °C for temperature and 0.1 Siemens m^{-1} for conductivity were used for the median filter. After running the filter, there were no temperature or conductivity points replaced by the median.

A 3-point triangular running mean filter was used to smooth the temperature and conductivity data after passing the glitch detection.

The thermosalinograph aboard the Ship Hi'ialakai was set to record data every five seconds. However, occasionally, due to an error in the acquisition software rounding routine, a record is written at a longer interval. There were no timing errors during WHOTS-15.

Data were visually scanned to flag spikes likely caused by contamination due to the introduction of bubbles to the flow-through system during transits or rough conditions. Of 799,508 data points, 22,555 conductivity data points (2.8%) were flagged as bad.

Bottle salinity and CTD Salinity Comparisons

The thermosalinograph salinity was calibrated by comparing it to bottle salinity samples drawn from a water intake next to the thermosalinograph every 8 hours throughout the cruise. Of the 22 thermosalinograph bottles sampled, bottle 17 was identified as a conductivity outlier and discarded from the analysis. Samples were analyzed as described in Section IV.B. The comparison was made in conductivity to eliminate the effects of temperature. The conductivity of each bottle sample was computed using the salinity of the bottle, thermosalinograph temperature, and a pressure of 3.44 dbar, which includes the pressure of the flow-through system's pump.

Salinity samples were drawn from the flow-through system, located less than 0.5 m from the SBE-21. Consequently, there should be virtually no delay between when the water passes through the thermosalinograph and sampled. A 90-second average centered on the sample draw time was chosen for processing purposes.

In order to make the comparison in conductivity units, the CTD conductivity was calculated using the 4 dbar downcast CTD salinity, the internal thermosalinograph temperature, and a pump pressure of 3.44 dbar. There were 12 CTD casts conducted during WHOTS-15 while the thermosalinograph was running. Casts 1 and 4 were removed from the analysis as temperature outliers and cast 1, 9, and 10 as conductivity outliers.

A cubic spline was fit to the time series of the differences between the bottle and TSG conductivity, and a correction was obtained for the TSG conductivities. Salinity was calculated using these corrected conductivities, the thermosalinograph temperatures, and 3.44 dbar pressure. After correction, the mean difference between the bottle and thermosalinograph salinities was 0.000005 psu with a standard deviation of 0.003339 psu. The mean CTD - thermosalinograph difference was -0.001385 psu with a standard deviation of 0.001677 psu.

CTD Temperature Comparisons

There were 12 CTD casts conducted during WHOTS-15, one of which was a test cast offshore Honolulu (Station 20) and five at Station 52 (WHOTS-14), and six at Station 50 (WHOTS-15), respectively. The 4 dbar downcast CTD temperature data from those casts were used to compare with the thermosalinograph data at the time of the casts. This comparison gives an estimate of the quality of the thermosalinograph measurements. Of the 12 casts, two were

identified as temperature outliers after comparing it against the thermosalinograph data and removed from the analysis. The mean difference between the CTD and the internal temperature sensor was -0.00992 °C, with a standard deviation of ± 0.04096 °C.

2. WHOTS-16 Cruise

Near-surface temperature and salinity data during the WHOTS-16 cruise were acquired from the thermosalinograph (TSG) system installed on the NOAA Ship Oscar Sette. The sensors were sampling water from the continuous seawater system running through the ship. They were comprised of one thermosalinograph model SBE-21 (SN 3168) and a micro-thermosalinograph model SBE-45 (SN 0290), both with (internal) temperature and conductivity sensors located in the ship's chemistry lab, about 70 m from the hull intake; and an SBE-38 (SN 266) external temperature sensor located at the entrance of the water intake. All instruments recorded data every second. The water intake is located at the ship's bow, forward from the starboard side bow thruster at a depth of 3 m. The system has a flow meter in the chemistry lab, showing a flow rate of about 1.1 liters/minute during the cruise. Only the SBE-45 has a debubbler. Salinity water samples were taken every 8 hours from the exhaust in the Chemistry lab using 0.25-liter glass bottles, to be measured in the UH lab to correct any drift in the thermosalinograph conductivities.

Temperature Calibration

External temperature data from the SBE-38 sensor (last calibrated at Sea-Bird on December 29th, 2019) were used to measure the seawater temperature. These data were compared to the data collected during CTD casts.

Nominal Conductivity Calibration

Data from the SBE-45 conductivity and temperature sensors were used to calculate the intake seawater salinity. These sensors were last calibrated at Sea-Bird on February 19th, 2019. All conductivity data from the thermosalinograph were nominally calibrated with coefficients from this calibration. However, all the final salinity data reported here were calibrated against bottle data, as explained below.

Data Processing

Daily files containing navigation data recorded every second were concatenated with the thermosalinograph data. The thermosalinograph data were then screened for gross errors, with upper and lower bounds of 18 °C and 35 °C for temperature and 3 and 6 Siemens m $^{-1}$ for conductivity. There were no points outside the valid temperature range and no points outside the valid conductivity range.

A 5-point running median filter was used to detect one- or two-point temperature and conductivity glitches in the thermosalinograph data. Glitches in temperature and conductivity detected by the 5-point median filter were immediately replaced by the median. Threshold values of 0.3 °C for temperature and 0.1 Siemens m^{-1} for conductivity were used for the median filter. After running the filter, there were no temperature or conductivity points replaced by the median.

A 3-point triangular running mean filter was used to smooth the temperature and conductivity data after passing the glitch detection.

The thermosalinograph aboard the Ship *Oscar Sette* was set to record data every second. The system had to be secured on the last day of the cruise due to the bad weather because it kept shutting down due to air going into the plumbing, causing the pumps to stop working.

Data were visually scanned to flag spikes likely caused by contamination due to the introduction of bubbles to the flow-through system during transits or rough conditions. Of 69,311,136 data points, 141,365 conductivity data points (2%) were flagged as bad.

Bottle salinity and CTD Salinity Comparisons

The thermosalinograph salinity was calibrated by comparing it to bottle salinity samples drawn from a water intake next to the thermosalinograph every 8 hours throughout the cruise. Of the twenty-one thermosalinograph bottles sampled, bottle #18, #19, #20, and #21 were identified as a conductivity outlier and were discarded from the analysis. Samples were analyzed as described in Section IV.B. The comparison was made in conductivity to eliminate the effects of temperature. The conductivity of each bottle sample was computed using the salinity of the bottle, thermosalinograph temperature, and a pressure of 10 dbar, which includes the pressure of the flow-through system's pump.

Salinity samples were drawn from the flow-through system, located less than 0.5 m from the SBE-45. Consequently, there should be virtually no delay between when the water passes through the thermosalinograph and sampled. A 90-second average centered on the sample draw time was chosen for processing purposes.

In order to make the comparison in conductivity units, the CTD conductivity was calculated using the 4 dbar downcast CTD salinity, the internal thermosalinograph temperature, and a pump pressure of 10 dbar. There were twelve CTD casts conducted during WHOTS-16 while the thermosalinograph was running. Casts 4, 5, 6, 7, and 9 were removed from the analysis as temperature and conductivity outliers.

A cubic spline was fit to the time series of the differences between the bottle and TSG conductivity, and a correction was obtained for the TSG conductivities. Salinity was calculated using these corrected conductivities, the thermosalinograph temperatures, and ten dbar pressure. After applying corrections, the mean difference between the bottle and thermosalinograph salinities was -0.00004 psu with a standard deviation of 0.001886 psu. The mean CTD - thermosalinograph difference was -0.0028 psu with a standard deviation of 0.001118 psu.

CTD Temperature Comparisons

There were 11 CTD casts conducted during WHOTS-16, one of which was a test cast offshore Honolulu (Station 20) and five at Station 52 (WHOTS-16), and five at Station 50 (WHOTS-15), respectively. The 4 dbar downcast CTD temperature data from those casts were used to compare with the thermosalinograph data at the time of the casts. This comparison gives an estimate of the quality of the thermosalinograph measurements. Of the 11 casts, five were

identified as temperature outliers after comparing it against the thermosalinograph data and removed from the analysis. The mean difference between the CTD and the internal temperature sensor was -0.05813 °C, with a standard deviation of ± 0.05561 °C.

D. Shipboard ADCP

1. WHOTS-15 Deployment Cruise

Currents were measured for the cruise duration over the depth range of 30-1000 m with a 75 kHz RDI Ocean Surveyor (OS75) ADCP working in narrowband mode with a vertical resolution of 16 m and broadband mode with a vertical resolution of 8 m. The system yielded useful data (see Santiago-Mandujano *et al.*, 2019). The times of the datasets from the OS75 are shown in Table IV-2.

Table IV-2.ADCP record times (UTC) for the Narrow Band 75 kHz ADCP during the WHOTS-15cruise

WHOTS-15	OS75nb	OS75bb
File beginning time	21-Sept-2018 19:00:19	21-Sept-2018 19:55:20
File ending time	03-Oct-2018 01:55:22	03-Oct-2018 01:50:21

2. WHOTS-16 Deployment Cruise

Currents were measured for the cruise duration over the depth range of 30-700 m with a 75 kHz RDI Ocean Surveyor (OS75) ADCP working in narrowband mode with a vertical resolution of 16 m and broadband mode with a vertical resolution of 8 m. The system yielded good data (see Santiago-Mandujano *et al.*, 2020) during operations near the WHOTS-15 and WHOTS-16 moorings. The broadband system only recorded good data in the upper 200 m. The times of the datasets from the OS75 kHz are shown in Table IV-3.

Table IV-3. ADCP record times (UTC) for the 75 kHz ADCP during the WHOTS-16 cruise.

WHOTS-16	OS75nb	OS75bb
File beginning time	04-Oct-2018 19:38:54	04-Oct-2018 19:38:54
File ending time	12-Oct-2018 20:14:15	12-Oct-2018 20:14:15

V. Moored Instrument Observations

A. MicroCAT/SeaCAT data processing procedures

Each moored MicroCAT temperature, conductivity, and pressure (when installed) was calibrated at Sea-Bird before their deployment and after their recovery on the dates shown in Table V-1. The internally-recorded data from each instrument were downloaded onboard the ship after the mooring recovery. The nominally-calibrated data were plotted for a visual assessment of the data quality. The data processing included checking the internal clock data against external event times, pressure sensor drifts correction, temperature sensor stability, and conductivity calibration against CTD data from casts conducted near the mooring during HOT and WHOTS cruises. The detailed processing procedures are described in this section.

Table V-1. WHOTS-15 MicroCAT temperature sensor calibration dates and sensor drift during deployments.

Nominal deployment depth (m)	Sea-Bird Serial number	Pre-deployment calibration	Post-recovery calibration	Temperature sensor's annual drift during WHOTS-15 (mili^{o}C)
1.5	SBE 37-5994	30-Nov-16	11-Mar-19	-0.10
7.0	SBE 37-6892	24-Sep-17	09-Jul-20	-0.64
15.0	SBE 37-3382	24-Sep-17	09-Jun-20	-0.93
25.0	SBE 37-4663	24-Sep-17	09-Jun-20	-0.49
35.0	SBE 37-3633	22-Sep-17	09-Jul-20	0.11
40.0	SBE 37-3381	24-Sep-17	10-Jul-20	0.29
45.0	SBE 37-3668	28-Sep-17	09-Jul-20	-0.23
50.0	SBE 37-3619	23-Sep-17	11-Jun-20	0.26
55.0	SBE 37-3620	22-Sep-17	10-Jun-20	-0.48
65.0	SBE 37-3621	22-Sep-17	13-Jun-20	-1.00
75.0	SBE 37-3632	22-Sep-17	09-Jun-20	-0.59
85.0	SBE 37-4699	22-Sep-17	10-Jun-20	-0.47
95.0	SBE 37-3791	28-Sep-17	10-Jul-20	-0.69
105.0	SBE 37-769	28-Sep-17	08-Jul-20	-0.93
120.0	SBE 37-4700	22-Sep-17	18-Jul-20	0.20
155.0	SBE 37-4701	22-Sep-17	09-Jul-20	-0.79
4658	SBE 37-12247	20-Apr-18	28-Jul-20	0.20
4658	SBE 37- 12246	20-Apr-18	28-Jul-20	0.18

1. Internal Clock Check and Missing Samples

Before the WHOTS-15 mooring deployment and after its recovery (before the data logging was stopped), the MicroCATs temperature sensors were placed in contact with an ice pack to create a spike in the data, to check for any problems with their internal clocks, and for possible missing samples (Table III-4). The cold spike was detected by a sudden decrease in temperature. For all the instruments, the clock time of this event matched the time of the spike (within the sampling interval of each instrument) correctly. No missing samples were detected for any of the devices.

2. Pressure Drift Correction and Pressure Variability

Some of the MicroCATs used in the moorings were outfitted with pressure sensors (Table III-1). Biases were detected in the pressure sensors by comparing the on-deck pressure readings (which should be zero for standard atmospheric pressure at sea level of 1029 mbar) before deployment and recovery. Table V-2 shows the magnitude of the bias for each of the sensors before and after deployment. To correct this offset, a linear fit between the initial and final on-deck pressure offset as a function of time was obtained and subtracted from each sensor. Figure V-1 shows the linearly corrected pressures measured by the MicroCATs located above 200 m during the WHOTS-15 deployment. For all these sensors, the mean difference from the nominal instrument pressure (based on the deployed depth) was less than 1 dbar. The standard deviation of the pressure for the duration of the record was also less than 1 dbar for all sensors, with the deeper sensors showing a slightly larger standard deviation. The range of variability for all sensors was about ± 3 dbar.

The causes of pressure variability can be several, including density variations in the water column above the instrument; horizontal dynamic pressure (not only due to the currents but also due to the motion of the mooring); mooring position (see WHOTS Data Report 1, Santiago-Mandujano *et al.*, 2007).

Table V-2. Pressure bias of MicroCATs with pressure sensors. The instrument at 135 m stopped recording data before it was recovered.

Deployment	Depth (m)	Sea-Bird Serial #	Bias before deployment (dbar)	Bias after recovery (dbar)
WHOTS-15	7	SBE 37-6892	0.00	-0.30
WHOTS-15	45	SBE 37-3668	-0.01	-0.10
WHOTS-15	85	SBE 37-4699	-0.02	-0.02
WHOTS-15	105	SBE 37-2769	-0.03	-0.05
WHOTS-15	120	SBE 37-4700	-0.40	-0.8
WHOTS-15	135	SBE 37-2965	-0.04	NA
WHOTS-15	136	SBE 37-15817	0.06	-0.20
WHOTS-15	154	SBE 37-15818	0.05	0.00
WHOTS-15	155	SBE 37-4701	-0.10	-0.10
WHOTS-15	4658	SBE 37-12247	0.40	1.70
WHOTS-15	4658	SBE 37-15818	0.40	1.50

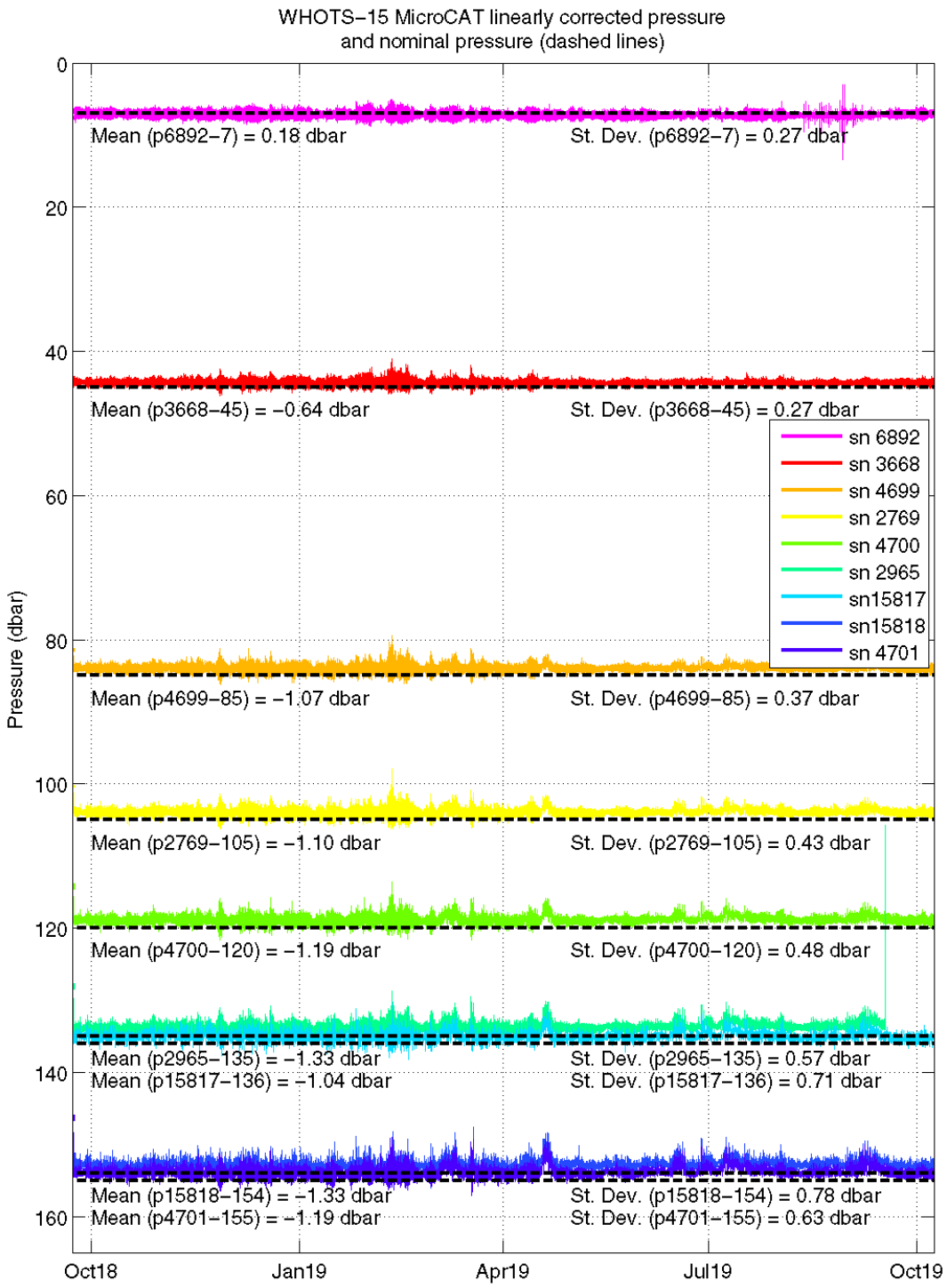

Figure V-1. Linearly corrected pressures from MicroCATs between 7 and 155 m during WHOTS-15 deployment. The horizontal dashed line is the sensor's nominal pressure, based on deployed depth. The text on the left (right) side of the figure indicates the mean (standard deviation) of the difference between each instrument's pressure and nominal pressure.

3. Temperature Sensor Stability

The MicroCAT temperature sensors were calibrated at Sea-Bird before and after each deployment, and their annual drift evaluations based on these calibrations are shown in Table V-1. These values turned out to be insignificant (not higher than 0.001 °C) for all sensors. Comparisons between the MicroCAT and CTD data from casts conducted near the mooring during HOT cruises confirmed that the rest of the moored instruments' temperature drift was insignificant. The instrument at 135 m failed during deployment and could not be calibrated after the recovery. The two MicroCATs (SN 12247 and SN 12246) deployed near the bottom were drift corrected. Figure V-7 (upper panel) shows the temperature differences between both instruments before and after the correction. After the correction, the temperature differences were in the $\pm 1.0 \times 10^{-3}$ °C range.

Temperature comparisons between one of the WHOTS-15 near-surface MicroCAT (SN 5994) and the four SBE-56 surface temperature sensors in the buoy hull Table III-2 are shown in Figure V-2. All of the SBE-56 instruments returned full records, and none of them show any obvious bias compared to the Microcat measurements.

Figure V-2. The temperature difference between MicroCAT SN 5994 at 1.5 m, and near-surface temperature sensors SN 6150 (top panel), 6239 (second panel), 6410 (third panel), and 6412 (bottom panel), during the WHOTS-15 deployment. The light blue line is a 24-hour running mean of the differences.

In addition to the Sea-Bird temperature sensors, there were additional temperature sensors in the VMCMs (at 10 and 30 m) and in the ADCPs (at 47.5 m and 125 m). Comparisons with the

temperatures from adjacent MicroCATs were conducted to evaluate the temperatures from those sensors.

Comparisons with VMCM and ADCP temperature sensors

The upper panel of Figure V-3 shows the difference between the 10-m VMCM and the 7-m MicroCAT temperatures during WHOTS-15, after adding a 0.0316 °C offset correction to the VMCM. The offset was the mean difference between the uncorrected VMCM and the 7-m MicroCAT data. Also shown for comparison in the middle panel of the figure are the differences between MicroCAT temperatures at 15 m. The lower panel shows the temperature fluctuations in the differences between the 7 and 15-m MicroCATs, which seem to be around zero.

Temperature differences between the 30-m VMCM and the temperatures from adjacent MicroCATs at 25 and 35-m during WHOTS-15 are shown in Figure V-4, after adding a 0.0126°C offset correction to the VMCM. The offset was the mean difference between the uncorrected VMCM and the 25-m MicroCAT data. For comparison, the differences between the MicroCATs temperatures are also shown in the lower panel.

Temperature differences between the 47.5-m ADCP and the temperatures from adjacent MicroCATs at 45 and 50-m during WHOTS-15 are shown in Figure V-5. The ADCP stopped collecting data on 2018/11/2 for unknown reasons. For comparison, the differences between the MicroCATs temperatures are also shown in the lower panel.

Temperature differences between the 125-m ADCP and the temperatures from adjacent MicroCATs at 120 and 135-m during WHOTS-15 are shown in Figure V-6. For comparison, the differences between the MicroCATs temperatures are also shown in the lower panel. It is difficult to assess the quality of the ADCP temperature from these comparisons. These sensors were located at the top of the thermocline, where we expect to find substantial temperature differences between adjacent sensors. However, an indication of the ADCP temperatures' quality is given in the upper panel plot, which shows temperatures fluctuating closely around zero.

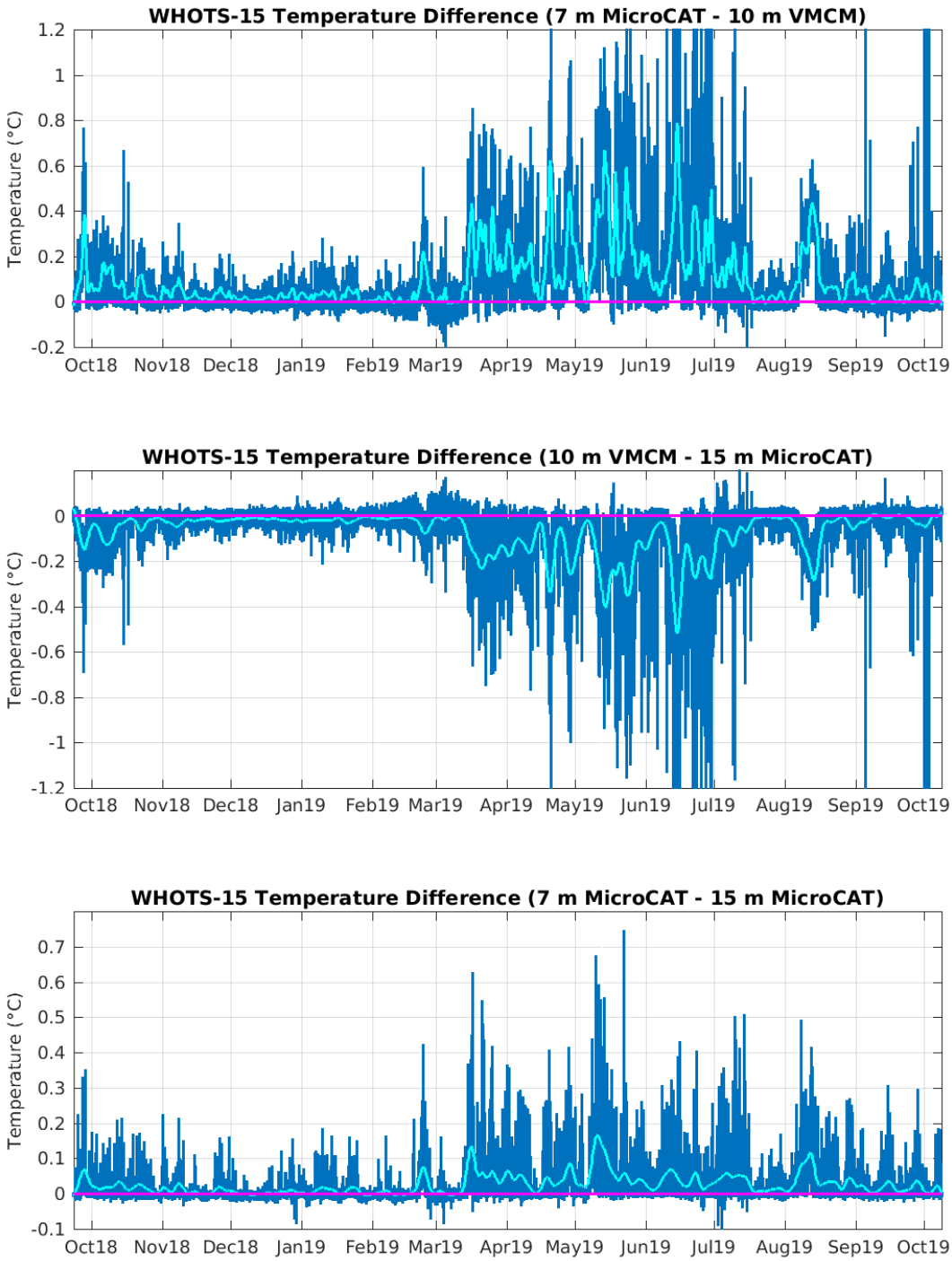

Figure V-3. The temperature difference between the 7-m MicroCAT and the 10-m VMCM (upper pane)l; between the 15-m MicroCAT and the 10-m VMCM (middle panel); and between the 7-m and the 15-m MicroCATs (lower panel) during the WHOTS-15 deployment. The light blue line is a 24-hour running mean of the differences.

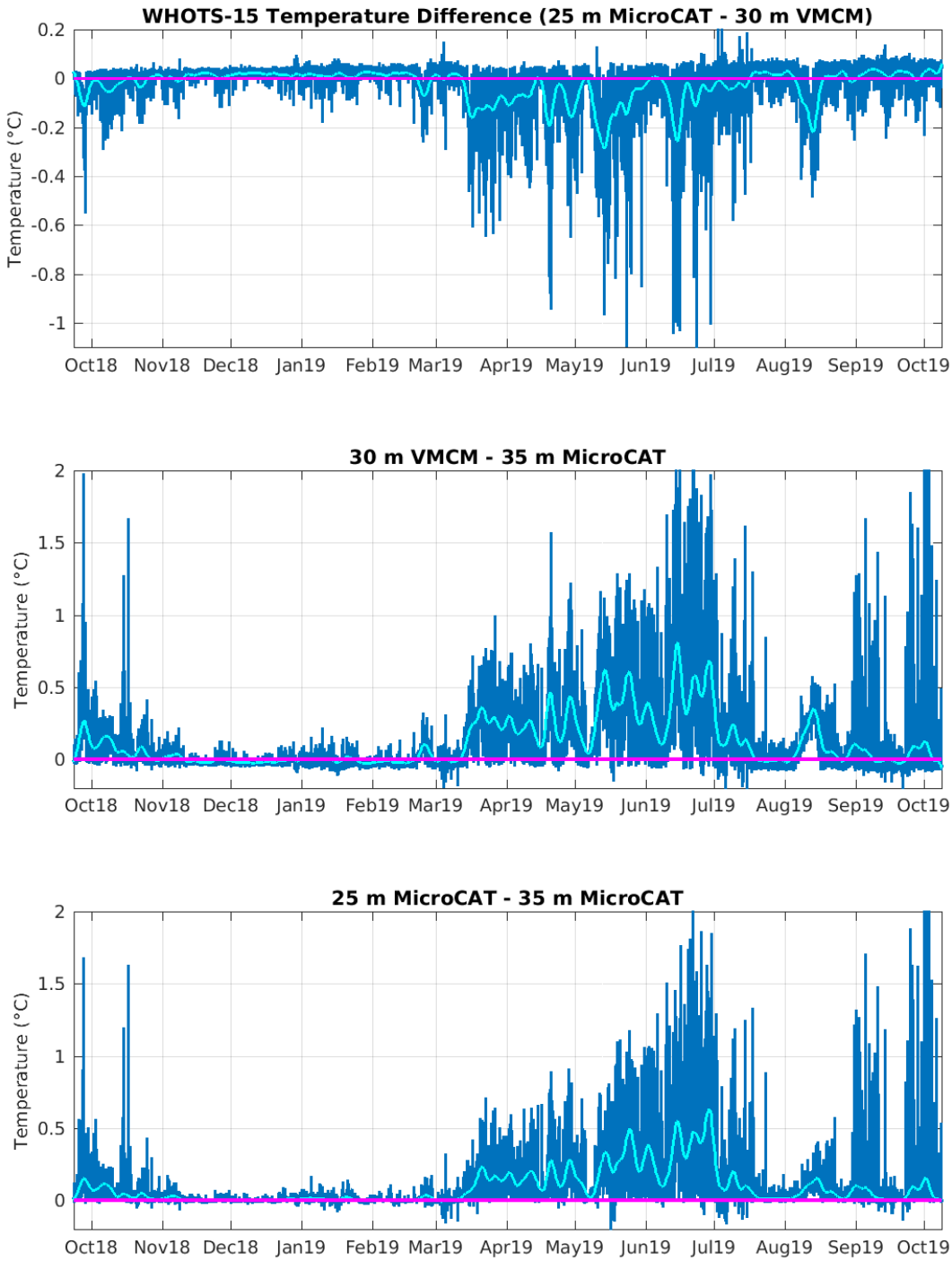

Figure V-4. The temperature difference between the 25-m MicroCAT and the 30-m VMCM (upper panel); between the 35-m MicroCAT and the 30-m VMCM (middle panel); and between the 25-m and the 35-m MicroCATs (lower panel) during the WHOTS-15 deployment. The light blue line is a 24-hour running mean of the differences.

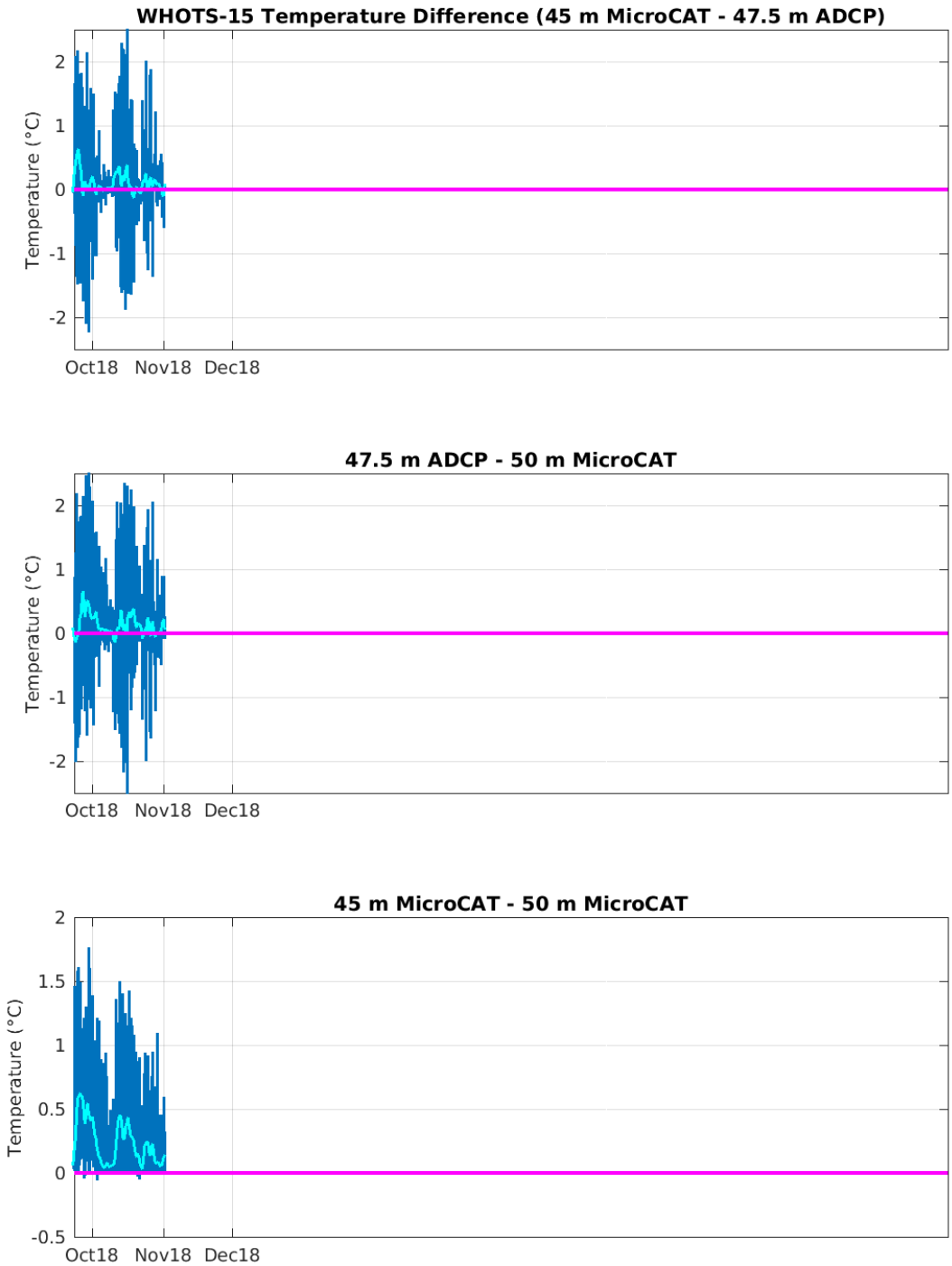

Figure V-5. The temperature difference between the 45-m MicroCAT and the 47.5-m ADCP (upper panel). (The ADCP stopped collecting data on 2018/11/2); between the 50-m MicroCAT and the 47.5-m ADCP (middle panel); and between the 45-m and the 50-m MicroCATs (lower panel) during the WHOTS-15 deployment. The light blue line is a 24-hour running mean of the differences.

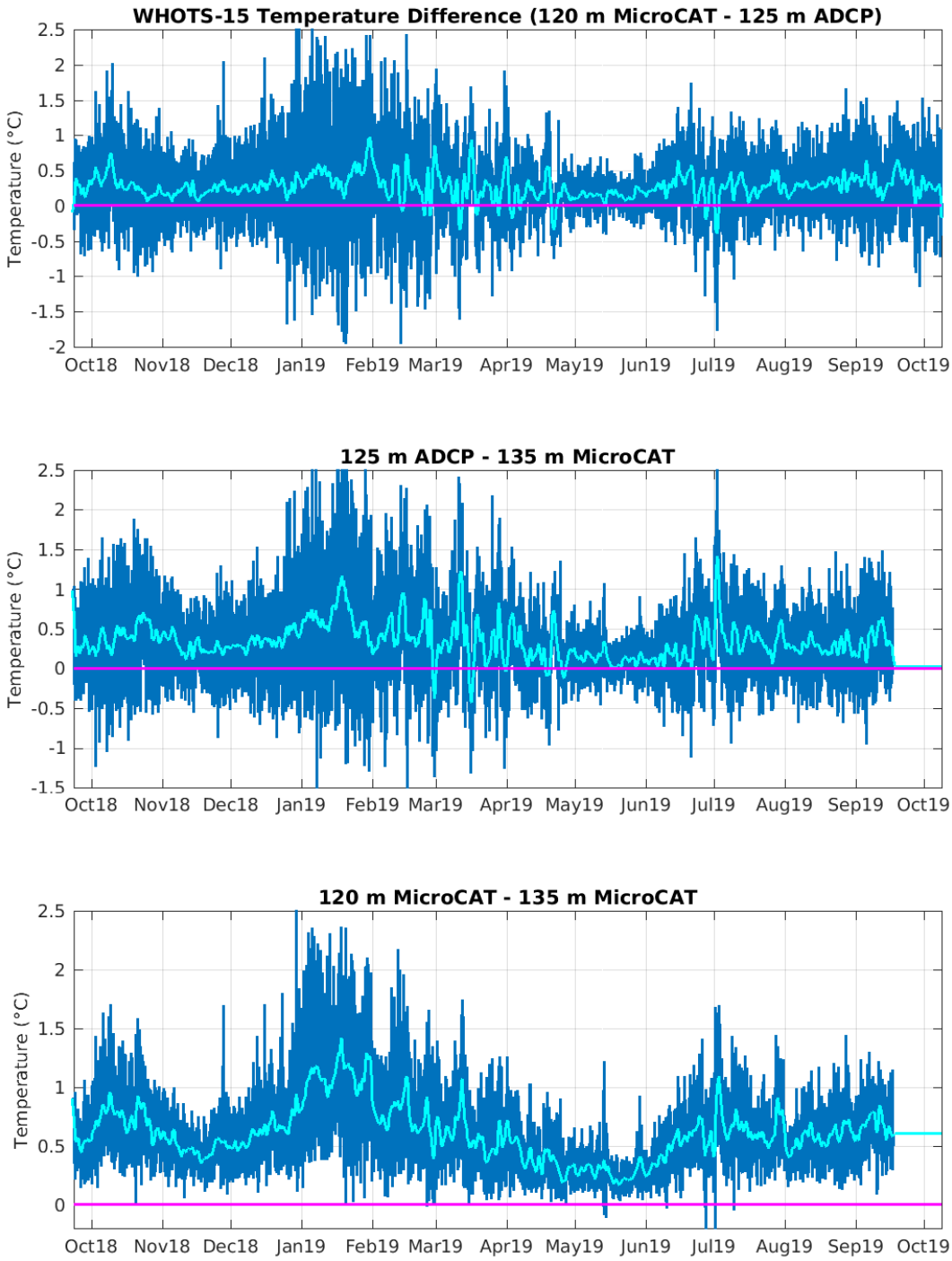

Figure V-6. The temperature difference between the 120-m MicroCAT and the 125-m ADCP (upper panel); between the 135-m MicroCAT and the 125-m ADCP (middle panel); and between the 120-m and the 135-m MicroCATs (lower panel) during the WHOTS-15 deployment. The light blue line is a 24-hour running mean of the differences.

4. Conductivity Calibration

The results of the Sea-Bird post-recovery conductivity calibrations indicated that some of the MicroCAT conductivity sensors experienced relatively large offsets from their pre-deployment calibration. These were qualitatively confirmed by comparing the mooring data against CTD data from casts conducted between 200 m and 5 km from the mooring during HOT cruises. The conductivity offsets are not apparent, and there may have been multiple causes (see Freitag *et al.* (1999) for a similar experience with conductivity cells during COARE). For some instruments, the offset was negative, caused perhaps by biofouling of the conductivity cell. In contrast, for others, the offset was positive, caused by scouring the inside of the conductivity cell (possibly by the instrument's continuous up and down motion in an abundant field of diatoms). A visual inspection of the instruments after recovery did not show any apparent signs of biofouling. There were no cell scourings reported in the post-recovery reviews at Sea-Bird.

Corrections of the MicroCATs conductivity data were conducted by comparing them against CTD data from profiles and yo-yo casts conducted near the mooring during HOT cruises and during deployment/recovery cruises. Casts led between 200 and 1000 m from the mooring were given extra weight in the correction compared to those conducted between 1 and 5 km away. Casts more than 5 km away from the mooring were not used. Given that the CTD casts are conducted at least 200 m from the mooring, CTD and MicroCAT data's alignment was done in density rather than in-depth. For cases where the alignment in density was not possible due to large conductivity offsets (causing unrealistic mooring density values), alignment in temperature space was done. A cubic least-squares fit (LSF) to the CTD-MicroCAT differences against time was applied as a first approximation, and the corresponding correction was applied.

Some of the sensors had large offsets and noticeable variability that could not be explained by a cubic LSF (see below). For these sensors, a stepwise correction was applied to match the data to the available CTD cast data and then to use the differences between consecutive sensors to determine when the sensor started to drift. For instance, during periods of weak stratification, the conductivity difference between neighboring sensors A, B, and C could reach near-zero values, in particular for instruments near the surface, which are the ones most prone to suffer conductivity offsets. A sudden conductivity offset observed during this period between sensors A and B, but not between sensors A and C could indicate the beginning of an offset for sensor B.

Given that the most in-depth instruments on the mooring are less likely to be affected by biofouling and consequent sudden conductivity drift, the deep instruments served as an excellent reference to find any possible malfunction in the shallower ones. Therefore the most profound instruments' conductivity was corrected first, and the correction was continued sequentially upwards toward the shallower ones.

As a quality control to the conductivity corrections, the buoyancy frequency between neighboring instruments was calculated using finite differences. Over- or under-corrected conductivities yielded instabilities in the water column (negative buoyancy frequency) that were easy to detect and were not real when lasting for several days. Based on this, the conductivity correction of the corresponding sensors was revised.

Corrections of the in-depth MicroCATs conductivity data were conducted following similar procedures for the shallow instruments by comparing them against CTD data from near-bottom profiles conducted during HOT cruises (Figure V-7, bottom panel). After correction, the salinity differences between both instruments were in the ±0.001 range.

Another characteristic of the offsets in the conductivity sensors is that their development is not always linear in time. Their behavior can be highly variable (see WHOTS Data Report 1, Santiago-Mandujano *et al.*, 2007). The corrections applied to each of the conductivity sensors during WHOTS-15 can be seen in Figure V-8 to 15. Most of the instruments had a drift of less than 0.025 Siemens/m for the duration of the deployment, corrected with a linear or cubic least-squares fit. Most of the instruments deployed above 85 m showed a negative drift starting a few months before the end of the deployment, apparently due to the anti-foulant expiration. The instrument at 15 m showed a large conductivity offset in April 2019. After this time, the data could not be corrected, and it was flagged as bad (the instrument was recovered with a bend in its conductivity guard). Similarly, the instrument at 105 m had a large conductivity offset in May 2019, and the data after this time was flagged as bad. The instrument at 135 m (SN 2965) stopped recording data one month before recovery, and the post-recovery inspection at Sea-Bird revealed that the instrument had a non-replaceable faulty board.

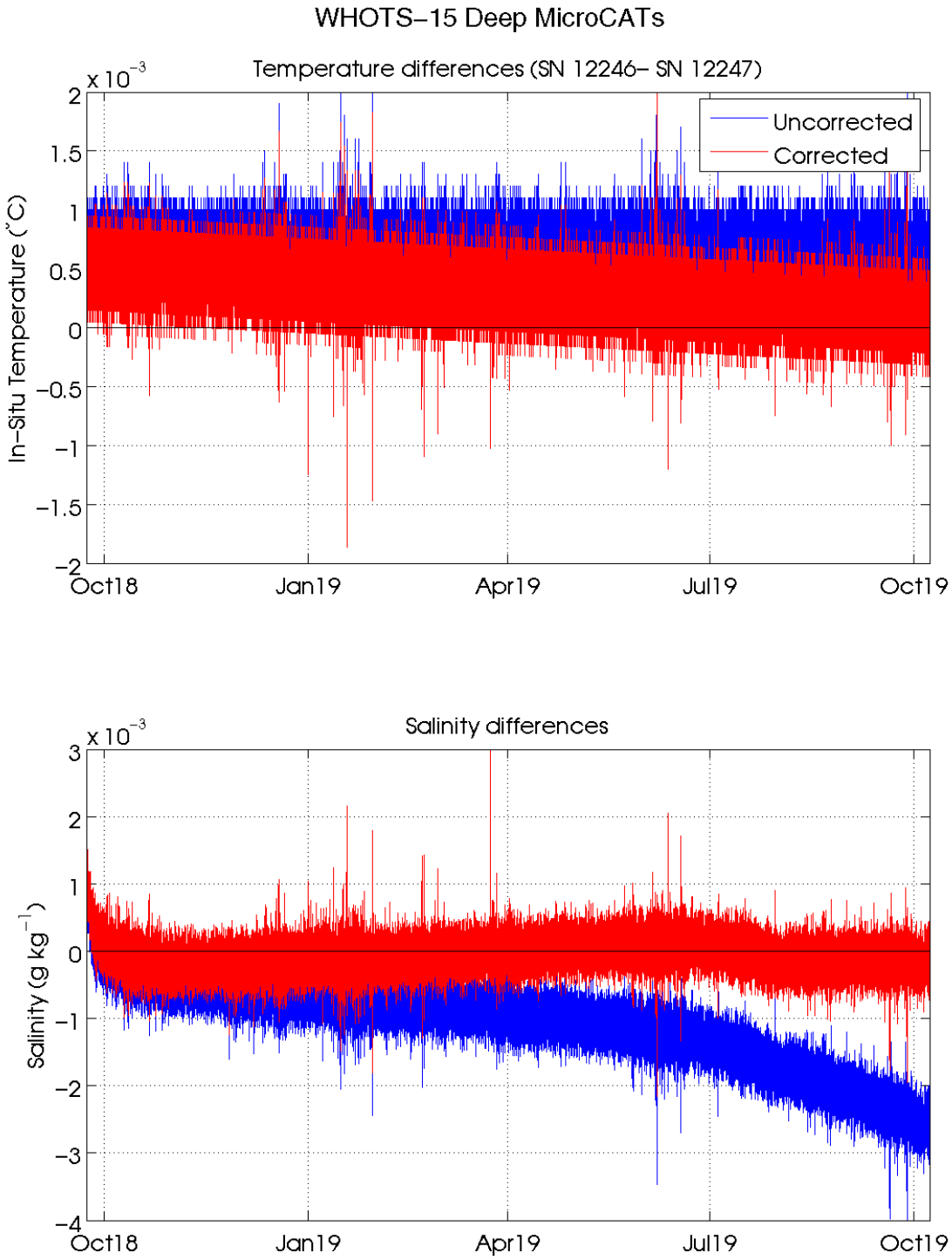

Figure V-7. Temperature differences (top panel) and salinity differences (bottom panel) between MicroCATs #12246 and #12246 during WHOTS-15. The blue (red) lines are the differences before (after) correcting the data following the text's procedures.

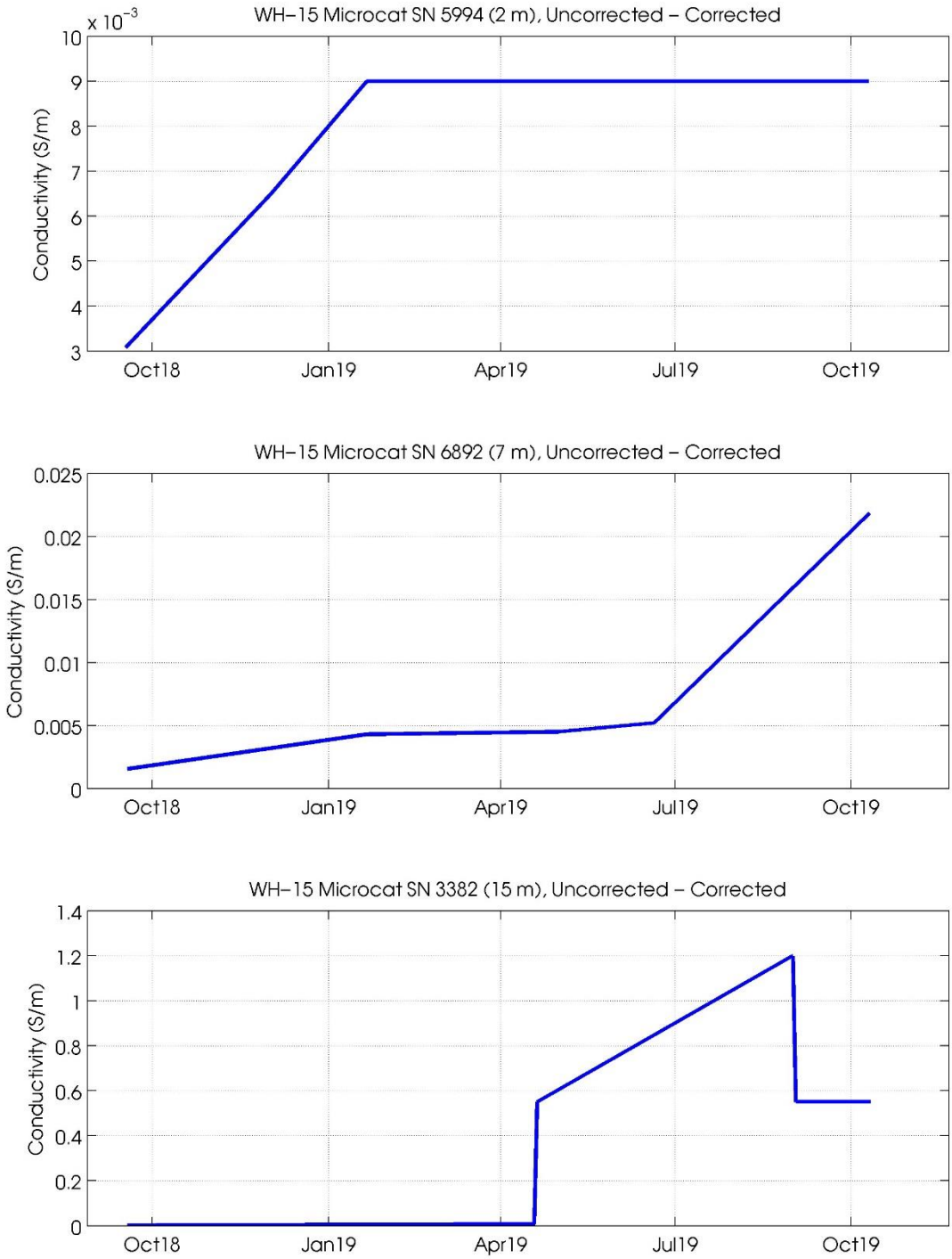

Figure V-8. Conductivity sensor corrections for MicroCATs from 2 to 15 meters during WHOTS-15.

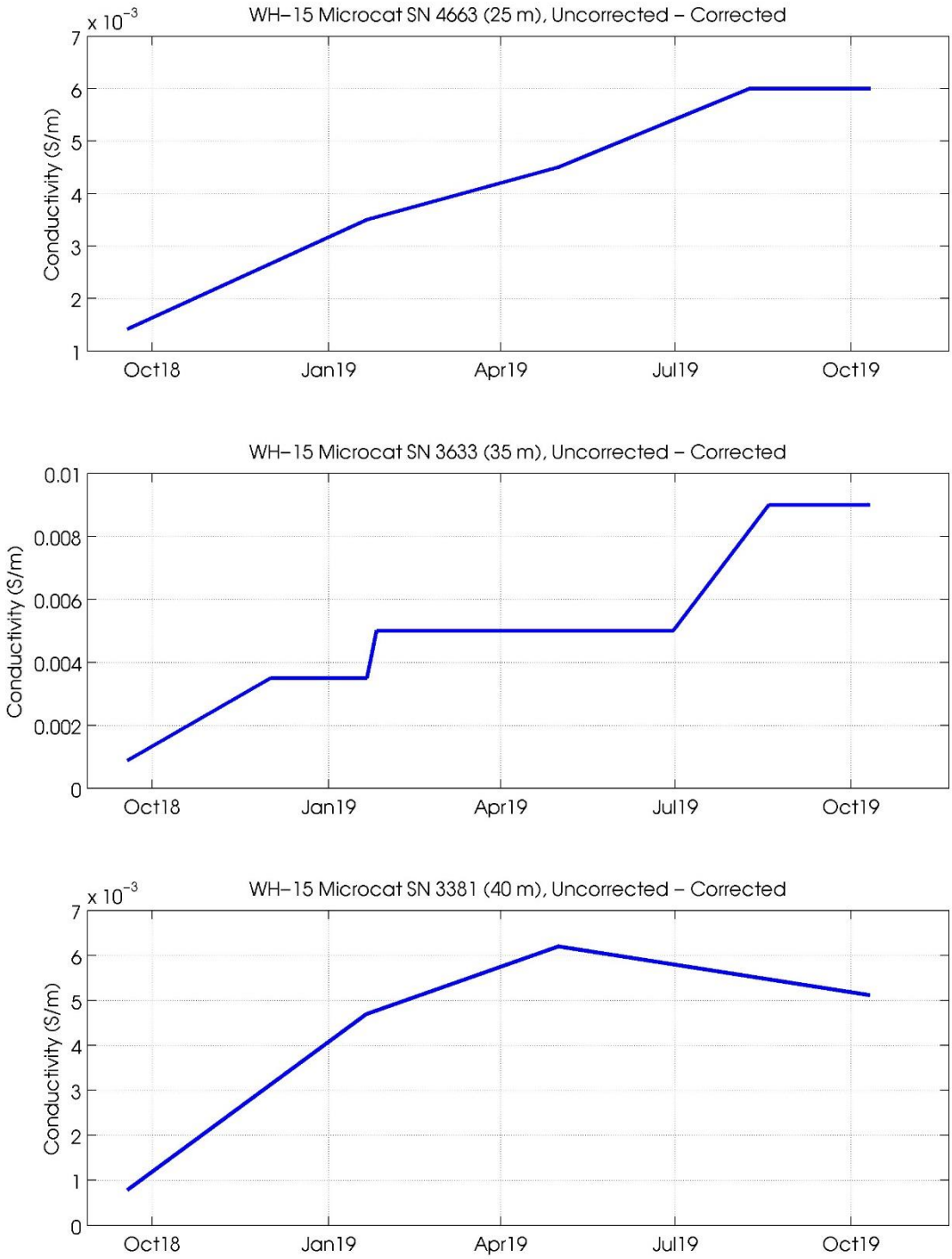

Figure V-9.Conductivity sensor corrections for MicroCATs from 25 to 40 meters during WHOTS-15

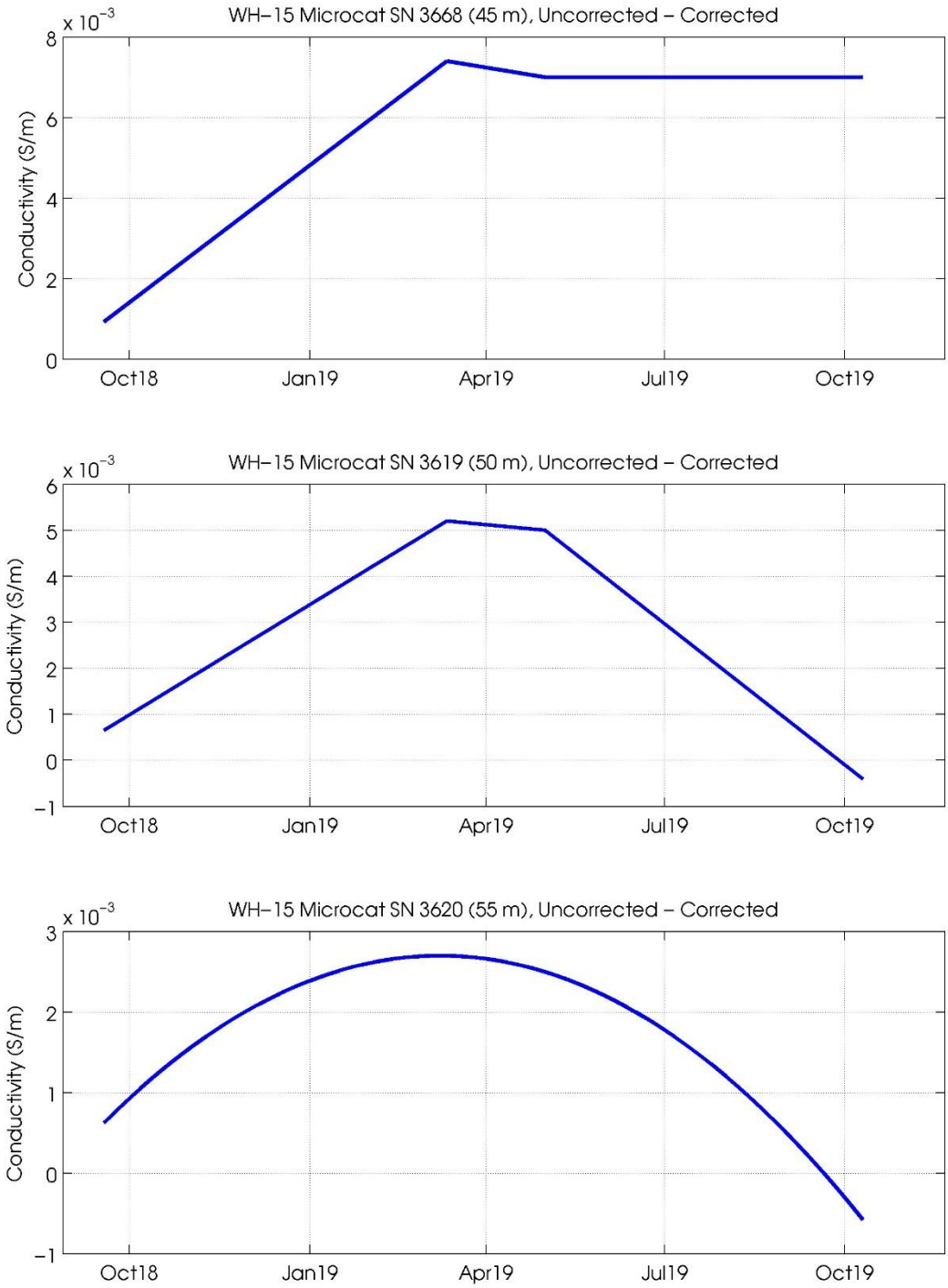

Figure V-10. Conductivity sensor corrections for MicroCATs from 45 to 55 meters during WHOTS-15

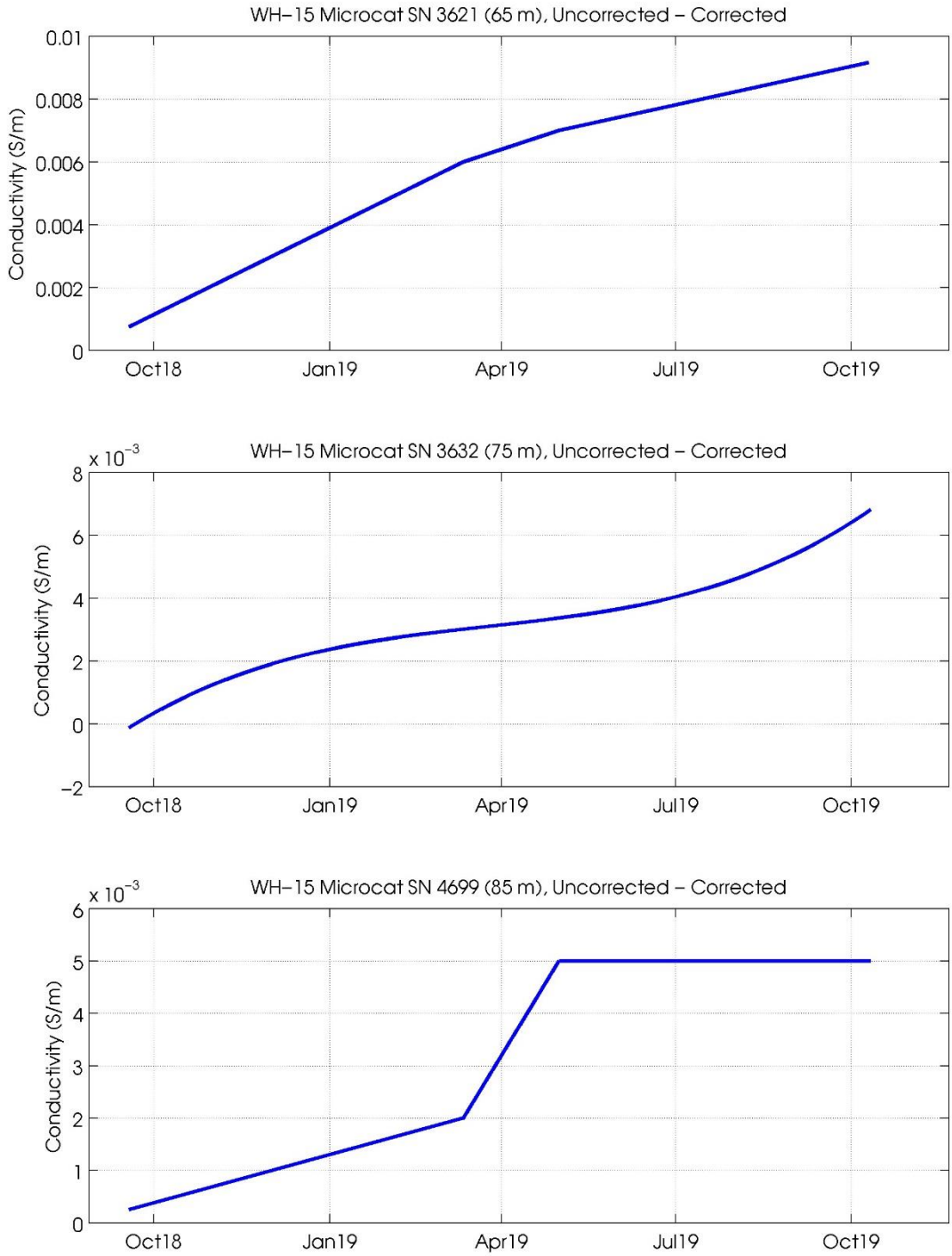

Figure V-11.Conductivity sensor corrections for MicroCATs from 65 to 85 meters during WHOTS-15.

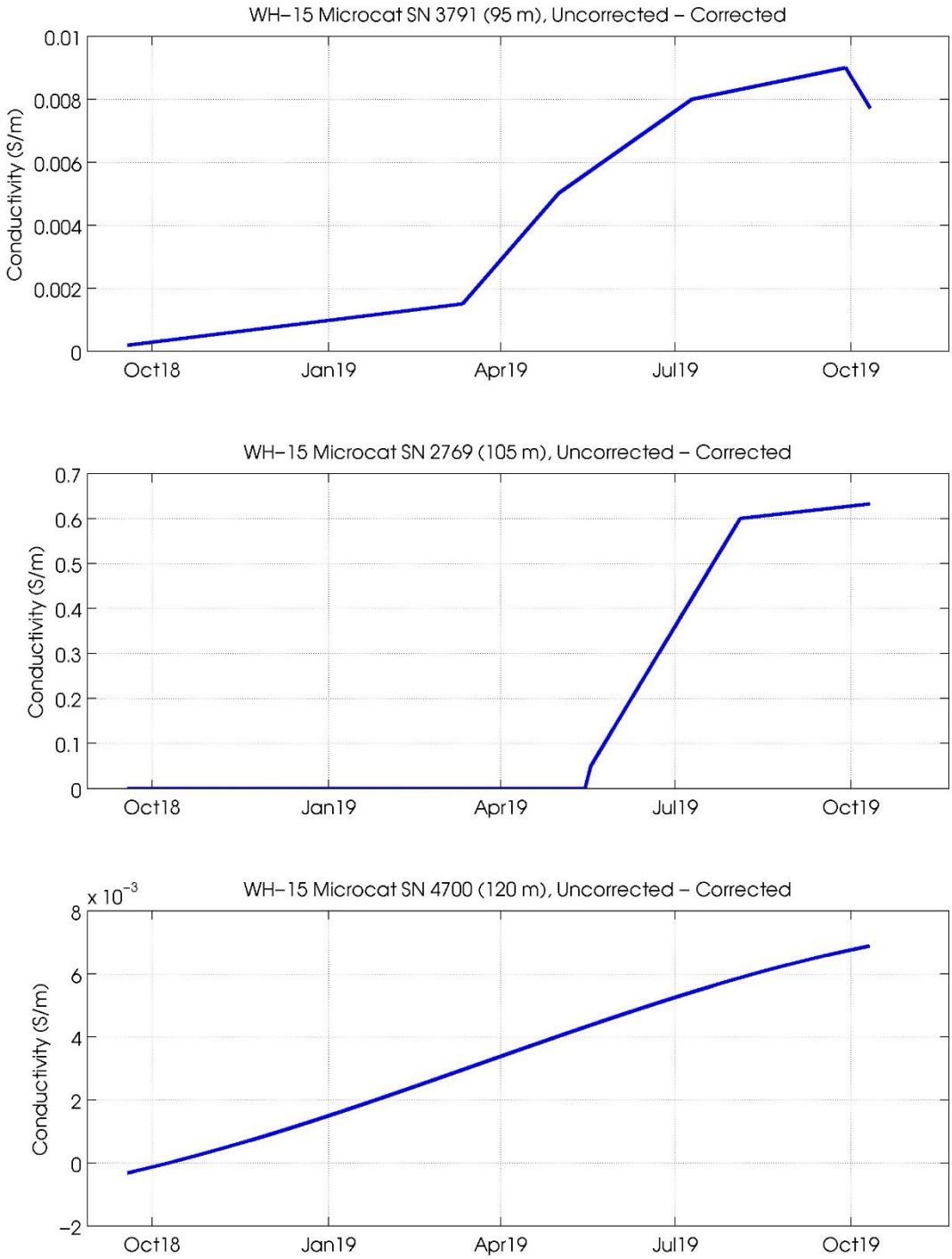

Figure V-12.Conductivity sensor corrections for MicroCATs from 95 to 120 meters during WHOTS-15.

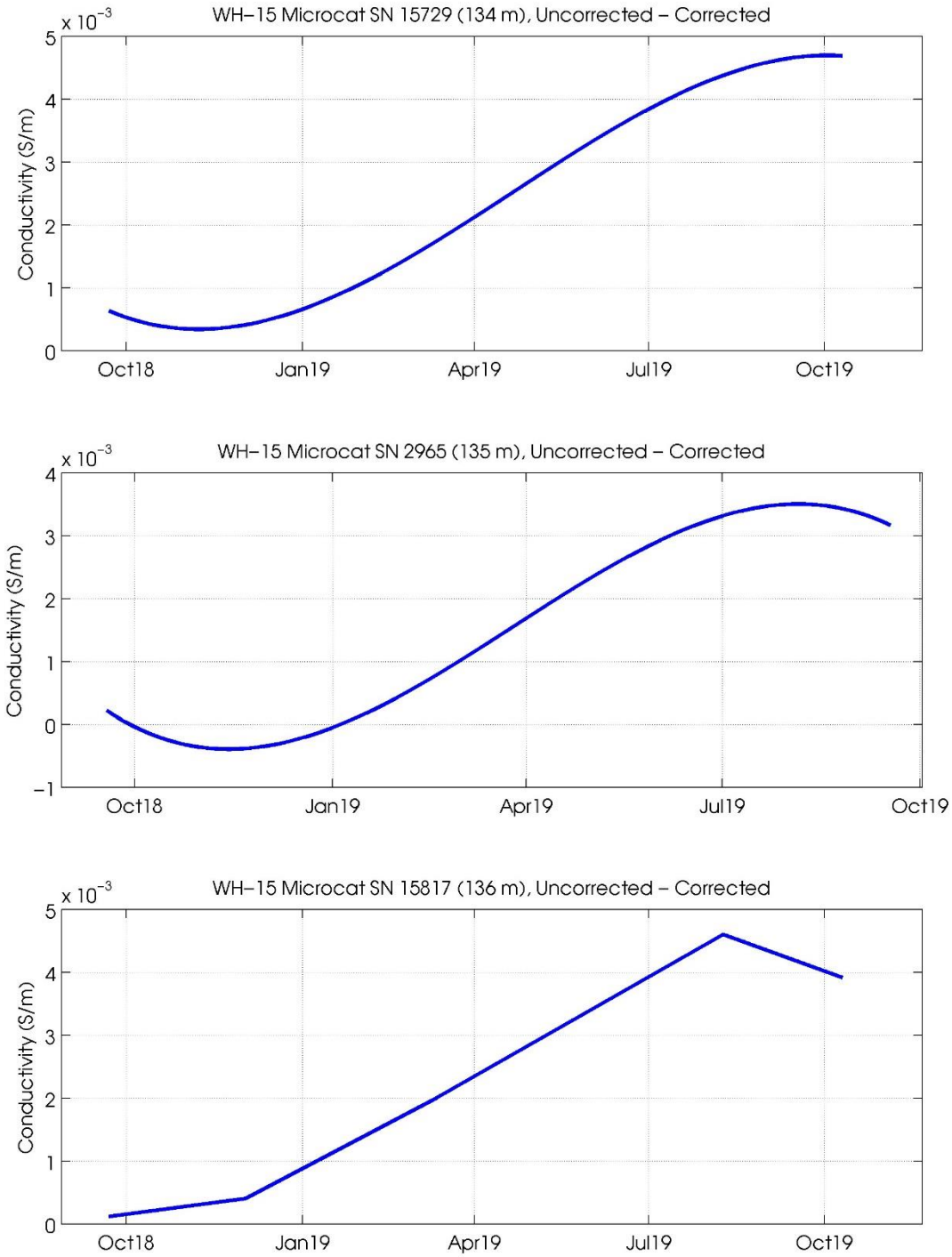

Figure V-13.Conductivity sensor corrections for MicroCATs from 134 to 136 meters during WHOTS-15

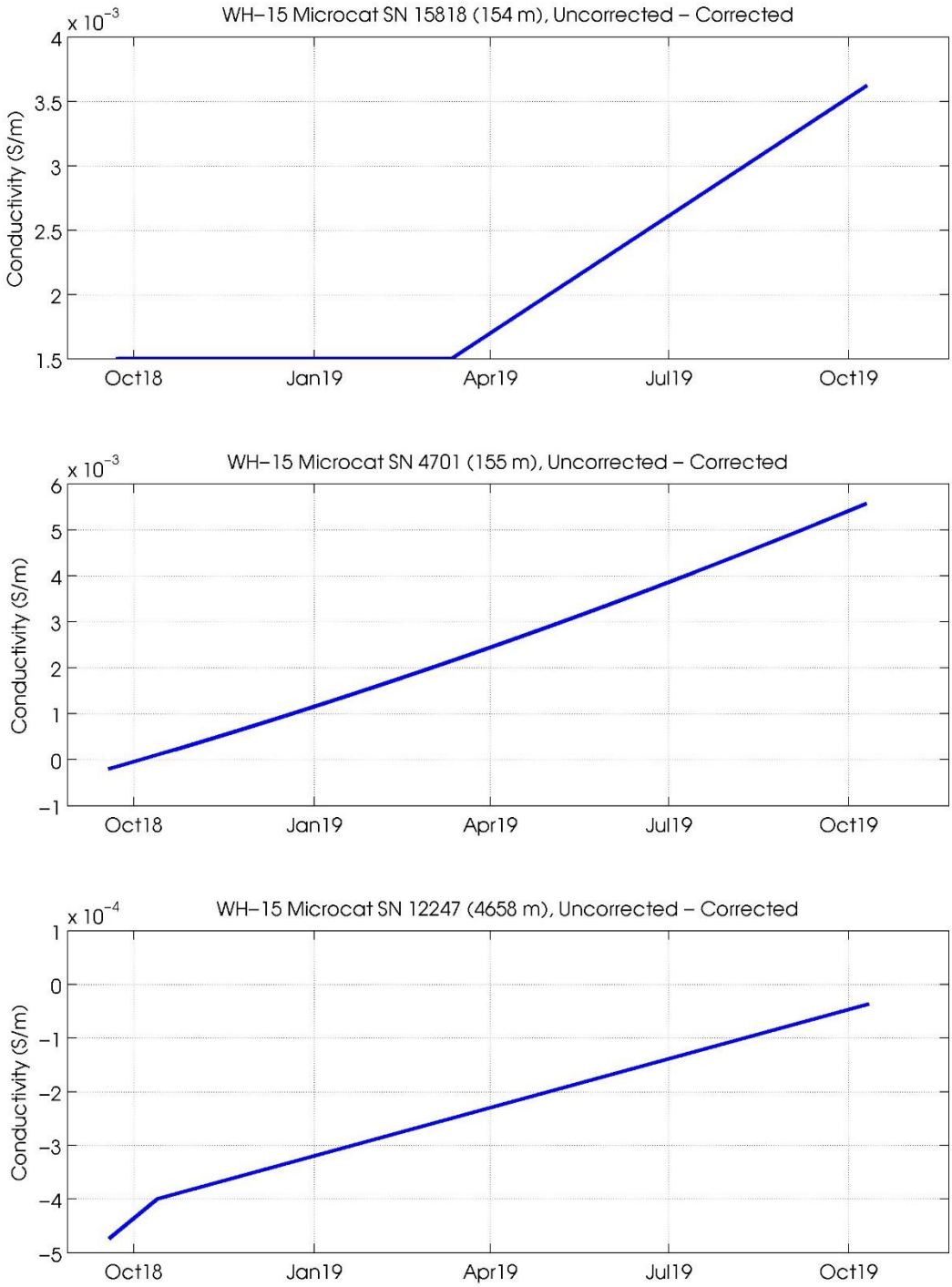

Figure V-14.Conductivity sensor corrections for MicroCATs at 154, 155 and 4658 meters during WHOTS-15.

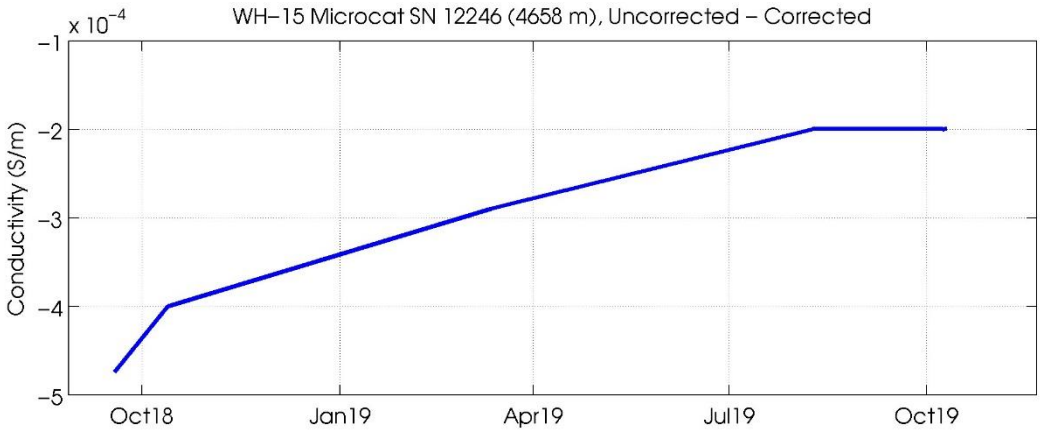

Figure V-15.Conductivity sensor correction for MicroCAT at 4658 meters during WHOTS-15

B. Acoustic Doppler Current Profiler

Two TRDI broadband Workhorse Sentinel ADCP's were deployed on the WHOTS-15 mooring. A 600 kHz ADCP was deployed at 47.5 m depth in the upward-looking configuration, and a 300 kHz ADCP was deployed at 125 m, also in the upward-looking configuration. The instruments were installed in aluminum frames and an external battery module to provide sufficient power for the intended period of deployment. The four ADCP beams were angled at 20° from the vertical line of the instrument. The 300 kHz ADCP was set to profile across 30 range cells of 4 m with the first bin centered at 6.22m from the transducer. The 600 kHz ADCP was set to profile across 25 range cells of 4 m with the first bin centered at 3.11m from the transducer. The specifications of the instrument are shown in Table V-3.

Table V-3. Specifications of the ADCP's used for the WHOTS-15 mooring.

Instrument	Description
ADCP	*TRDI Workhorse Sentinel, 300KHz* Model: WHS300-I-UG129; Serial Number: 7637 *TRDI Workhorse Sentinel, 600KHz* Model: WHS600-I; Serial Number: 13917

1. Compass Calibrations

Pre-Deployment

Before the WHOTS-15 deployment, field calibration of the internal ADCP compass was performed at the University of Hawaii's soccer field at Manoa on October 7th, 2018, for 300 kHz and the 600 kHz instruments. Each instrument was mounted in the deployment cage with the external battery module and was located away from potential sources of magnetic field disturbances. The ADCP was mounted to a turntable, aligned with the magnetic north using a surveyor's compass. Using the built-in RDI calibration procedure, the instrument was tilted in one direction between 10 and 20 degrees and then rotated through 360 degrees at less than 5 ° per second. The ADCP was then tilted in a different direction, and a second rotation was made. Based on the results from the first two rotations, calibration parameters are temporarily loaded, and the instrument, tilted in a third direction, is rotated once more to check the calibration. Results from each pre-deployment field calibration are shown in Table V-4 and Table V-5 (Figure V-16 and Figure V-17). Unfortunately, the results from the pre-deployment before calibration for the 600 kHz ADCP were not recorded.

Table V-4. Results from the WHOTS-15 pre-deployment 300 kHz ADCP compass field calibration procedure.

300 kHz (SN 7637)	Single Cycle Error (°)	Double Cycle Error (°)	Largest Double + Single Cycle Error (°)	RMS of 3rd Order and Higher + Random Error (°)	Overall Error (°)	Pitch Mean and Standard Deviation (°)	Roll Mean and Standard Deviation (°)
Before Calibration	4.87	0.41	5.28	0.17	4.94	0.09 ± 0.59	-1.40 ± 0.60
After Calibration	0.66	0.02	0.68	0.26	0.66	0.51 ± 0.60	16.97 ± 0.68

Table V-5. Results from the WHOTS-15 pre-deployment 600 kHz ADCP compass field calibration procedure.

600 kHz (SN 13917)	**Single Cycle Error (°)**	**Double Cycle Error (°)**	**Largest Double + Single Cycle Error (°)**	**RMS of 3rd Order and Higher + Random Error (°)**	**Overall Error (°)**	**Pitch Mean and Standard Deviation (°)**	**Roll Mean and Standard Deviation (°)**
Before Calibration	NaN	NaN	NaN	NaN	1.40	NaN	NaN
After Calibration	0.27	0.12	0.39	0.23	0.34	-0.09± 0.78	14.44 ± 0.42

Post-Deployment

After the WHOTS-15 mooring was recovered, the ADCP compass's performance was tested at the University of Hawai'i's soccer field at Manoa on October 29th, 2019, with an identical compass calibration procedure as during the pre-deployment calibration. Results from the WHOTS-15 post-deployment ADCP compass field calibration procedure are listed in Table V-6 and

Table V-7. (Figure V-16 and Figure V-17).

Table V-6. Results from the WHOTS-15 post-deployment 300kHz ADCP compass field calibration procedure.

300 kHz (SN 7637)	**Single Cycle Error (°)**	**Double Cycle Error (°)**	**Largest Double + Single Cycle Error (°)**	**RMS of 3rd Order and Higher + Random Error (°)**	**Overall Error (°)**	**Pitch Mean and Standard Deviation (°)**	**Roll Mean and Standard Deviation (°)**
After Calibration	1.01	0.42	1.42	0.12	1.24	2.44 ± 0.57	-0.45 ± 0.52

Table V-7. Results from the WHOTS-15 post-deployment 600kHz ADCP compass field calibration procedure.

600 kHz (SN 13917)	**Single Cycle Error (°)**	**Double Cycle Error (°)**	**Largest Double + Single Cycle Error (°)**	**RMS of 3rd Order and Higher + Random Error (°)**	**Overall Error (°)**	**Pitch Mean and Standard Deviation (°)**	**Roll Mean and Standard Deviation (°)**
After Calibration	2.86	0.24	3.10	0.28	2.90	-0.24 ± 0.43	2.37 ± 0.53

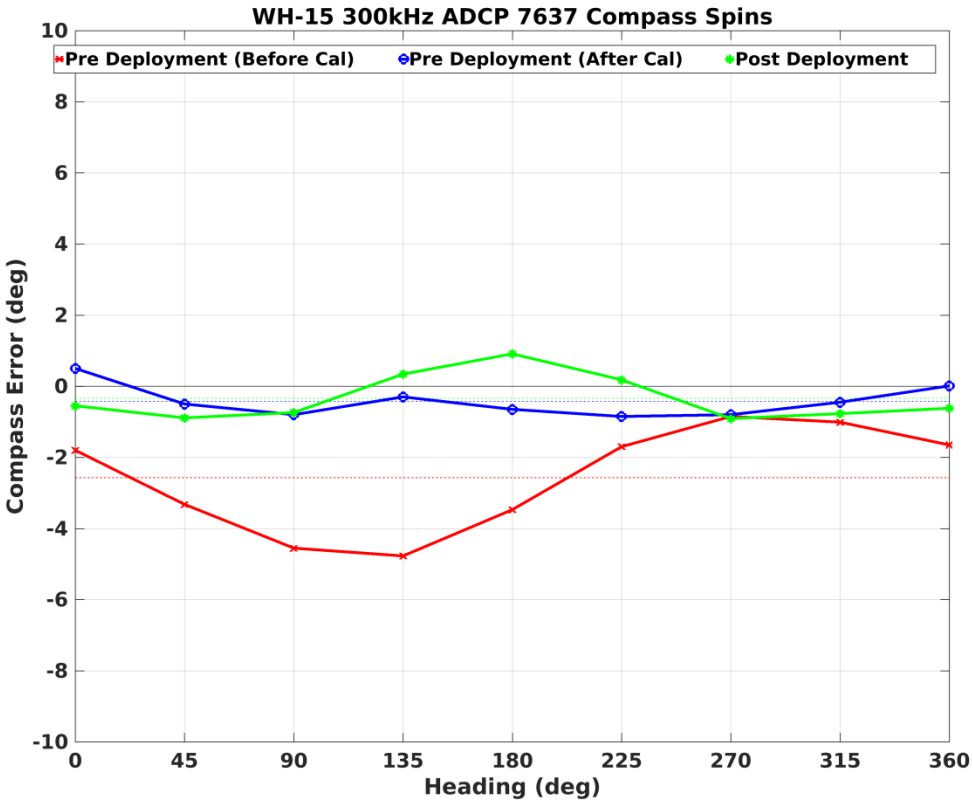

Figure V-16.Results of the post-cruise compass calibration, conducted October 29th, 2019, on ADCP SN 7637 at the University of Hawai'i at Manoa.

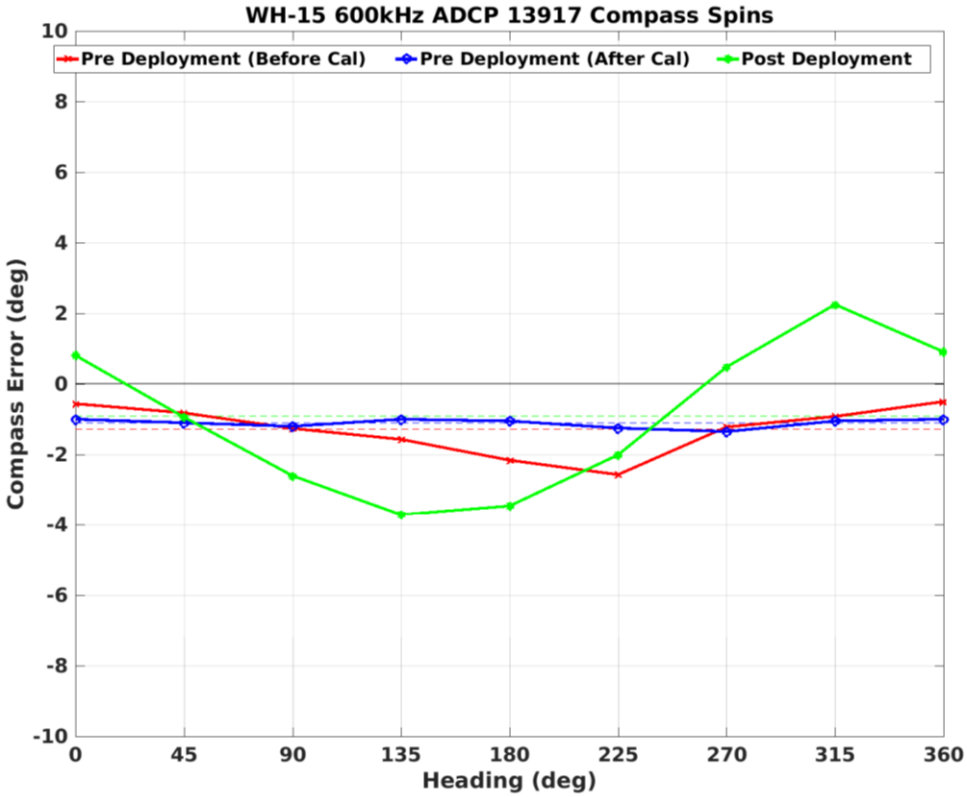

Figure V-17.Results of the post-cruise compass calibration, conducted October 29th, 2019, on ADCP SN 13917 at the University of Hawai'i at Manoa.

2. ADCP Configurations

Individual configurations for the two ADCP's on the WHOTS-15 mooring are detailed in Section VIII.A, and Section VIII.B. The salient differences for each of the ADCP's are summarized below.

300 kHz (SN/7637 - 125m)

The ADCP, set to a beam frequency of 300 kHz, was configured in a burst sampling mode consisting of 40 pings per ensemble to resolve low-frequency wave orbital motions. The interval between each ping was 4 seconds, so the ensemble length was 160 seconds. The interval between ensembles was 10 minutes. Data were recorded in earth coordinates, with a heading bias of 9.34° E due to magnetic declination. False targets, usually fish, were screened by setting the threshold maximum to 70 counts. Velocity data were rejected if the difference in echo intensity among the four beams exceeded this threshold.

600 kHz (SN/13917 - 47.5m)

The ADCP, set to a beam frequency of 600 kHz, was configured in a burst sampling mode consisting of 80 pings per ensemble. The interval between each ping was 2 seconds, so the ensemble length was also 160 seconds. The interval between ensembles was 10 minutes. Data were recorded in earth coordinates with a heading bias of 9.34° E. The threshold maximum was also set to 70 counts. Velocity data were rejected if the difference in echo intensity among the four beams exceeded this threshold.

3. ADCP data processing procedures

Binary files output from the ADCP were read and converted to MATLAB™ binary files using scripts developed by Eric Firing's ADCP lab (http://current.soest.hawaii.edu). The beginning of the raw data files was truncated to a time after the mooring anchor was released to allow time for the anchor to reach the seabed and for the mooring motions that follow the anchor's impact on the seafloor to dissipate. The pitch, roll, and ADCP temperature were examined to pick reasonable times that ensured good data quality without unnecessarily discarding too much data (Figure V-18, Figure V-19). Truncation at the end of the data files was chosen to be the ensemble before the acoustic release signal was sent to avoid contamination due to the instrument's ascent. The times of the first ensemble from the raw data, deployments, and recovery time, along with the truncated records of both deployments, are shown in Table V-8.

Table V-8. ADCP record times (UTC) during WHOTS-15 deployment

Activities		300 kHz	600 kHz
Raw file	Beginning	09/22/18, 00:00:00	09/22/18, 00:00:00
	End	10/10/2019 03:49:59	11/02/18 13:39:59
Deployment and Recovery	In water	09/22/18, 19:57:00	09/22/18, 19:45:00
	Anchor over	9/23/2018 01:17	9/23/2018 01:17
	Release fired	10/8/2019 17:00	10/8/2019 17:00
	on deck	10/9/19 17:15	10/9/19 17:30

ADCP Clock Drift

Upon recovery, a spike was produced in the ADCP data by gently rubbing each instrument's transducer by hand for 20 seconds (see Table III-5) to compare the ADCP clocks with the ship's time server. It was found that for 300 kHz (SN 7637) ADCP, the instrument's clock was slow by less than 3 minutes. The clock on the 600 kHz ADCP could not be evaluated because the instrument stopped working before recovery. Past deployments of the ADCP's suggest a 3-minute difference is not unusual. Since the drift represents just one ensemble out of over 58,000, no corrections were made. However, this drift may be significant if the data are used for time-dependent analysis, such as tidal or spectrum analysis. A drift correction needs to be applied in those cases.

Heading Bias

As mentioned in the ADCP configuration section, the data were recorded in the earth coordinates. A heading bias, the angle between magnetic north and true north, can be included in the setup to obtain output data in true-earth coordinates. Magnetic variation was obtained from the National Geophysical Data Center 'Geomag' calculator. (https://www.ngdc.noaa.gov/geomag/calculators/magcalc.shtml#declination). A constant value is acceptable for a yearlong deployment because the change in declination is small, approximately -0.02° year^{-1} at the WHOTS location. A heading bias of 9.34° was entered in the setup of the WHOTS-15 ADCP's.

Speed of sound

Due to the constant proportionality between the Doppler shift and water speed, the speed of sound needs only be measured at the transducer head (Firing, 1991). The sound speed used by the ADCP is calculated using a constant value of salinity (35) and the temperature recorded by the transducer temperature sensor of the ADCP. Using CTD profiles close to the mooring during HOT cruises, HOT-306:315, except for HOT-308, and from the WHOTS deployment/recovery cruises, the mean salinity at 125 dbar was 35.06 while the mean salinity at 47.5 dbar was 34.92. The mean ADCP temperature at 125 dbar was 21.10°C and 25.64°C at 47.5 dbar Figure V-18 through Figure V-20). The maximum associated mean sound speed variability at 47.5 and 125 dbar is about 10 m s^{-1} and 8 m s$^{-1,}$ respectively.

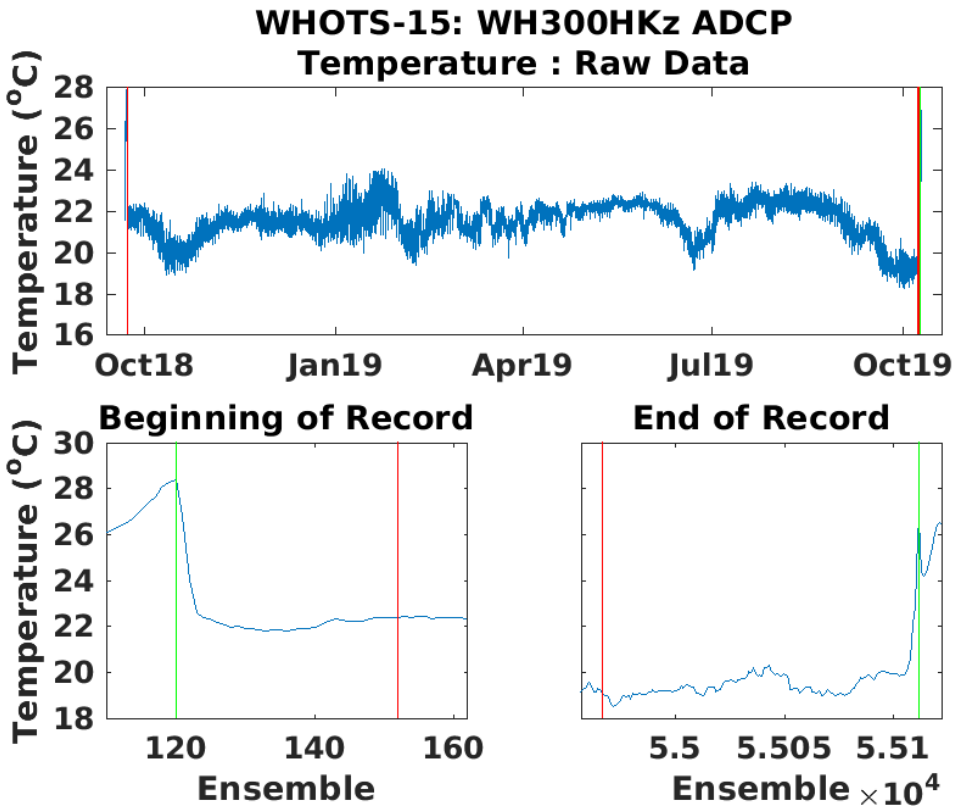

Figure V-18. Temperature record from the 300 kHz ADCP during WHOTS-15 mooring (top panel). The bottom panel shows the beginning and end of the record, with the green vertical line representing the in-water time during deployment and out-of-water recovery time. The red line represents the anchor release and acoustic release trigger for deployment and recovery, respectively.

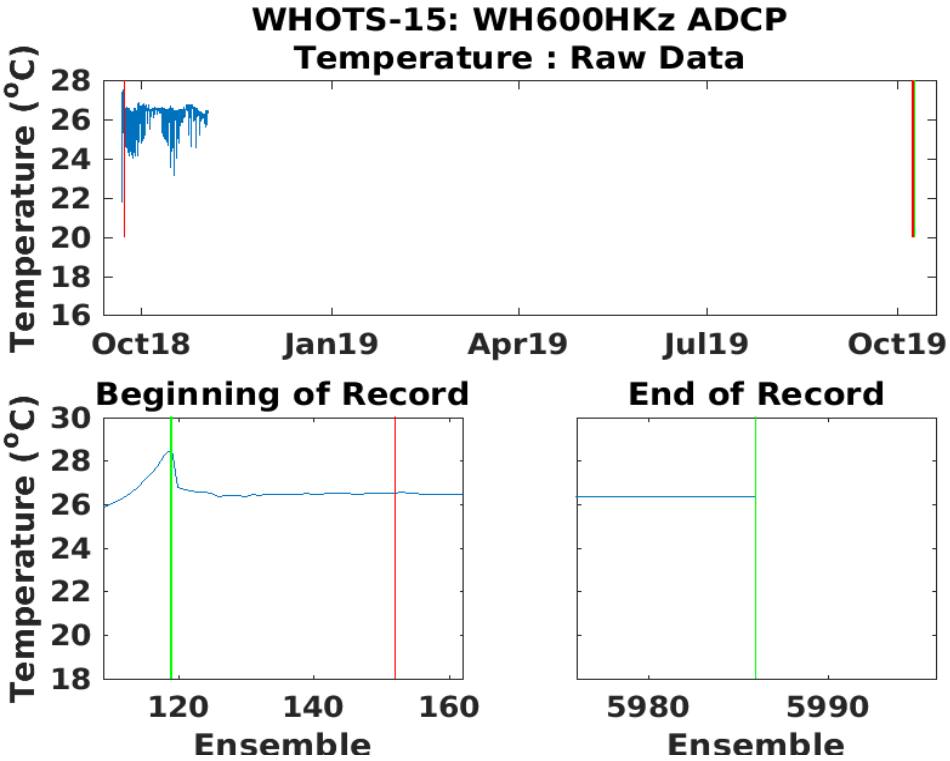

Figure V-19. Same as Figure V-18, but for the 600 kHz ADCP.

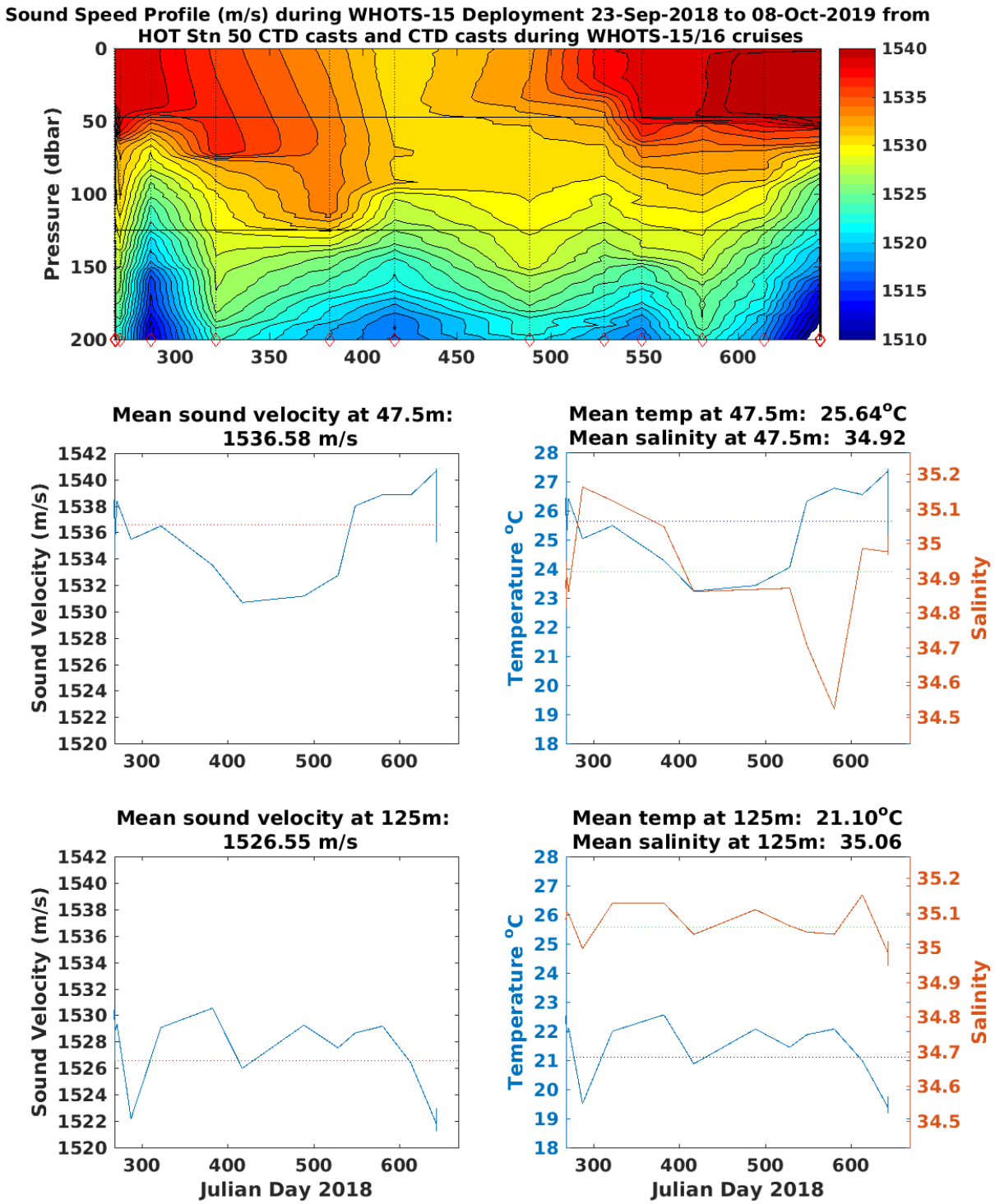

Figure V-20. Sound speed profile (top panel) during the deployment of the WHOTS-15 mooring from 2 dbar CTD data taken during regular HOT cruises and CTD profiles taken during the WHOTS-15 and -16 deployment cruises (individual casts marked with a red diamond). The bottom left panels show the sound velocity at a depth of the ADCP's (47.5 m and 125 m), with the mean sound velocity indicated with a red line. The lower right panels show the temperature and salinity at each ADCP depth for the time series, with the mean temperatures indicated with blue lines and mean salinity indicated with green lines.

Quality Control

Quality control of the ADCP data involved the thorough examination of the velocity, instrument orientation, and diagnostic fields to develop the basis of the QC flagging procedures. Details of the methods used can be found in the WHOTS Data Report 1 (Santiago-Mandujano *et al.*, 2007). The following QC procedures were applied to the WHOTS-15 deployment of ADCP data.

1) The first bin (closest to the transducer) is sometimes corrupted due to what is known as ringing. A period of time is needed for the sound energy produced during a transducer's transmit pulse to dissipate before the ADCP can adequately receive the returned echoes. This "blanking interval" is used to prevent useless data from being recorded. If it is too short, signal returns can be contaminated by the lingering noise from the transducer. The blanking interval is expressed as a distance. The default value of 1.76 m was used for the 300 kHz ADCP, whereas an interval of 0.88 m was used for the 600 kHz ADCP. As a result, bin one was flagged and replaced with Not a Number (NaN) in the quality-controlled dataset (Figure V-21).

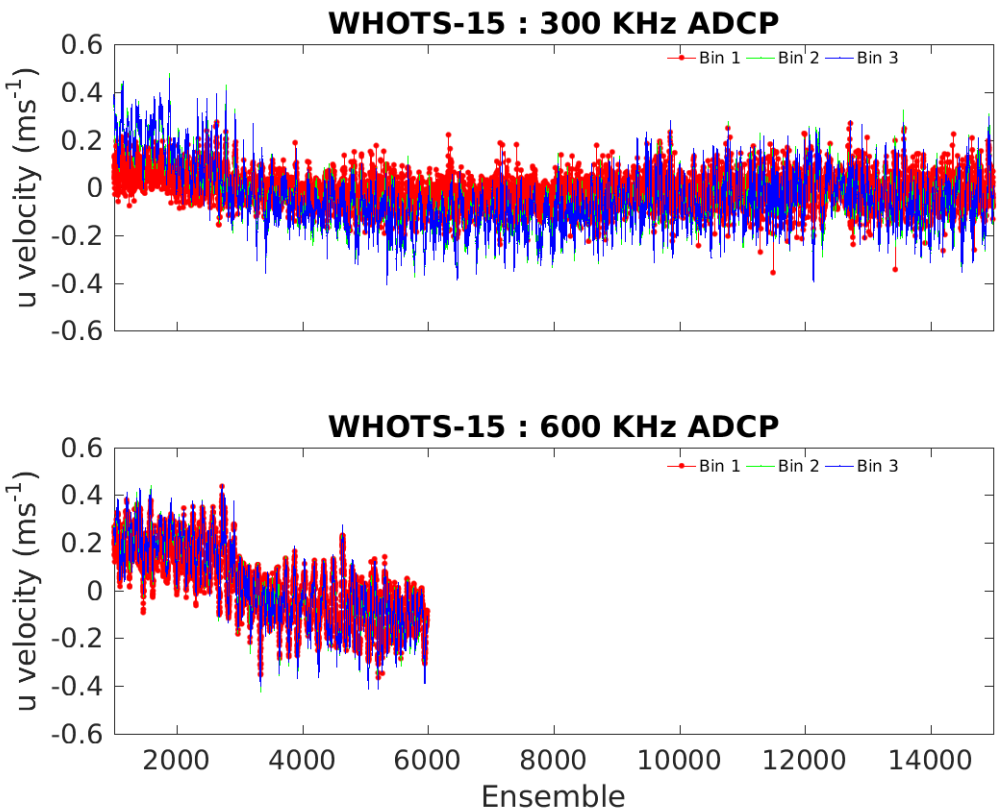

Figure V-21. Eastward velocity component for the 300 kHz (top panel) and the 600 kHz (bottom panel) ADCPs are showing the incoherence between depth bins 1 (red), 2 (green), and 3 (blue).

2) For an upward-looking ADCP with a beam angle of 20° within range of the sea surface, the upper 6% of the depth range is contaminated with sidelobe interference (Teledyne RD Instruments, 2011). This contamination results from the much stronger signal reflection from the sea surface than from scatters, overwhelming the sidelobe suppression of the

transducer. Data quality is quantified using echo intensity, a measure of the backscattered echo's strength for each depth cell. With distance from the transducer sensor, echo intensity is expected to decrease. Sharp increases in echo intensity indicate contamination from surface reflection. Most of the data within the upper four bins (~14% of the vertical range) were flagged. These top four bins range from about 15 m up to the sea surface.

3) The Janus configuration of four beams (along with instrument orientation) is used to resolve currents into their component earth-referenced velocities, providing a second estimate of the vertical velocity. The scaled difference between these estimates is defined as the error velocity, and it is useful for assessing data quality. Error velocities with an absolute magnitude more significant than 0.15 m s^{-1} (value comparable to the standard deviation of observed horizontal velocities) were flagged and removed.

4) An indication of data quality for each ensemble is given by the "percent good" data indicator, which accompanies each beam for each bin. The use of the percent good indicator is determined by the coordinate transformation mode used during the data collection. For profiles transformed into earth coordinates, the percent good field shows the percentage of pings that could be used to create the earth coordinate velocities. The percent good fields show the percentage of data made using 4 and 3 beam solutions in each depth cell within an ensemble and the percentage that was rejected due to failing one of the criteria set during the instrument setup (see Appendix 1: WHOTS-15 300 kHz). Data were flagged when data in each depth cell within an ensemble made from 3 or 4 beam solutions was 20% or less.

5) Data were rejected using correlation magnitude, which is the pulse-to-pulse correlation (in ping returns) for each depth cell. Correlation magnitude represents how the shape of the received signal corresponds to the outgoing signal for each ping. If at least three of the beams exhibited a correlation magnitude more significant than 64 counts for a given bin, the profile could be transformed into earth coordinates. Low correlation magnitudes may indicate sudden changes in particle density or sudden changes in ADCP tilt. More research is needed at this time into relationships between ADCP tilt and correlation magnitude. If any beam had a correlation magnitude of 20 counts or less, that data point was flagged.

6) Histograms of raw vertical velocity data and partially cleaned data from the ADCP [see Figure V-22 and Figure V-23] and the WHOTS Data Report 1 (Santiago-Mandujano *et al.*, 2007) showed vertical velocities larger than expected, some exceeding 1 m s^{-1}. Recall that the instruments' burst sampling (4-second intervals for the 300 kHz and 2-second intervals for the 600 kHz, for 160 seconds every 10 minutes) was designed to minimize aliasing by occasional large ocean swell orbital motions (Section III), and therefore are not the source of these speeds in the data. These significant vertical speeds are possibly fish swimming in the beams based on the histograms of the partially cleaned data; depth cells with an absolute value of vertical velocity greater than 0.3 m s^{-1} were flagged.

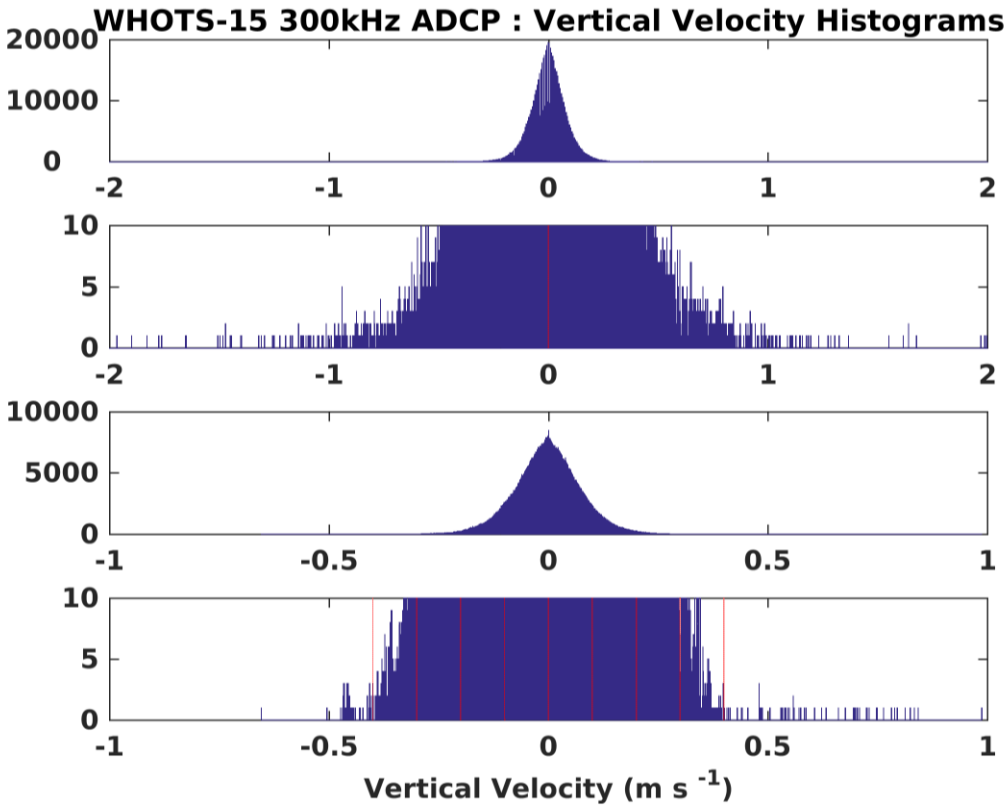

Figure V-22. Histogram of the vertical velocity of the 300 kHz ADCP for raw data (top panel) and enlarged for clarity (upper middle panel), and partial quality controlled data (lower middle panel) and enlarged for clarity (bottom).

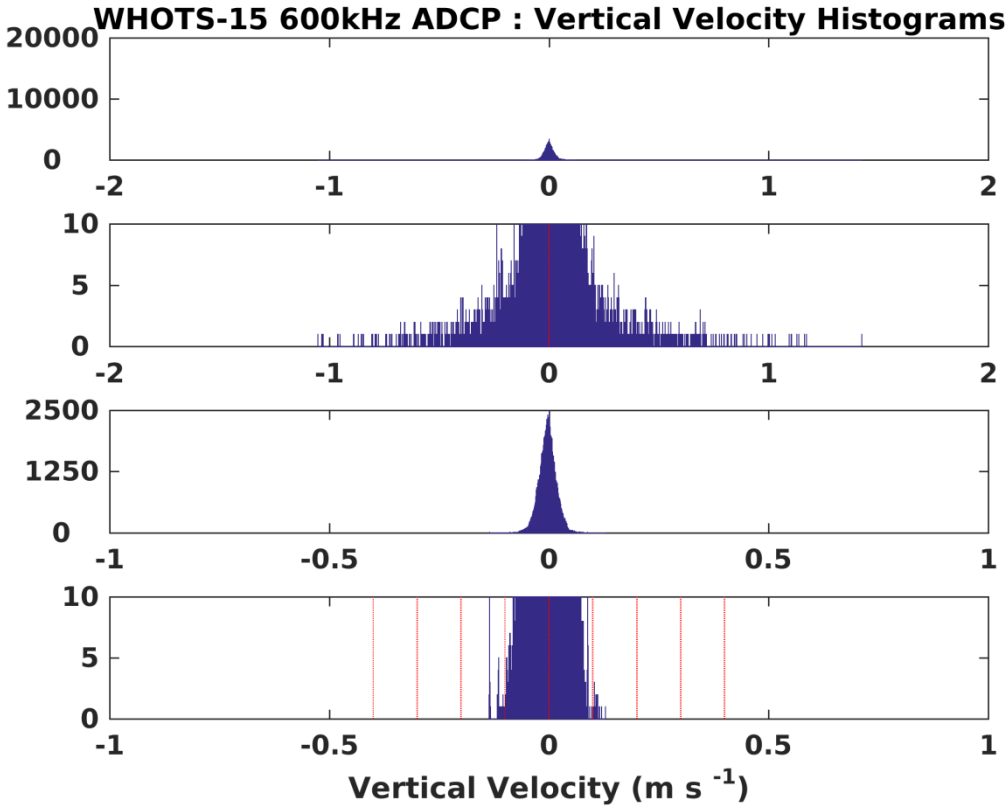

Figure V-23.Same as Figure V-22, but for 600kHz ADCP.

7) A quality control routine known as ‘edgers’ identifies outliers in surface bins using a five-point median differencing method. The median velocity from surface bins was calculated for each ensemble, and then a five-point running median of the surface bin median was calculated. This last median was then compared to individual velocity observations in the surface bins, and those differing by greater than 0.48 m/s were flagged.

8) A 5-pole low pass Butterworth filter with a cutoff frequency of 1/4 cycles/hour was used upon the time-series' length to isolate low-frequency flow for each bin independently. The low-frequency flow is then subtracted, giving a time series of high-frequency velocity component fluctuations for each bin. Data points were considered outliers when their values exceeded four standard deviations from the mean (for each bin) and were removed.

9) A median residual filter used a 7-point (70 minutes) median differencing method to define velocity fluctuations. A 7-point running median is calculated for each bin independently, and the result is subtracted out, giving time series of variations relative to the running median. Outliers higher than four standard deviations from the mean of the 7 points are flagged and removed for each bin.

10) Meticulous verification of all the quality control routines was performed through visual inspections of the quality-controlled velocity data. Two methods were utilized; time-series of u and v components for multiple bins were evaluated, and individual vertical profiles. The time-series methodology involved inspecting u and v components separately, five bins at a time, over 600 ensembles (100 hours). Any instance showing one bin behaving erratically from the other four bins was investigated further. If it seemed that there could be no reasonable rationale for the erratic points from the identified bin, the points were flagged. The intent of the inspection of vertical profiles of u and v components was to find entire profiles that were not aligned with neighboring profiles. Thirty u and v profiles were stacked at a time and were visually inspected for any anomalous data.

C. Vector Measuring Current Meter (VMCM)

Vector measuring current meters (VMCM) were deployed on the WHOTS-15 mooring at depths of 10 m and 30 m, serial numbers SN 009 andc010, respectively. VMCM data were processed by the WHOI/UOP group, and the record times are shown in Table V-9

Table V-9.Record times (UTC) for the VMCMs at 10 m and 30 m during the WHOTS-15 deployment

	WHOTS-15	
	VMCM009	**VMM010**
Deployment and recovery times	22-Sept-2018 19:10 9-Oct-2019 19:01	22-Sept-2018 18:52 9-Oct-2019 19:24

Daily (24 hours) moving averages of quality controlled 600 kHz ADCP data are compared to VMCM data interpolated to the ADCP ensemble times in the top panels of Figure V-24 through Figure V-27, and the difference is shown in the middle panels. The absolute value of the mean difference plus or minus one standard deviation is shown at the top of the middle panel. Velocities are not compared if greater than 80% of the ADCP data within a 24-hour average was flagged. The absolute value of mean differences for all deployments and both velocity components varied between 3 and 4 cm/s, with standard deviations between 2.2 and 3.5 cm/s. The VMCM data does not appear to degrade over time for any deployment. Propeller fouling would dampen measured VMCM velocity magnitudes, but a decrease in VMCM velocity magnitude than ADCP velocity magnitude with time is not observed.

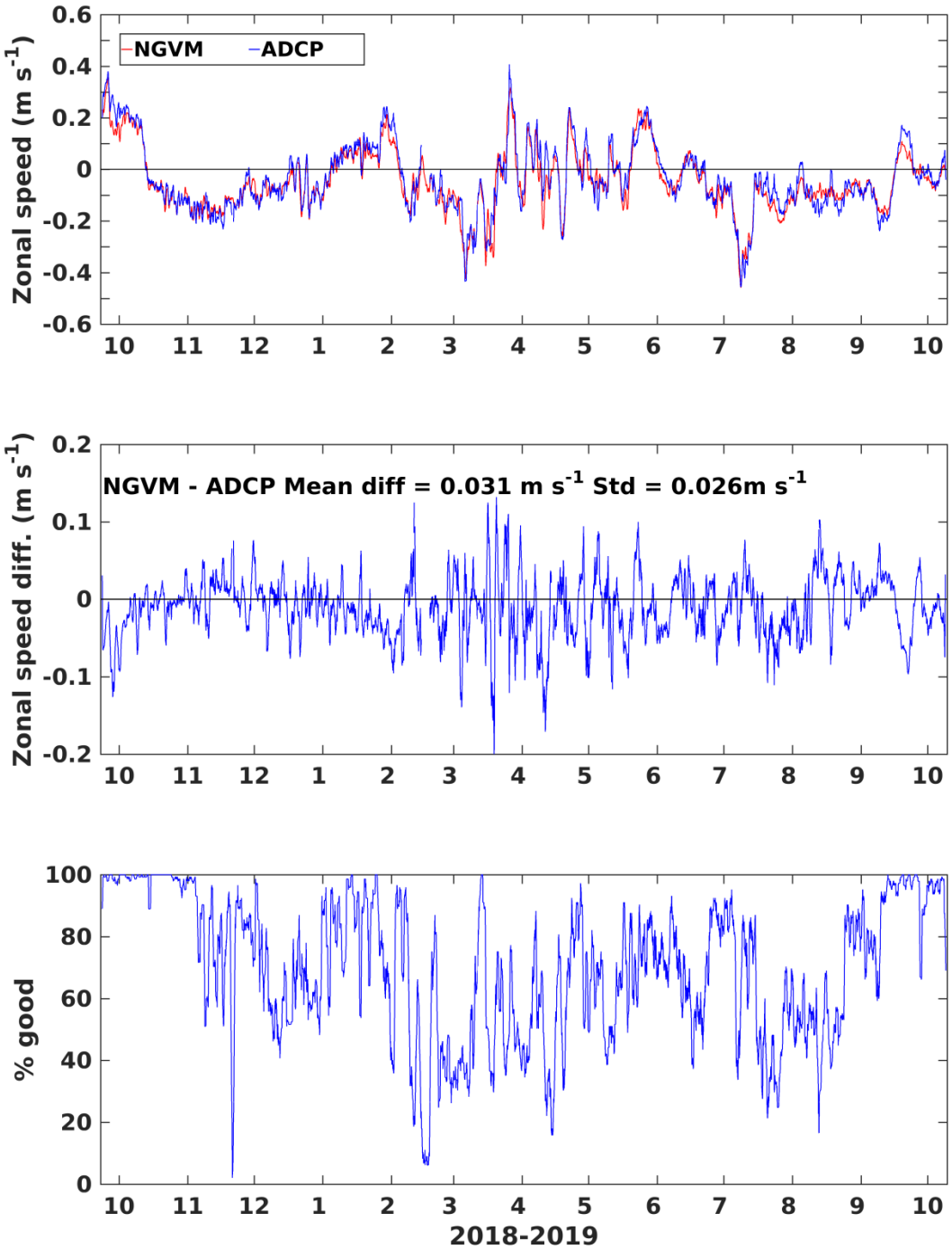

Figure V-24. A comparison of 30 m VMCM and ADCP U velocity for WHOTS-15. The top panel shows 24-hour moving averages of VMCM zonal (U) velocity at 30 m depth (red) and ADCP U velocity from the nearest depth bin to 30 m (30.22 m). The middle panel shows the U velocity difference, and the bottom panel shows the percentage of ADCP data within the moving average not flagged by quality control methods.

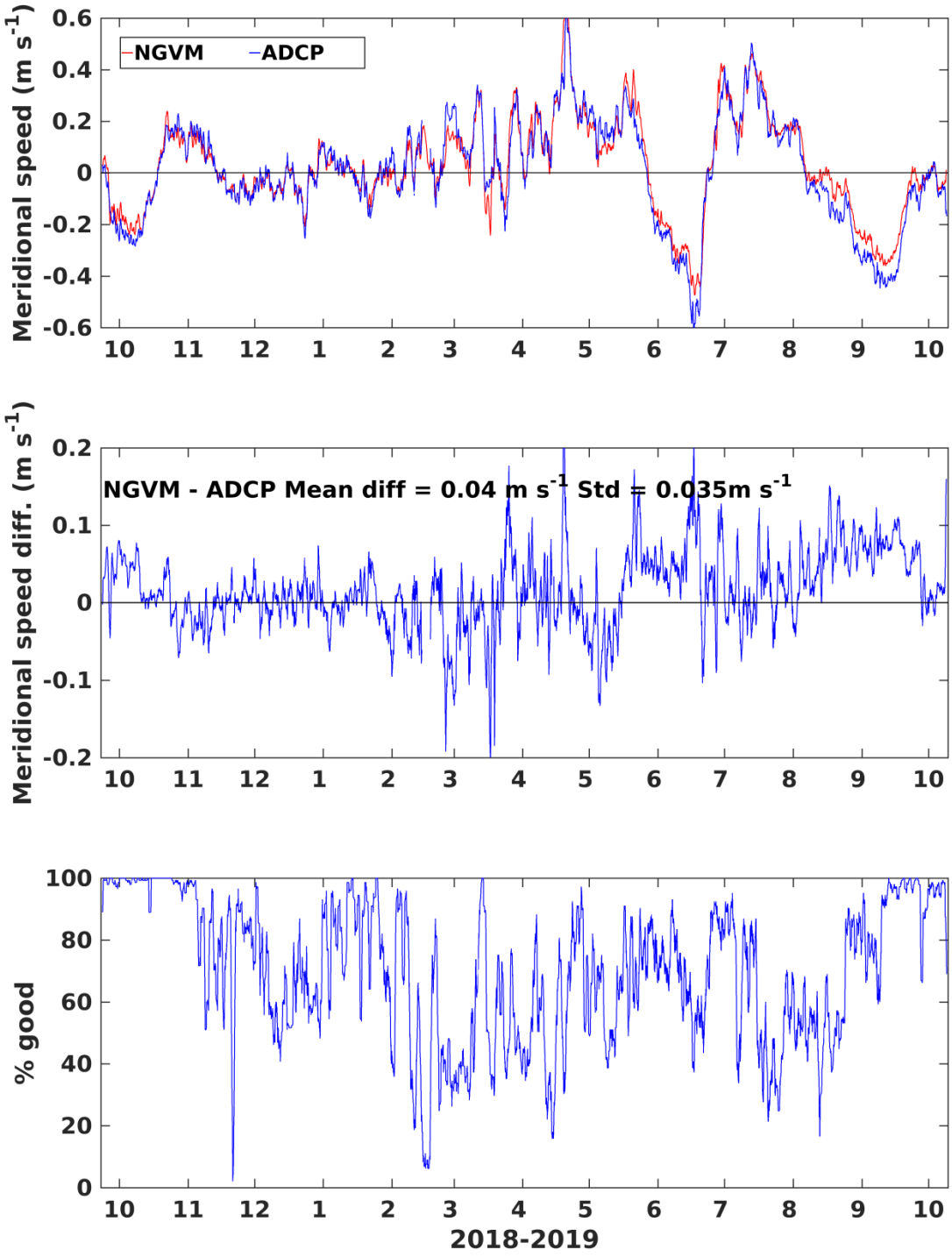

Figure V-25. Same as in Figure V-24 but for the meridional (V) velocity component.

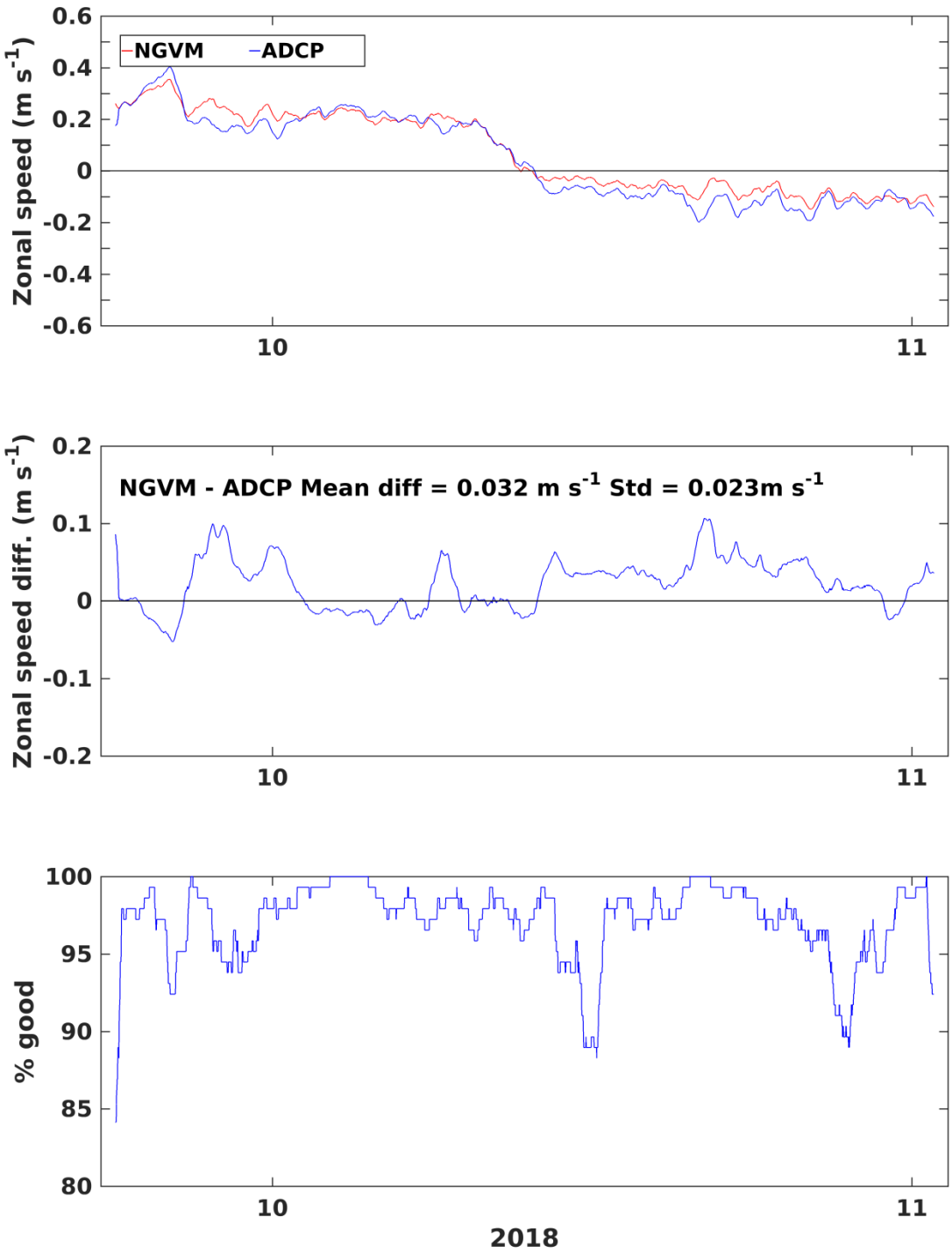

Figure V-26. Same as in Figure V-24 but for the 10 m VMCM.

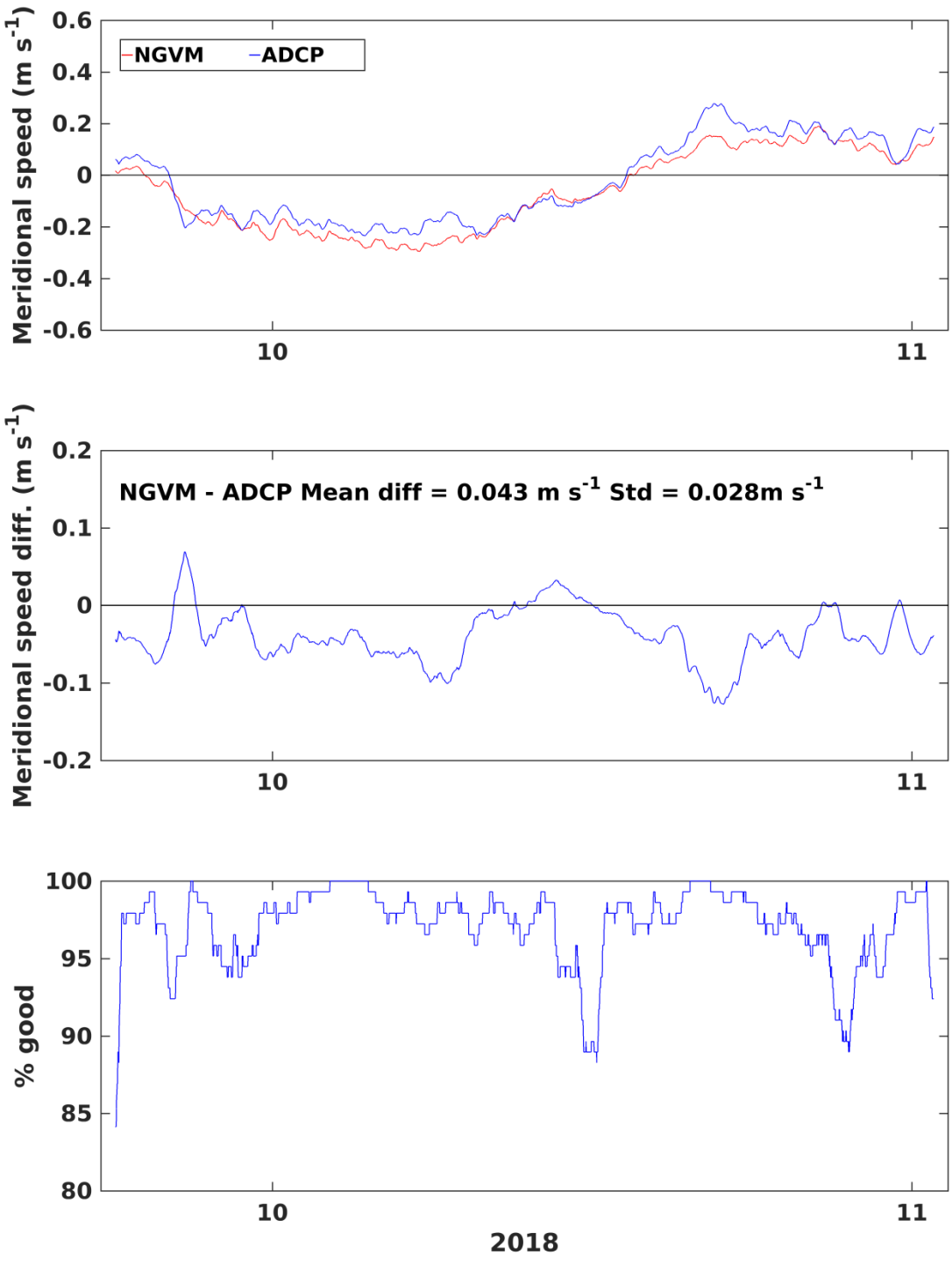

Figure V-27. Same as Figure V-26, but for the meridional (V) velocity component.

D. Global Positioning System Receiver

Xeos Global Positioning System receiver (GPS) was attached to the buoy's tower top during the WHOTS-15 deployment (see Section III). Data returns from the receiver were high (Table V-10). There was no ARGOS receiver for WHOTS-15.

Table V-10. GPS record times (UTC) during WHOTS-15

WHOTS-15	Xeos GPS
Raw file beginning and end times	15-Sept-2018 21:37 14-Oct-2019 18:00

VI. Results

During the WHOTS-15 cruise (WHOTS-15 mooring deployment, September 21-29, 2018), weather conditions on September 22-23 were favorable, with light east-southeast winds of about 5 kt increasing to up to 16 kt by the end of the deployment, and 1.5m waves from the east, with a strong surface current toward the east-northeast.

CTD casts conducted near the mooring site (Station 50 – Near the WHOTS-15 buoy) after the deployment (Figure VI-1 through Figure VI-4) displayed a subsurface salinity maximum at 150 dbar and a mixed layer nearly 50 m deep. Near-surface currents were about 1 kt North-eastward during transit to Station ALOHA, turning Northward and Eastward upon arrival to Station ALOHA, and remained so for approximately five days. There was a nearly stationary cyclonic eddy east of ALOHA, suggesting a possible increasing geostrophic flow towards the East, North-East. A combination of internal semidiurnal and diurnal tides and near-inertial oscillations was noticeable, especially in vertical shear.

During the WHOTS-16 cruise (WHOTS-15 mooring recovery, October 4-12, 2019), a weakening front north of the Hawaiian Islands acted to weaken trades across the region. This ridge to the north was eroding due to a weakening cold front north of the ridge, which led to a downward trend in winds. The front continued to weaken and sink southward through the weekend, keeping the winds light and variable. Regular trades returned by mid-week. There was no measurable precipitation during the deployment or recovery times of the WHOTS-16 and -15 moorings, respectively. On Thursday, October 10^{th,} winds in the morning increased to 25 kt gusting to 35 kt, and there was a brief rain event in the morning. Distant lightning caused a short delay (30 minutes) to the first CTD yo-yo cast. Waves during the week were also low, with a small swell from the north arriving mid-week.

Conditions during the WHOTS-16 deployment on October 5th were favorable, with light NNE winds of ~ 5 kt increasing to up to 10 kt by the end of the deployment. There were clear skies and no precipitation in the region, and 1.0 to 1.5 m waves from the east, with a strong surface current towards ENE.

CTD casts conducted near the mooring site (Station 50) before the recovery (Figure VI-7 through Figure VI-9)displayed a subsurface salinity maximum at 70 dbar and a mixed layer nearly 60 dbar deep. Near-surface currents were almost 1 kt northward during transit to Station ALOHA, turning southward upon arrival to Station ALOHA. Eventually, the current shifted due north again, became somewhat weaker (about 0.5 kt), and remained for approximately five days.

There was a nearly low sea level just to the east of Station ALOHA, not quite a fully formed eddy; it was reflected by northward flow to the east and southward flow to the west. A combination of internal semidiurnal and diurnal tides and near-inertial oscillations was noticeable, especially in vertical shear.

The temperature MicroCAT records during the WHOTS-15 deployment (Figure VI-16 through Figure VI-20) show noticeable seasonal variability in the upper 100 m and a sudden increase during January 2019. A decrease in June 2019 was evident in the instruments below 55 m. The salinity records (Figure VI-21 through Figure VI-25 do not show an apparent seasonal cycle, but instances of salinity decrease were recorded during March, especially in July-August 2019, and to a minor extent in May 2019 by the instruments located above 120 m.

Figure VI-31 and Figure VI-32 show contours of the WHOTS-15 MicroCAT data in context with data from the previous 14 deployments. The seasonal cycle is evident in the temperature record, with record temperatures (higher than 26 °C) in the summer of 2004, and again in 2014, 2015, 2017, and 2019. Salinities in the subsurface salinity maximum were relatively low during the first 6 years of the record, only to increase drastically after 2008 through 2015, with some lower salinity episodes in mid-2011 and early 2012. The salinity maximum extended to near the surface in early 2010, 2011, late 2012-early 2013, and February-March 2013. Salinities in the salinity minimum decreased after 2015, showing low salinities above 100 m in 2016, 2017, 2018, and reaching record low values (34.4) in July-August 2019. The low salinities observed in 2019 in the MicroCAT time-series plots (Figure VI-21 through Figure VI-25) are apparent in Figure VI-32 and Figure VI-33. When plotted in σ_θ coordinates (Figure VI-33), the salinity maximum seems to be centered roughly between 24 and 24.5 σ_θ.

Records from the WHOTS-15 MicroCATs (Figure VI-33) deployed near the bottom of the mooring (4658 m) detected temperature and salinity changes related to episodic 'cold events' apparently caused by bottom water moving between abyssal basins (Lukas et al., 2001). These events are being monitored by instruments at the ALOHA Cabled Observatory (ACO, Howe et al., 2011), a deep water observatory located at the bottom of Station ALOHA (about 6 nautical miles west from the WHOTS-15 anchor), since June 2011. Figure VI-33 shows temperature and salinity records from the WHOTS-15 MicroCATs superimposed on the ACO data. The MicroCAT data agreed with the temperature decrease and the salinity variability registered by ACO instruments during two cold events in December 2018 and June 2019, and a minor event in September 2019.

Figure VI-37 through Figure VI-39 shows the time series of the zonal, meridional, and vertical currents recorded with the moored ADCPs during the WHOTS-15 deployment. Figure VI-34, through Figure VI-36, shows the ADCP current components' contours in context with data from the previous deployments. Despite the gaps in the data, an apparent variability is seen in the zonal and meridional currents, apparently caused by passing eddies. There have been periods of intermittent positive or negative zonal currents on top of this variability, for instance, during 2007-2008. The contours of the vertical current component (Figure VI-36) show a transition in the magnitude of the contours near 47 m, indicating that the 300 kHz ADCP located at 126 m moves more vertically than the 600 kHz ADCP located at 47.5 m.

A comparison between the moored ADCP data and the shipboard ADCP data obtained during the WHOTS-15 cruise is shown in Figure VI-40, Figure VI-41, and a similar comparison

during the WHOTS-16 cruise is shown in Figure VI-42 and Figure VI-43. Some of the differences were seen, especially in the zonal component, maybe due to the mooring motion, which was not removed from the data. Comparisons between the available shipboard ADCP from HOT-306 to -315 cruises and the mooring data are shown in Figure VI-44 and Figure VI-45.

The Xeos-GPS receiver registered the WHOTS-15 buoy motion, and its positions are plotted in Figure VI-47. The buoy was located west of the anchor for most of the deployment, except from around April to June 2019, when it was east. The power spectrum of these data (Figure VI-48) shows extra energy at the inertial period (~31 hr). Combining the buoy motion with the tilt (a combination of pitch and roll) from the ADCP data (Figure VI-49) showed that the tilt increased as the buoy distance from the anchor WHOTS-15 increased. This was expected since the inclination of the cable increases as the buoy moves away from the anchor.

A. CTD Profiling Data

Profiles of temperature, salinity, and potential density (σ_θ) from the casts obtained during the WHOTS-15 deployment cruise are presented in Figure VI-1 through Figure VI-6, together with the results of bottle determination of salinity. Figure VI-7 through Figure VI-9 shows the results of the CTD profiles during the WHOTS-16 cruise.

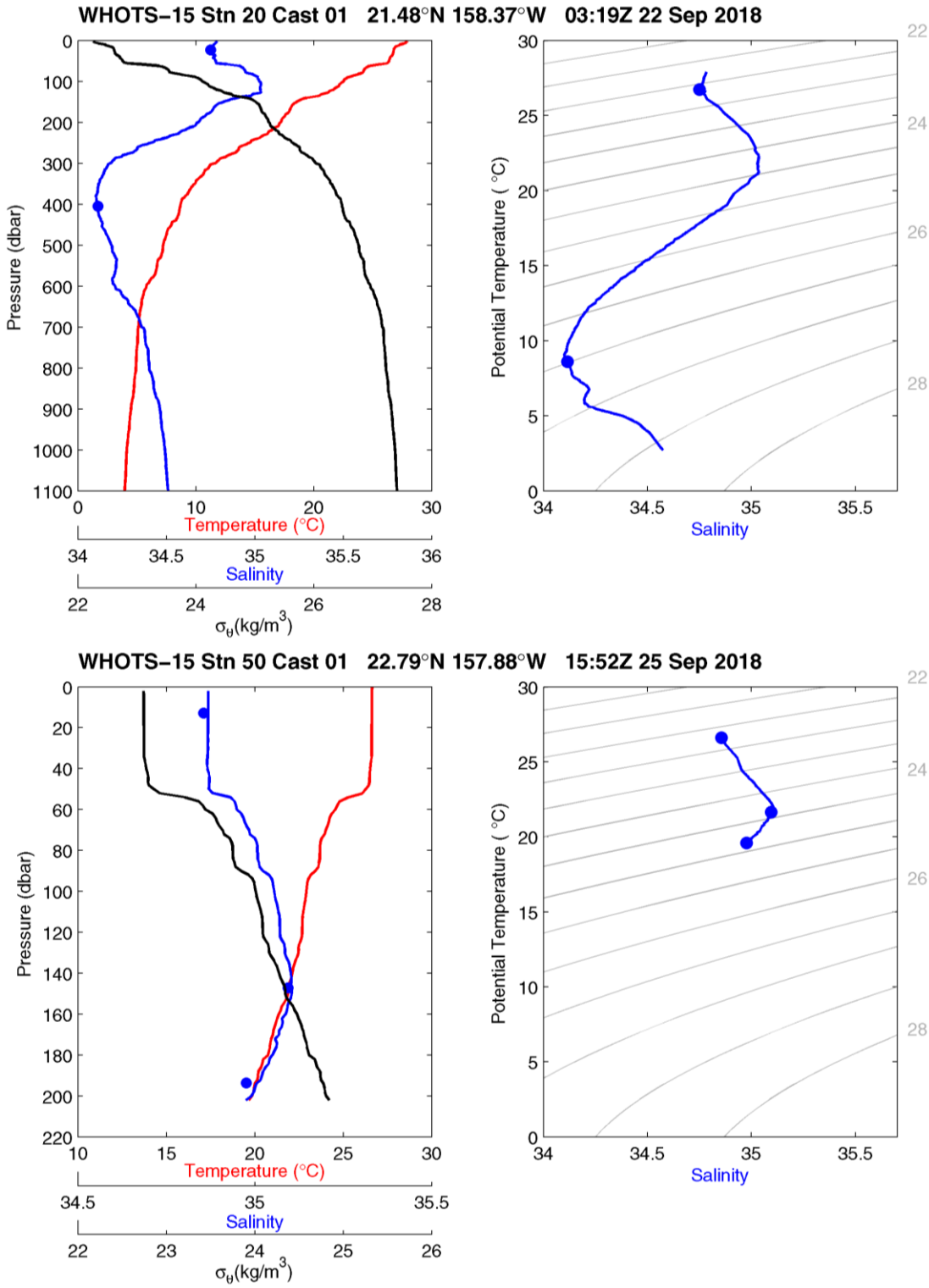

Figure VI-1. [Upper left panel] Profiles of CTD temperature, salinity, and potential density (σ_θ) as a function of pressure, including discrete bottle salinity samples (when available) for station 20 cast 1 during the WHOTS-15 cruise. [Upper right panel] Profiles of CTD salinity as a function of potential temperature, including discrete bottle salinity samples (when available) for station 20 cast 1 during the WHOTS-15 cruise. [Lower left panel] Same as in the upper left panel, but for station 50 cast 1. [Lower right panel] Same as in the upper right panel, but station 50 cast 1.

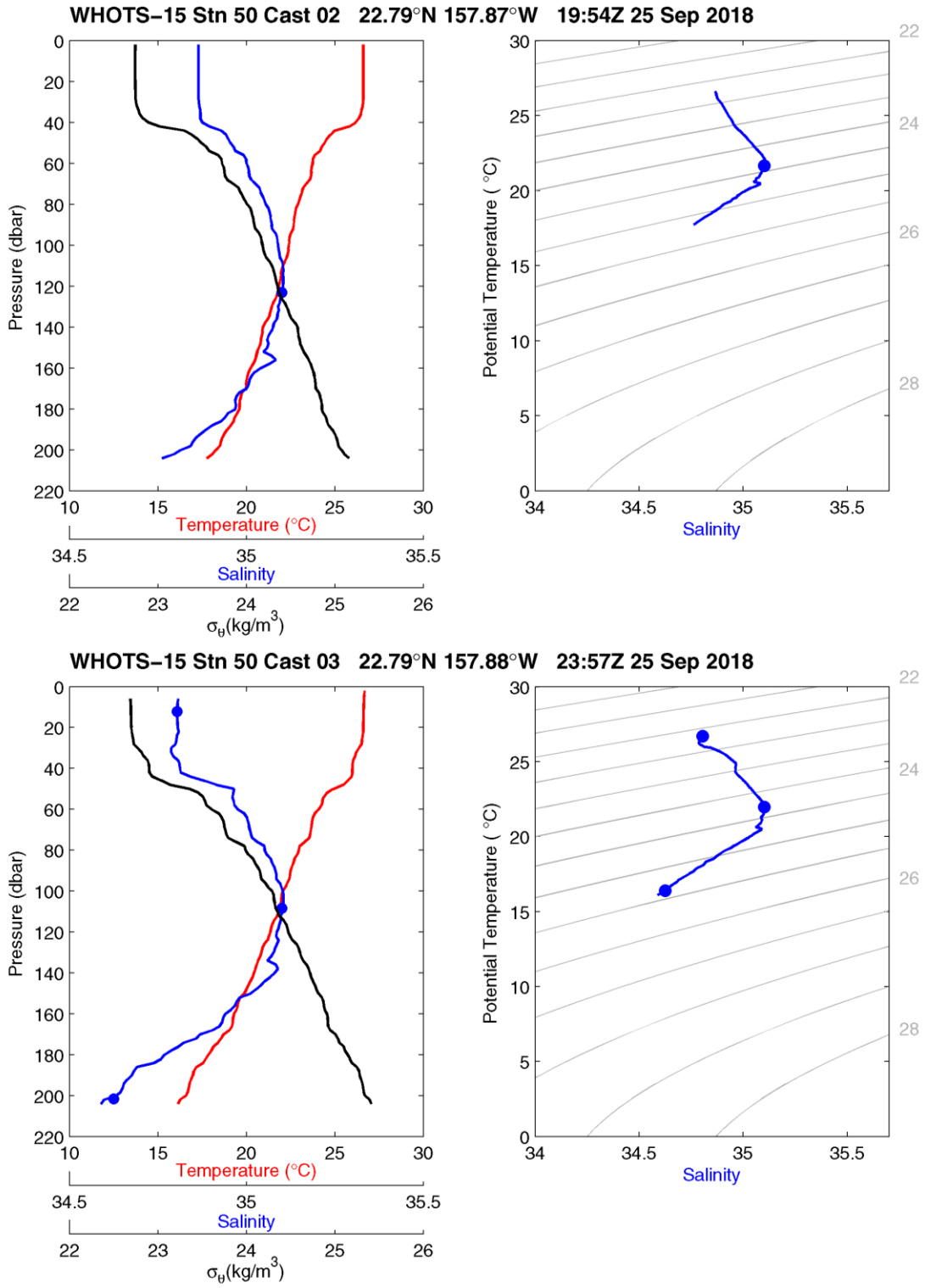

Figure VI-2.[Upper panels] Same as in Figure VI-1, but for station 50, cast 2. [Lower panels] Same as Figure VI-1, but for station 50, cast 3.

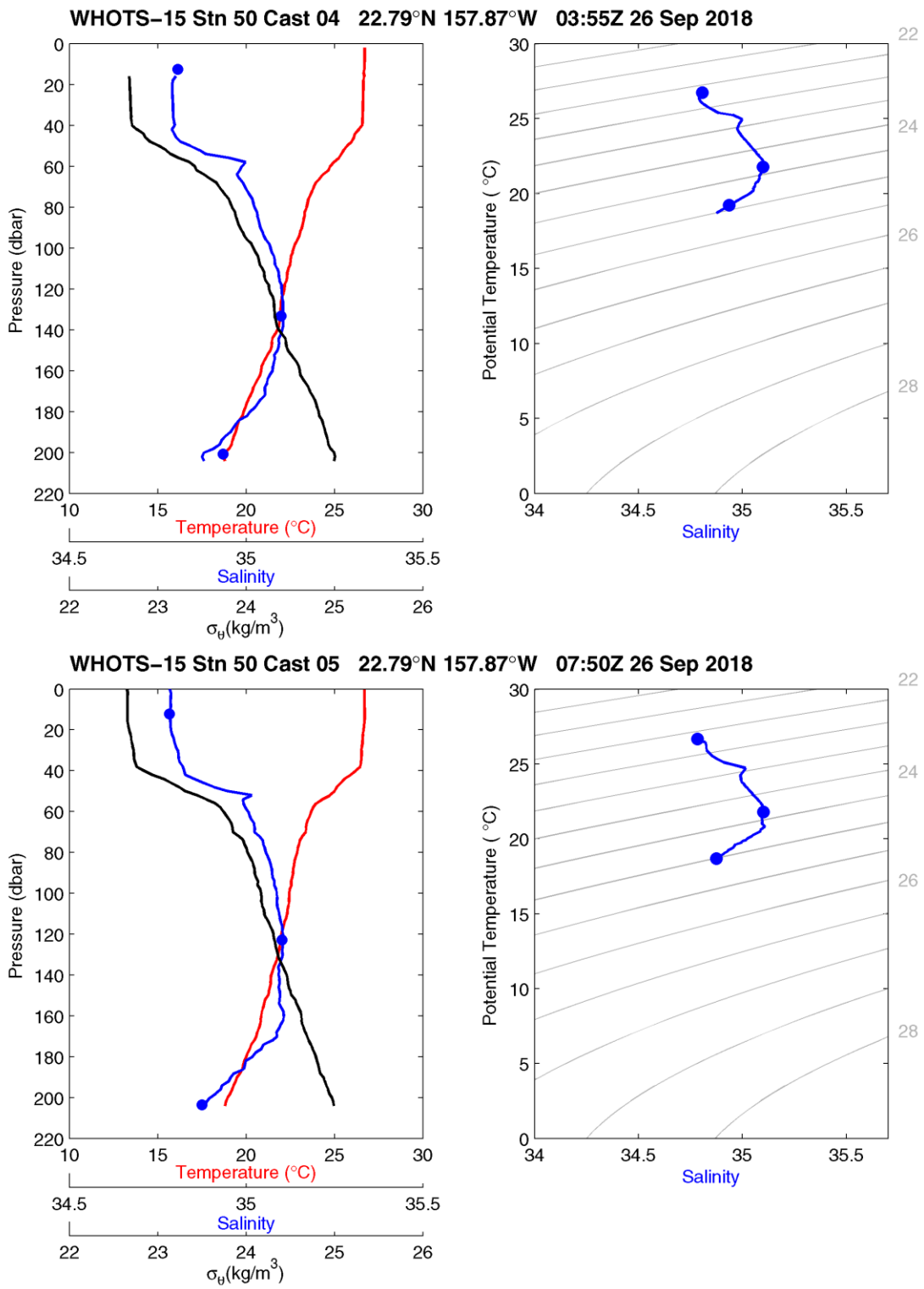

Figure VI-3.[Upper panels] Same as in Figure VI-1, but for station 50, cast 4. [Lower panels] Same as in Figure VI-1, but for station 50 cast 5.

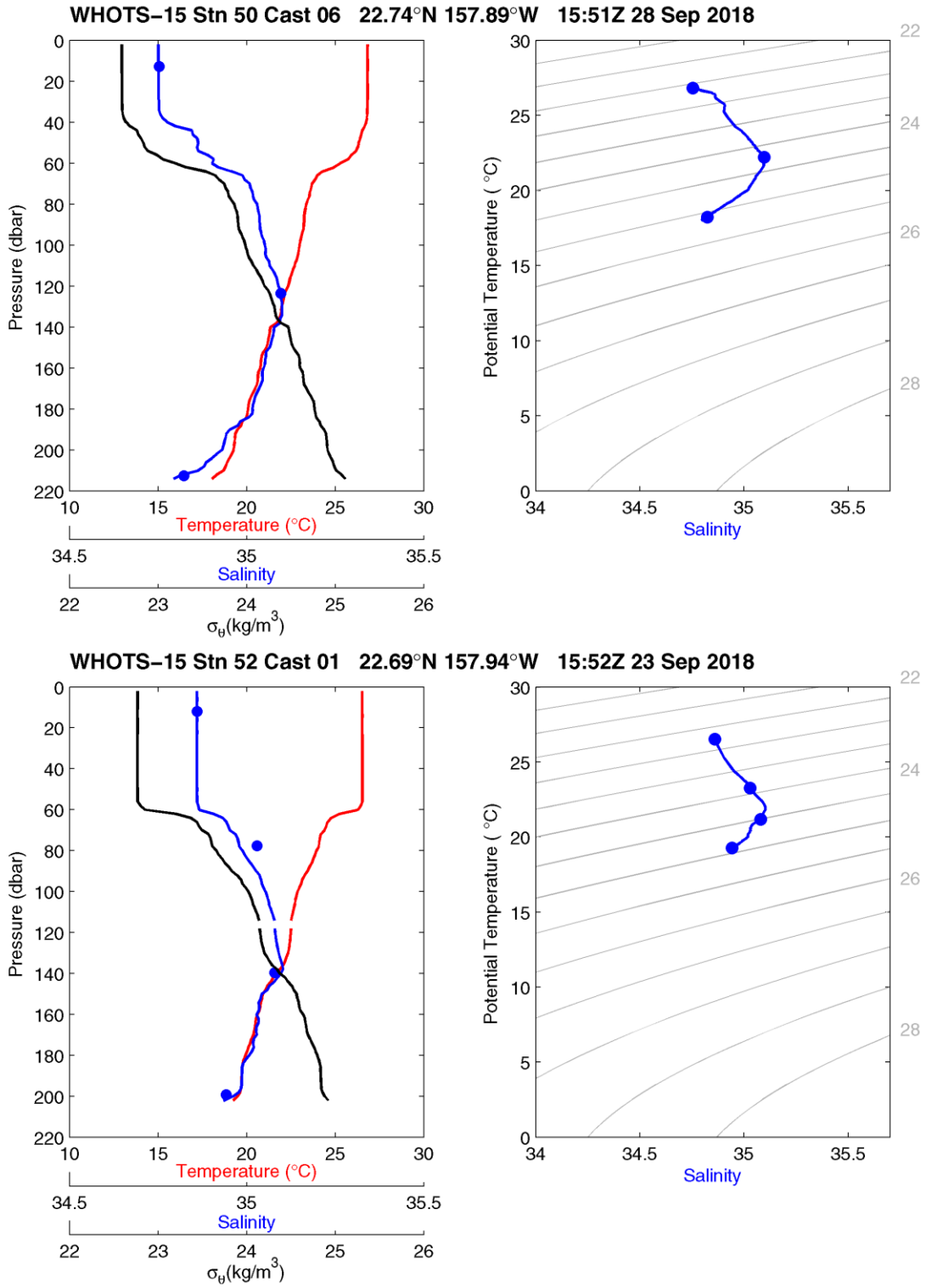

Figure VI-4.[Upper panels] Same as in Figure VI-1, but for station 50, cast 6. [Lower panels] Same as in Figure VI-1, but for station 52, cast 1.

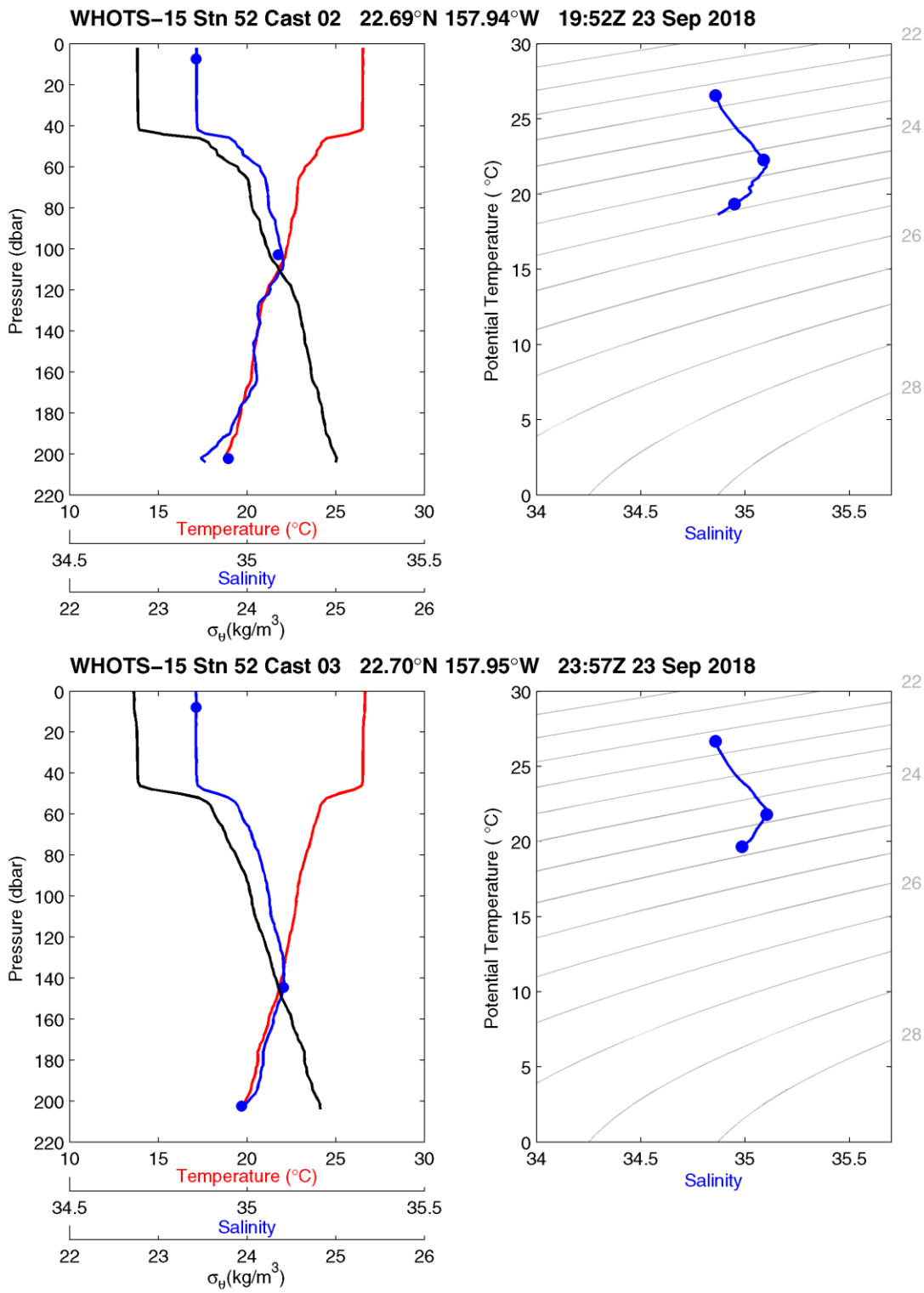

Figure VI-5. [Upper panels] Same as in Figure VI-1, but for station 52, cast 2. [Lower panels] Same as in Figure VI-1, but for station 52, cast 3.

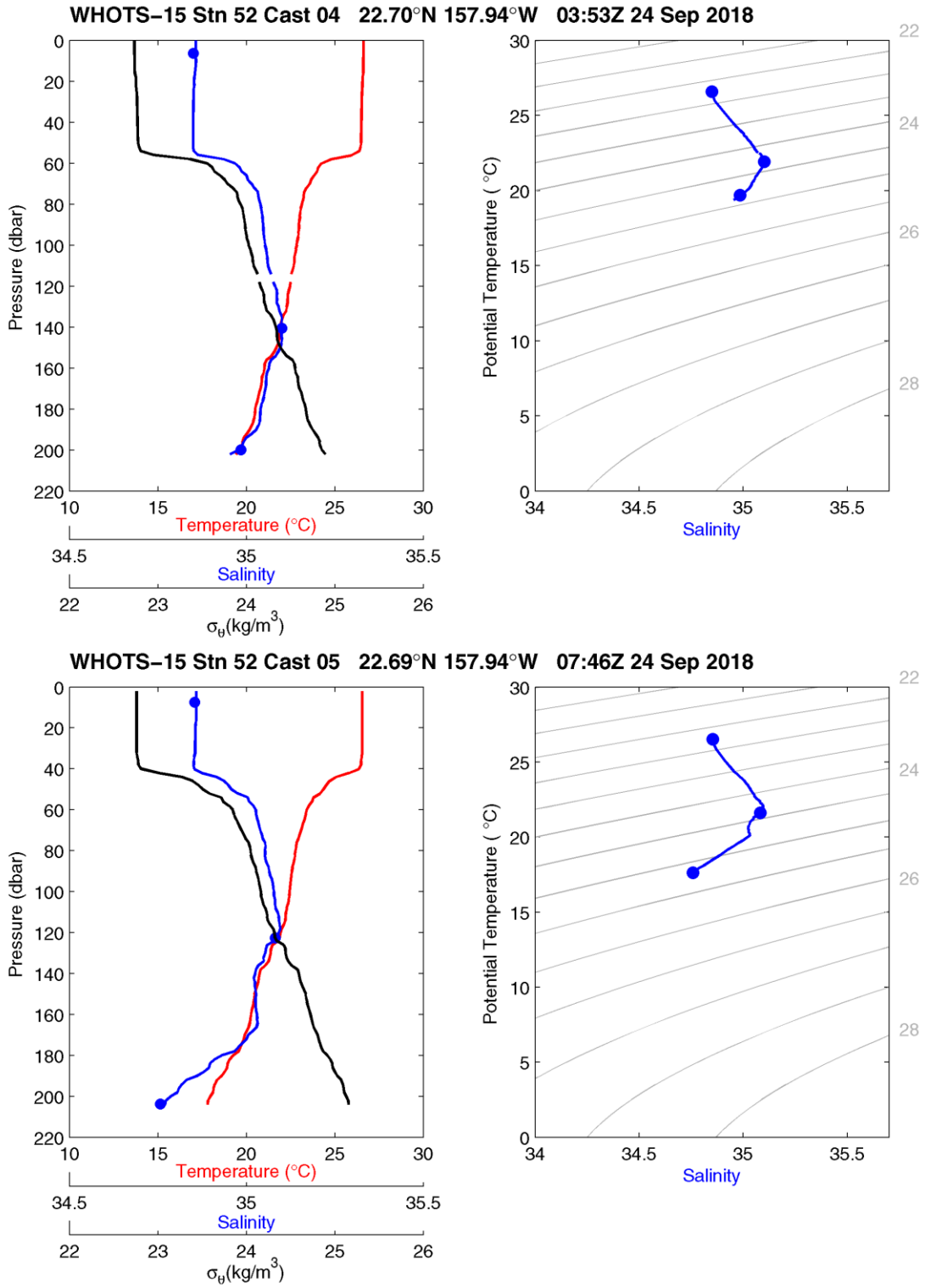

Figure VI-6.[Upper panels] Same as in Figure VI-1, but for station 52, cast 4. [Lower panels] Same as in Figure VI-1, but for station 52, cast 5.

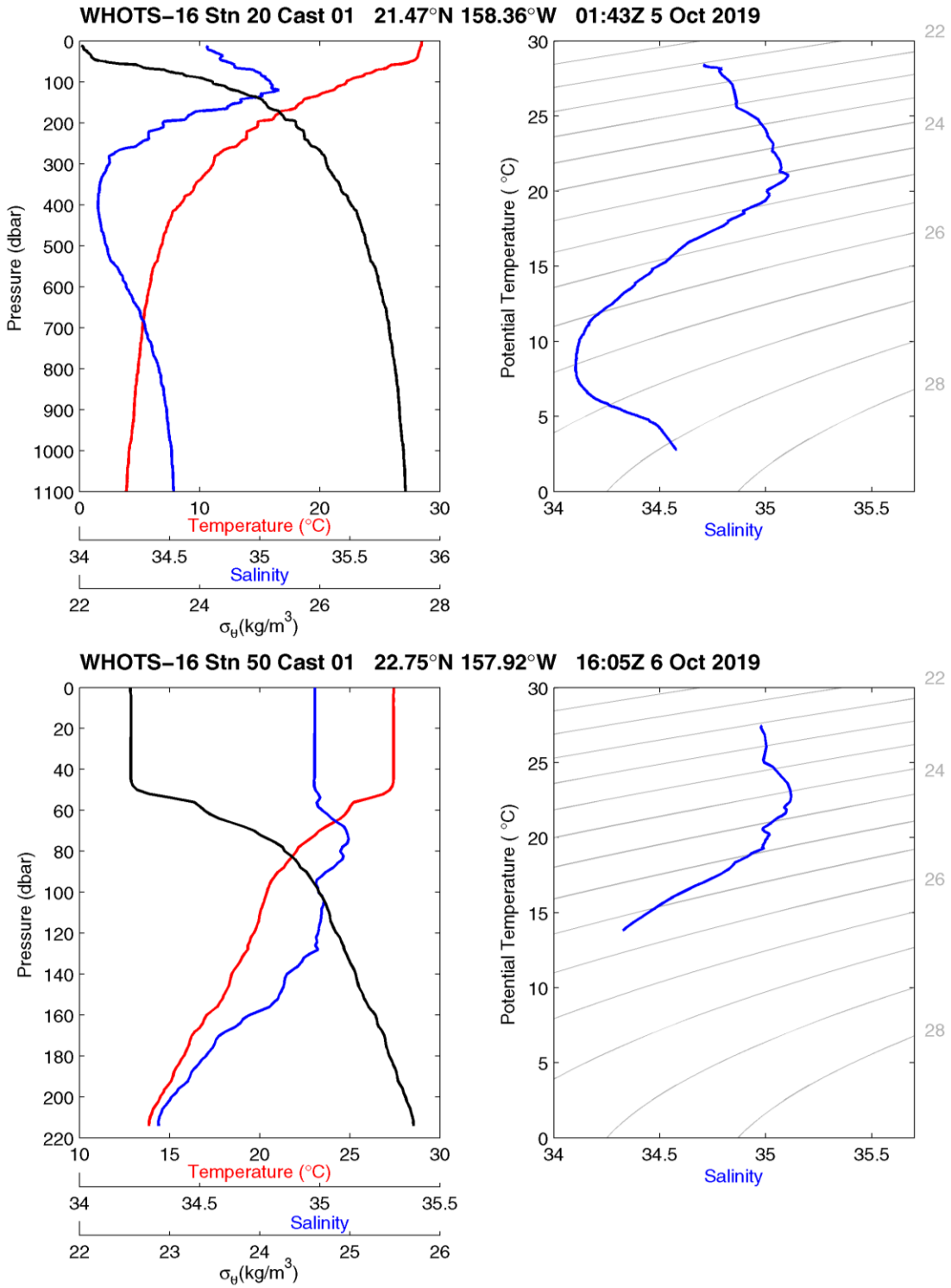

Figure VI-7.[Upper left panel] Profiles of CTD temperature, salinity, and potential density (σθ) as a function of pressure, including discrete bottle salinity samples (when available) for station 20 cast 1 during the WHOTS-16 cruise. [Upper right panel] Profiles of CTD salinity as a function of potential temperature, including discrete bottle salinity samples (when available) for station 20 cast 1 during the WHOTS-16 cruise. [Lower left panel] Same as in the upper left panel, but for station 50 cast 1. [Lower right panel] Same as in the upper right panel, but station 50 cast 1.

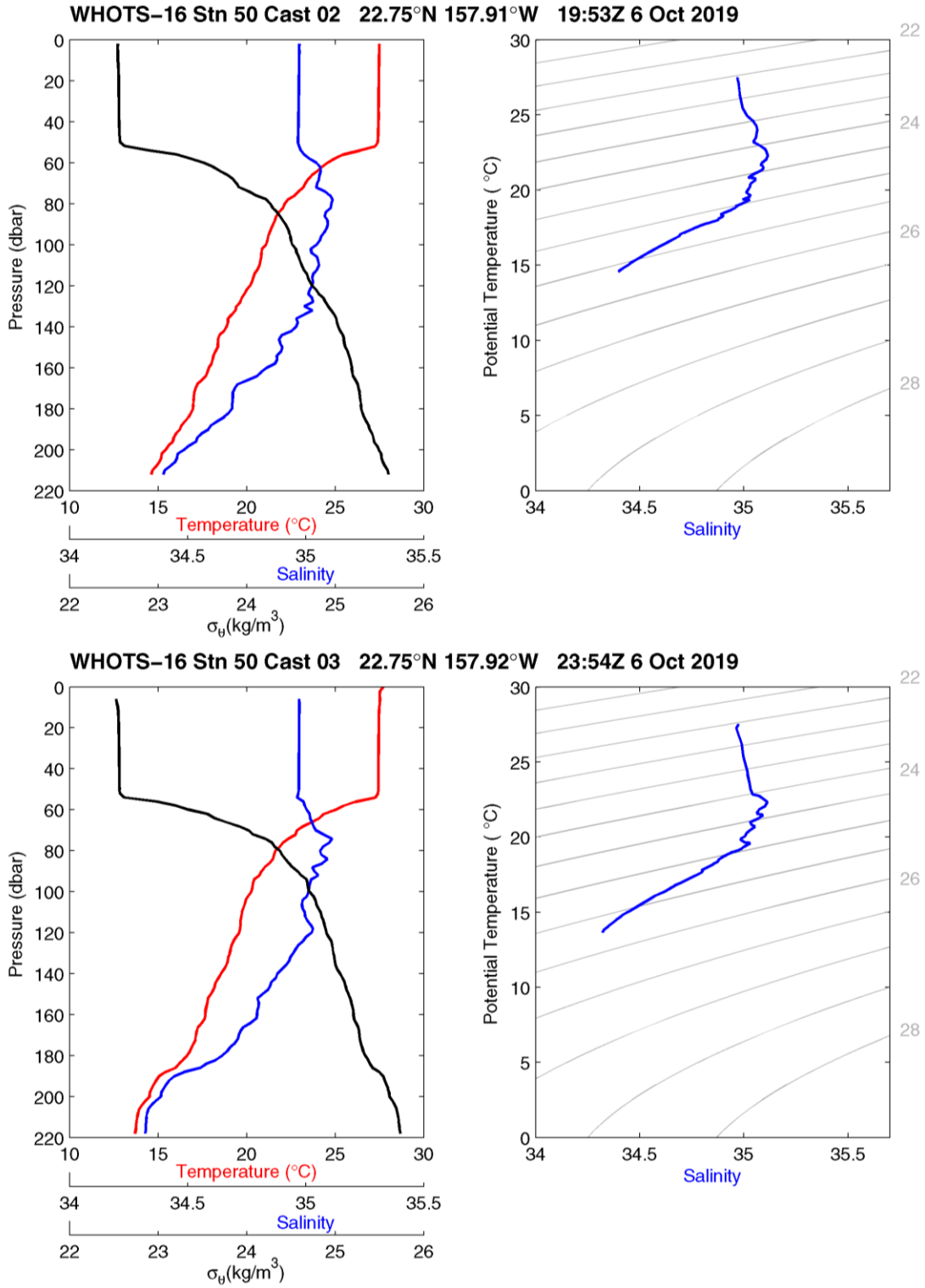

Figure VI-8.[Upper panels] Same as in Figure VI-7 but for station 50, cast 2. [Lower panels]Same as Figure VI-7., but for station 50 cast 3.

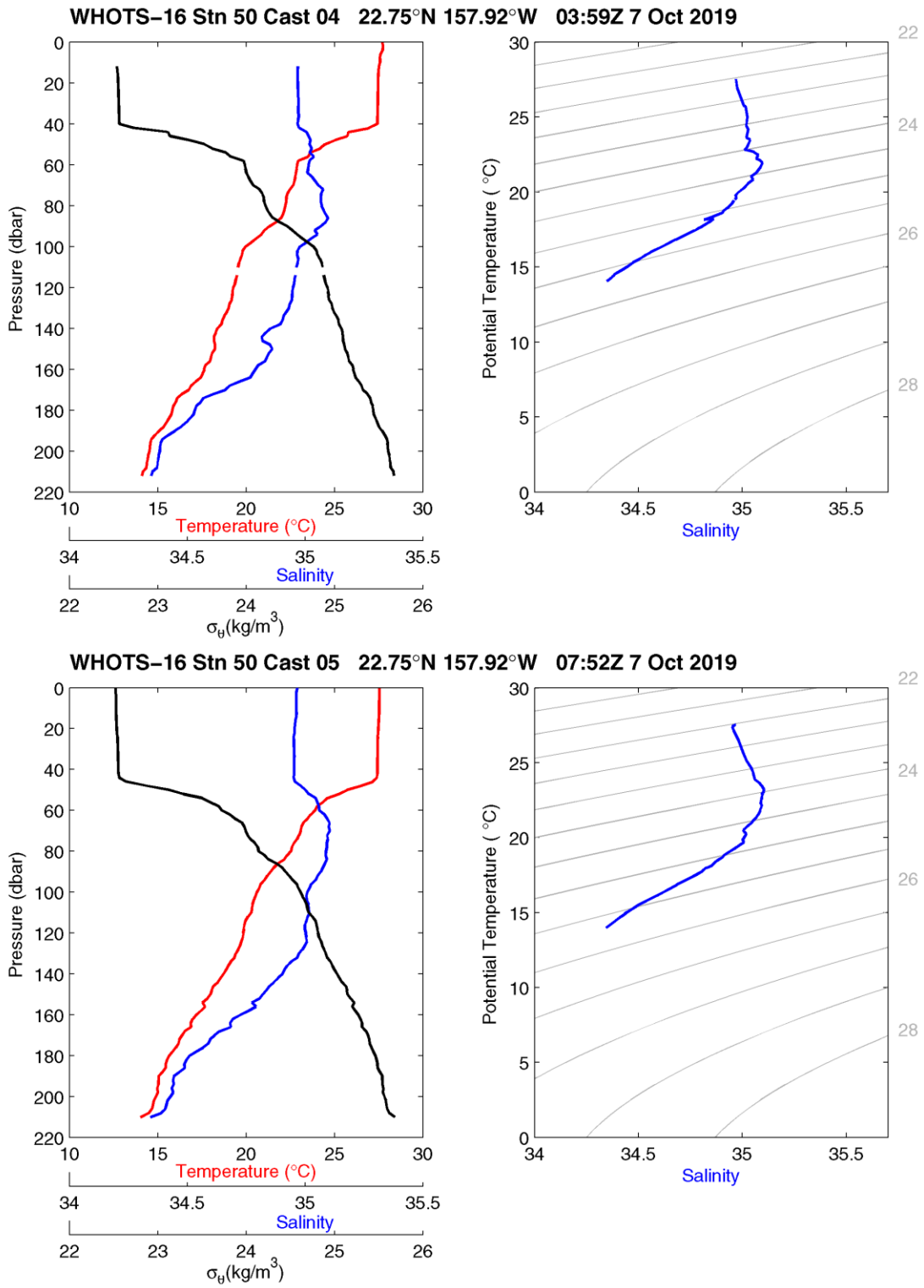

Figure VI-9. Same as in Figure VI-7, but for station 50, cast 4. [Lower panels] Same as in Figure VI-7, but for station 50 cast 5.

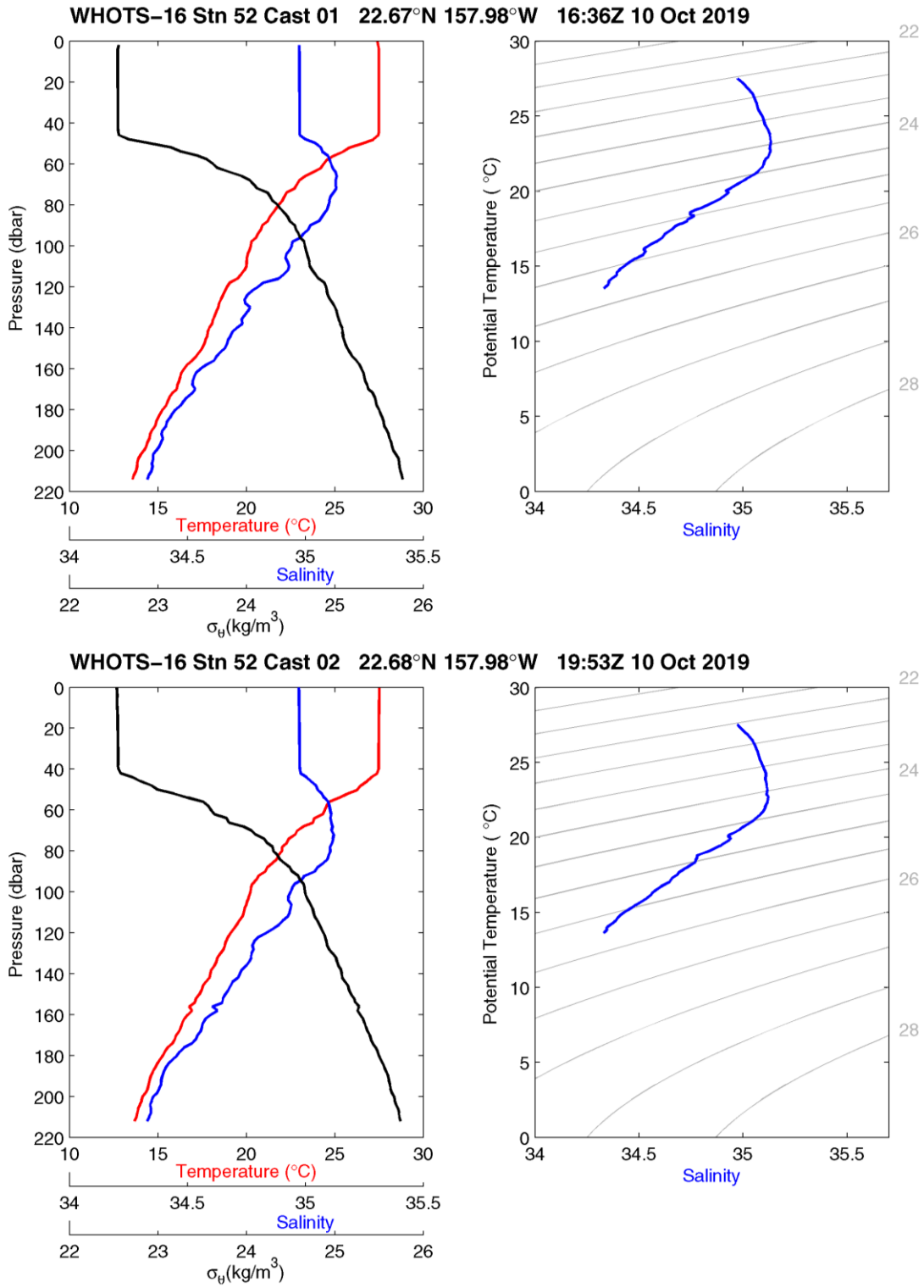

Figure VI-10. [Upper panels] Same as in Figure VI-7, but for station 52, cast 1. [Lower panels] Same as in Figure VI-7 but for station 52, cast 2.

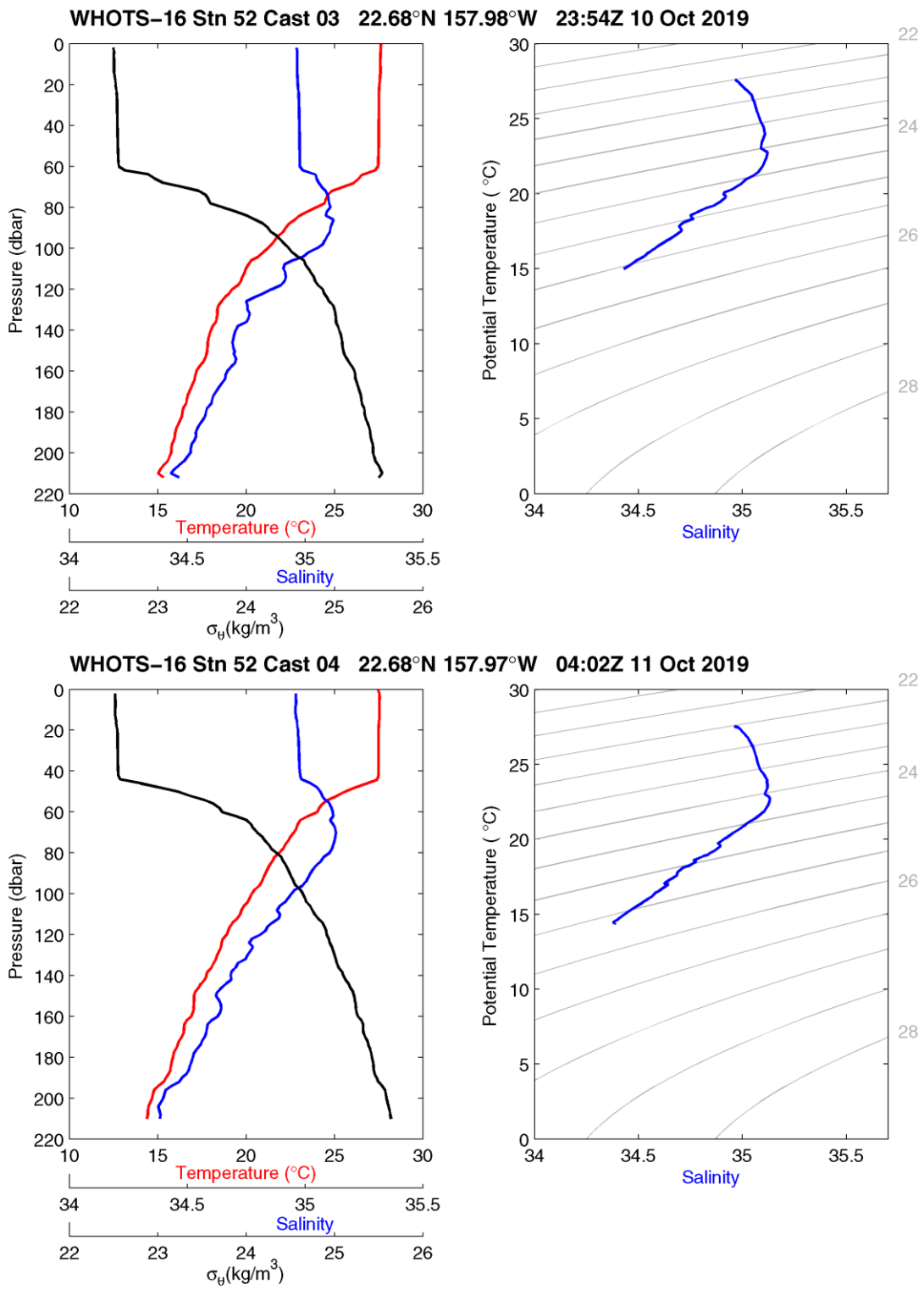

Figure VI-11.[Upper panels] Same as Figure VI-7 , but for station 52, cast 3. [Lower panels] Same as Figure VI-7 but for station 52 cast 4.

B. Thermosalinograph data

Underway measurements of near-surface temperature and salinity from the thermosalinograph (TSG) system onboard the R/V *Hi'ialakai* cruise are presented in Figure VI-12 and navigational data is shown in Figure VI-13 for the WHOTS-15 cruise. TSG and navigational data during the WHOTS-16 cruise, onboard the R/V *Oscar Sette*, are presented in Figure VI-14 and Figure VI-15, respectively. The WHOTS-16 underway seawater system that feeds the TSG failed on October 11th, 2019, due to air going into the plumbing, causing the pumps to stop working during deteriorated weather conditions.

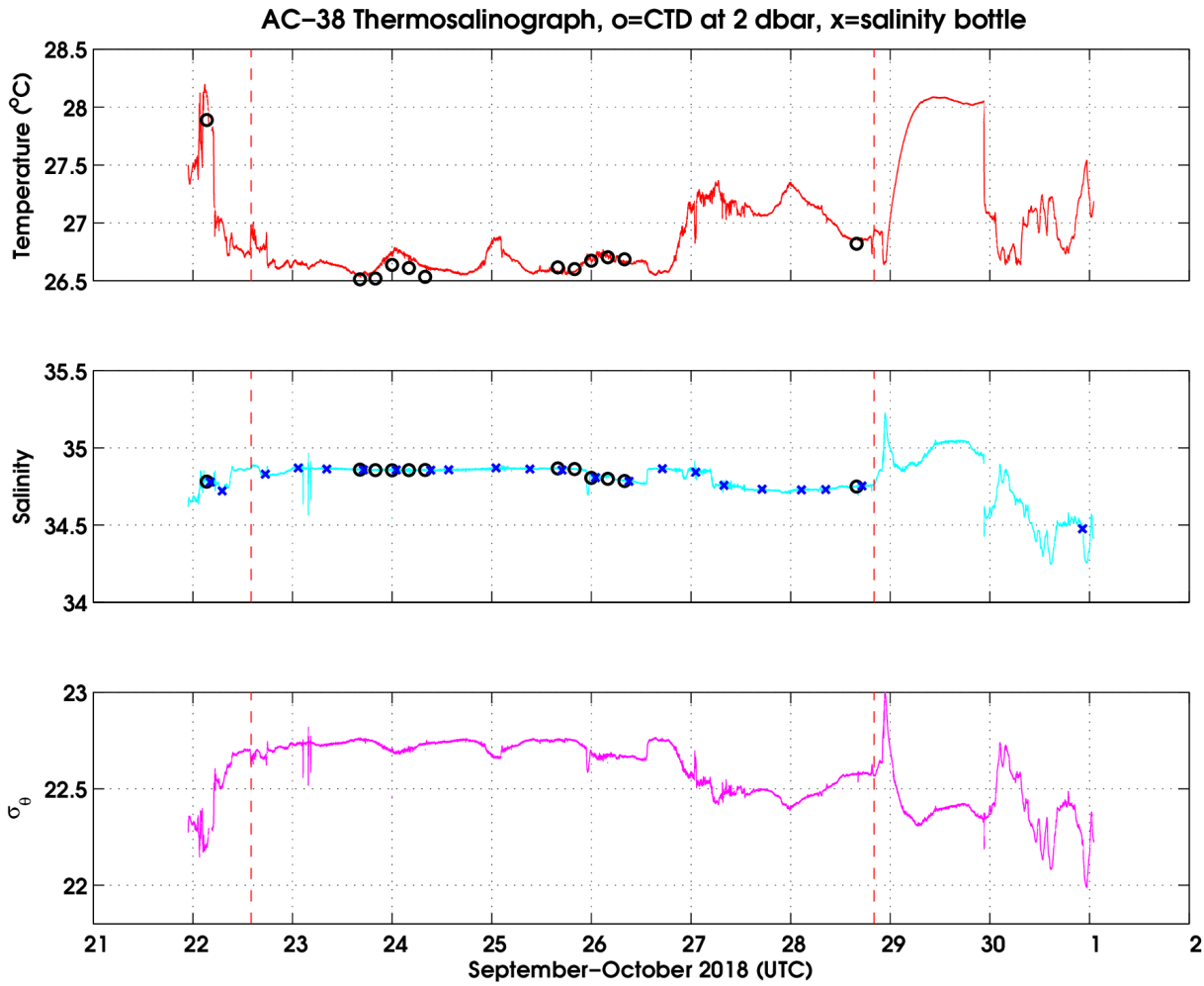

Figure VI-12. Final processed temperature (upper panel), salinity (middle panel), and potential density (σθ) (lower panel) data from the continuous underway system onboard the R/V Hi'ialakai during the WHOTS-15 cruise. Temperature and salinity taken from 6-dbar CTD data (circles) and salinity bottle sample data (crosses) are superimposed. The dashed vertical red line indicates the period of occupation of Station ALOHA and the WHOTS site.

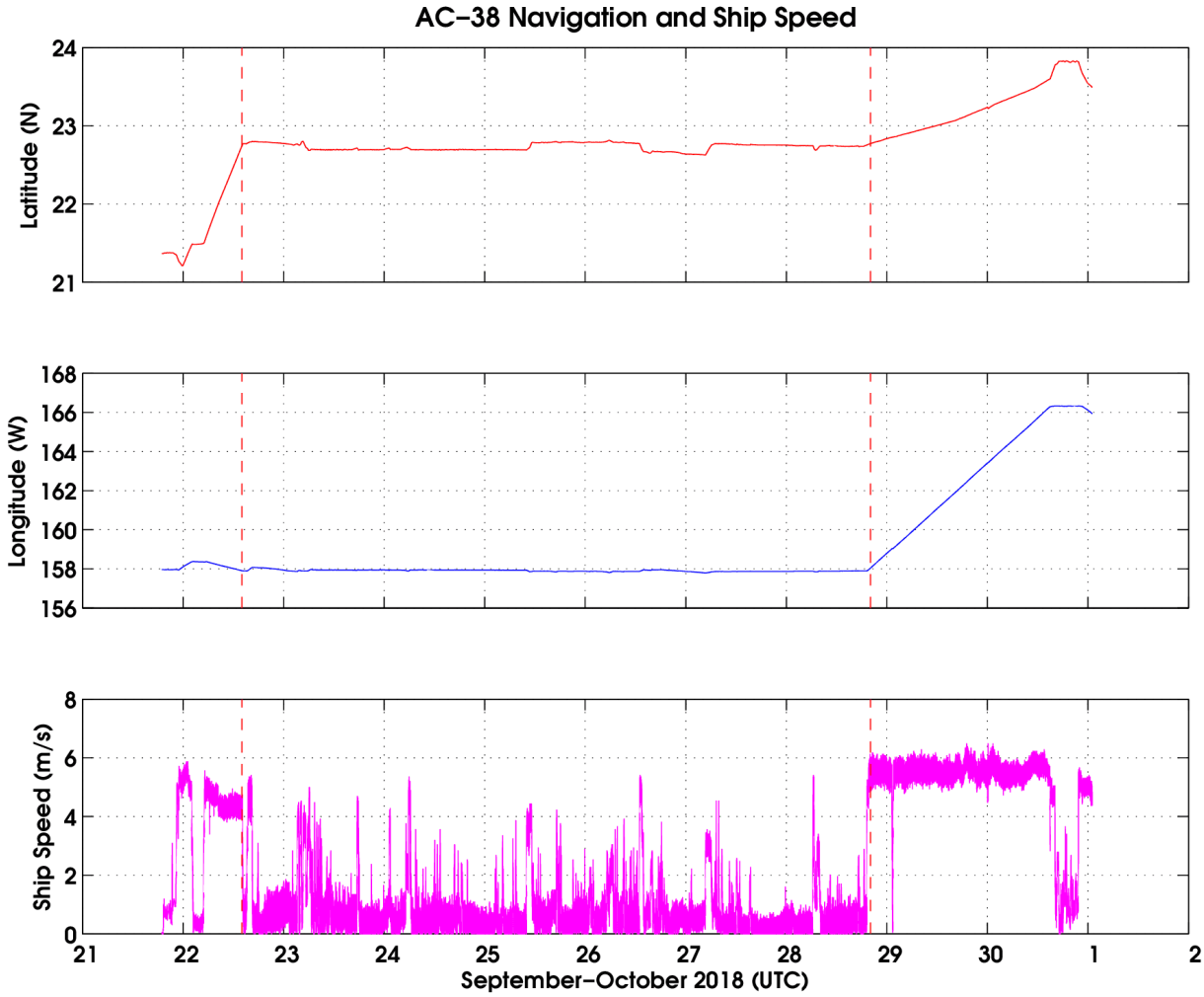

Figure VI-13. Timeseries of latitude (upper panel), longitude (middle panel), and ship's speed (lower panel) during the WHOTS-15 cruise.

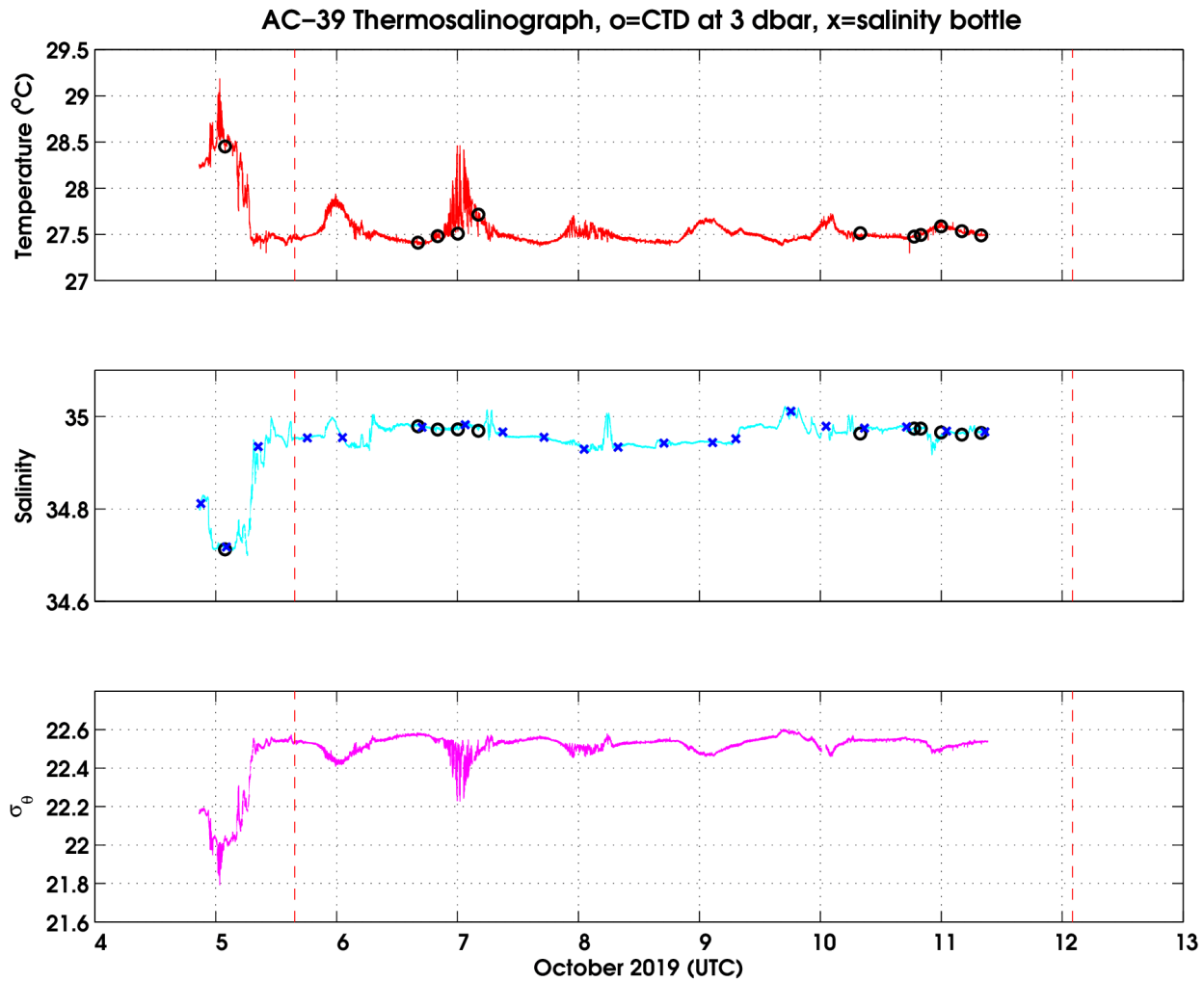

Figure VI-14. Final processed temperature (upper panel), salinity (middle panel), and potential density (σθ) (lower panel) data from the continuous underway system onboard the R/V Oscar Sette during the WHOTS-16 cruise. Temperature and salinity were taken from 6-dbar CTD data (circles), and salinity bottle sample data (crosses) are superimposed. The dashed vertical red line indicates the period of occupation of Station ALOHA and the WHOTS site.

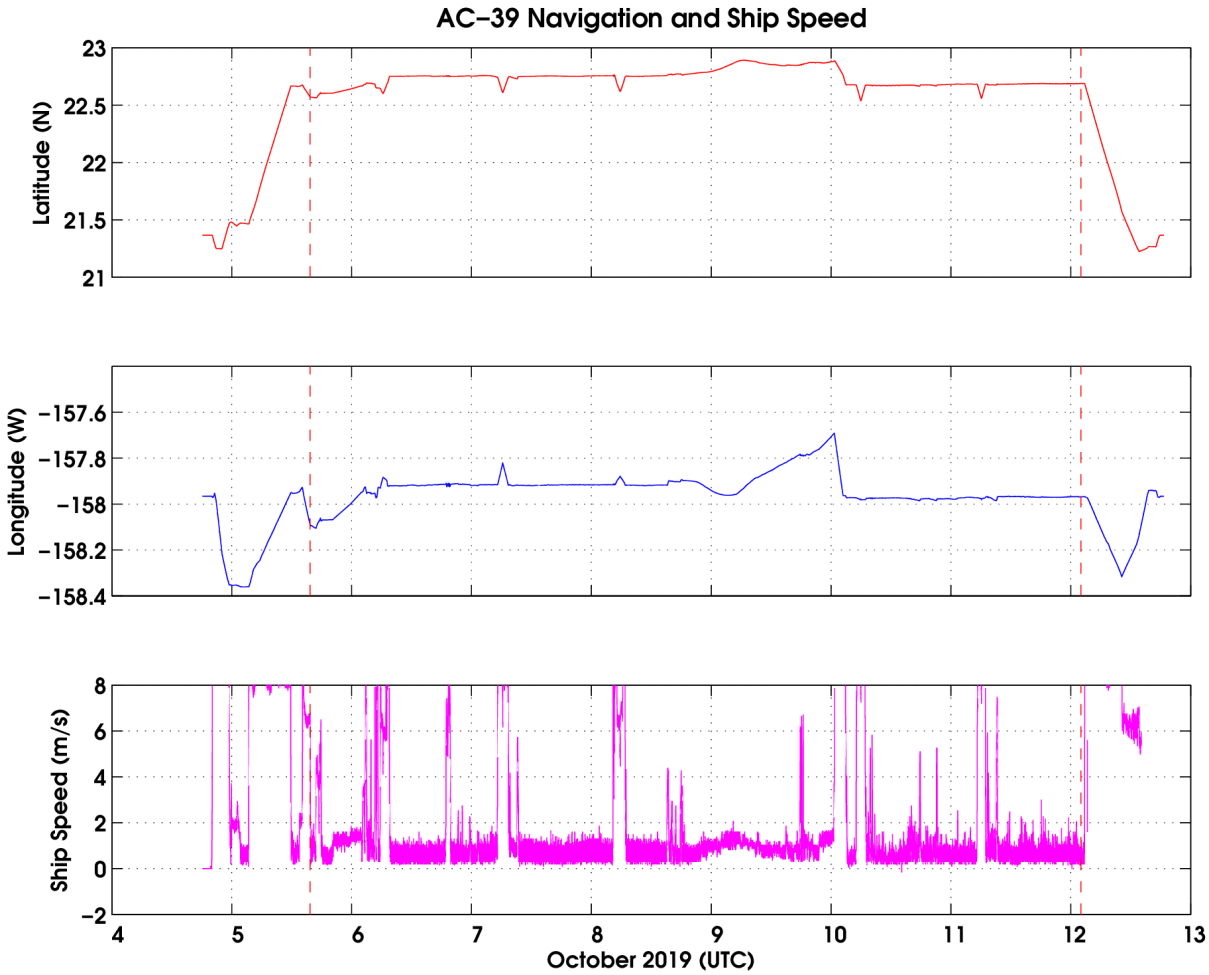

Figure VI-15. Timeseries of latitude (upper panel), longitude (middle panel), and ship's speed (lower panel) during the WHOTS-16 cruise.

C. MicroCAT data

The temperatures measured by MicroCATs during the mooring deployment for WHOTS-15 are presented in Figure VI-16 through Figure VI-20 for each of the depths where the instruments were located. The salinities are plotted in Figure VI-21 through Figure VI-25. The potential densities (σ_θ) are plotted in Figure VI-26 through Figure VI-30.

Contoured plots of temperature and salinity as a function of depth for the deployments WHOTS-1 through -15 are presented in Figure VI-31, and contoured plots of potential density (σ_θ) as a function of depth, and of salinity as a function of σ_θ are in Figure VI-32.

The potential temperature and salinity measured by the deep MicroCATs during the mooring deployment are shown in Figure VI-33. Also shown in the plot are the potential temperature and salinity data obtained with a MicroCAT (SBE-37) installed in the ALOHA Cabled Observatory, about six nautical miles west from the WHOTS-15 anchor. The instrument is located 2 m above the bottom.

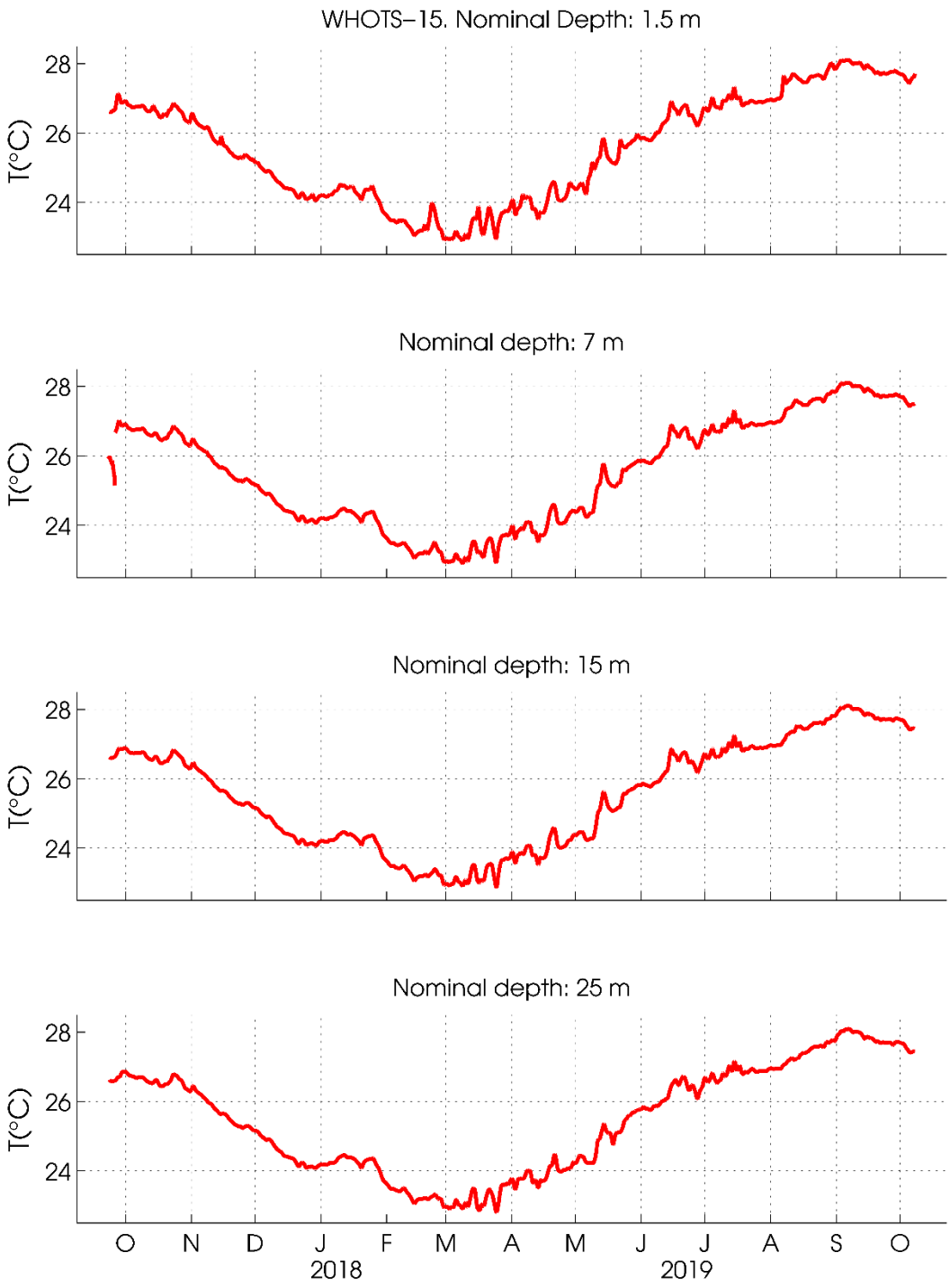

Figure VI-16. Temperatures from MicroCATs during WHOTS-15 deployment at 1.5, 7, 15, and 25 m.

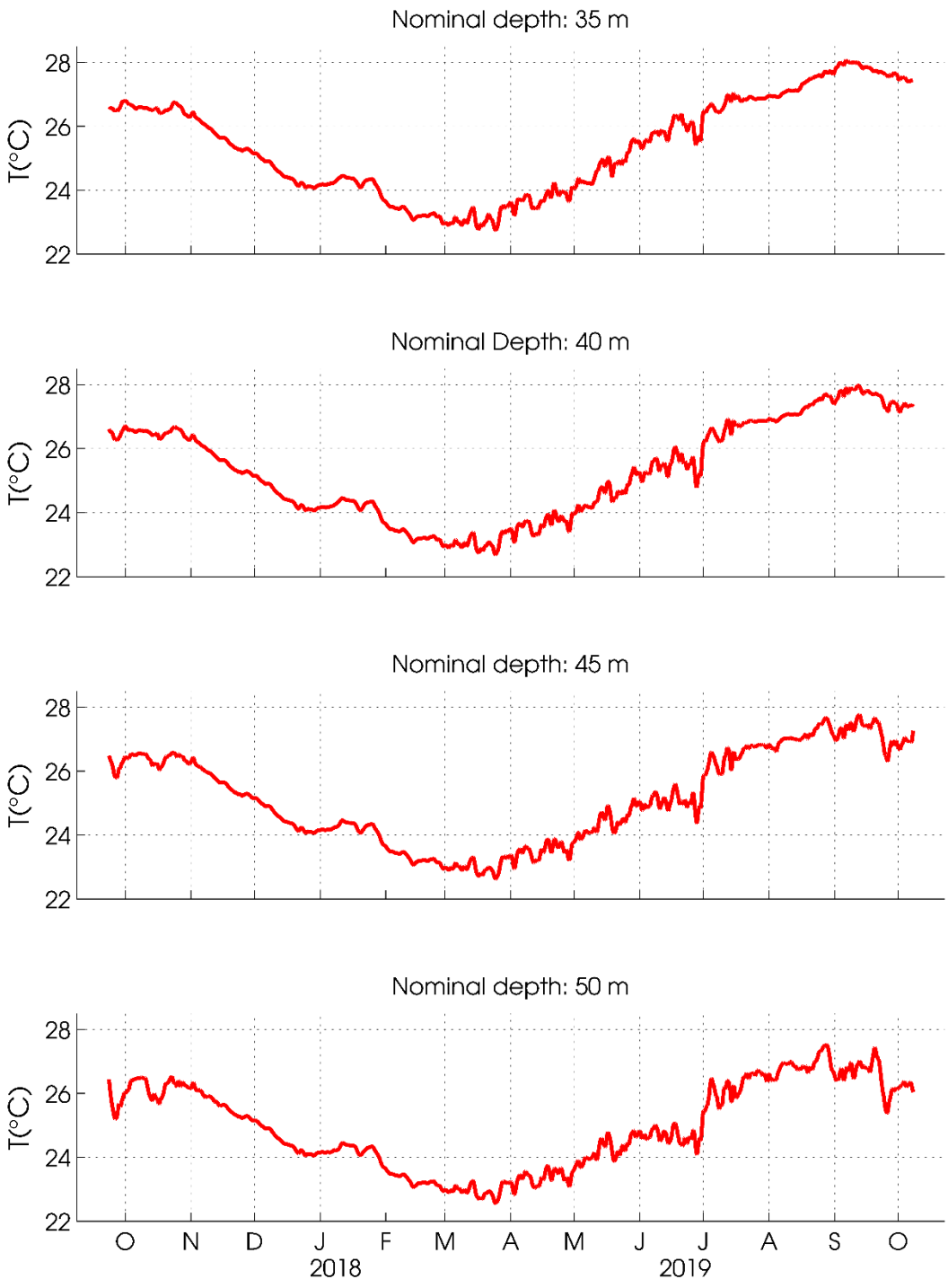

Figure VI-17. Same as in Figure VI-16, but at 35, 40, 45, and 50 m.

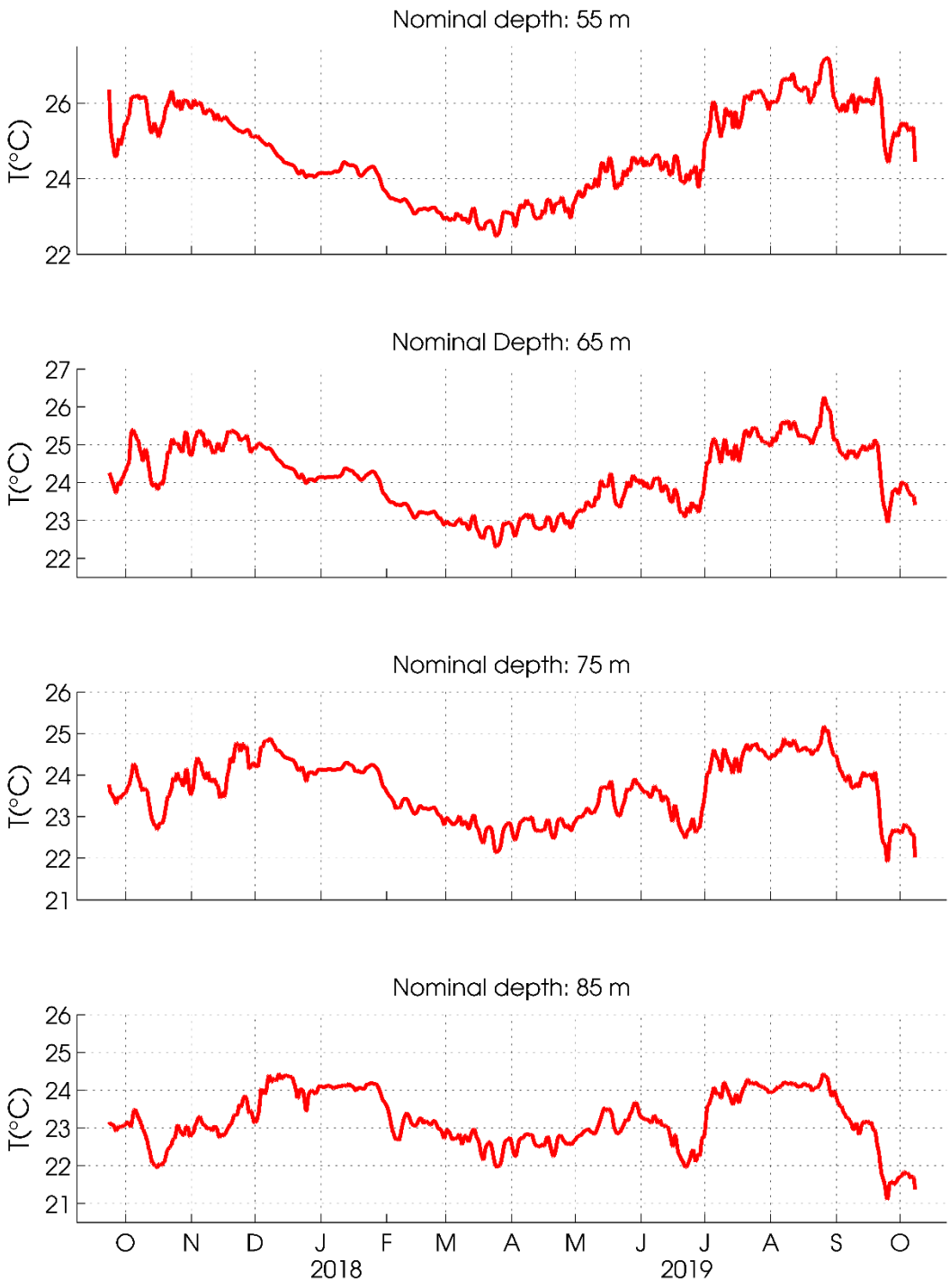

Figure VI-18. Same as in Figure VI-16, but at 55, 65, 75, and 85 m.

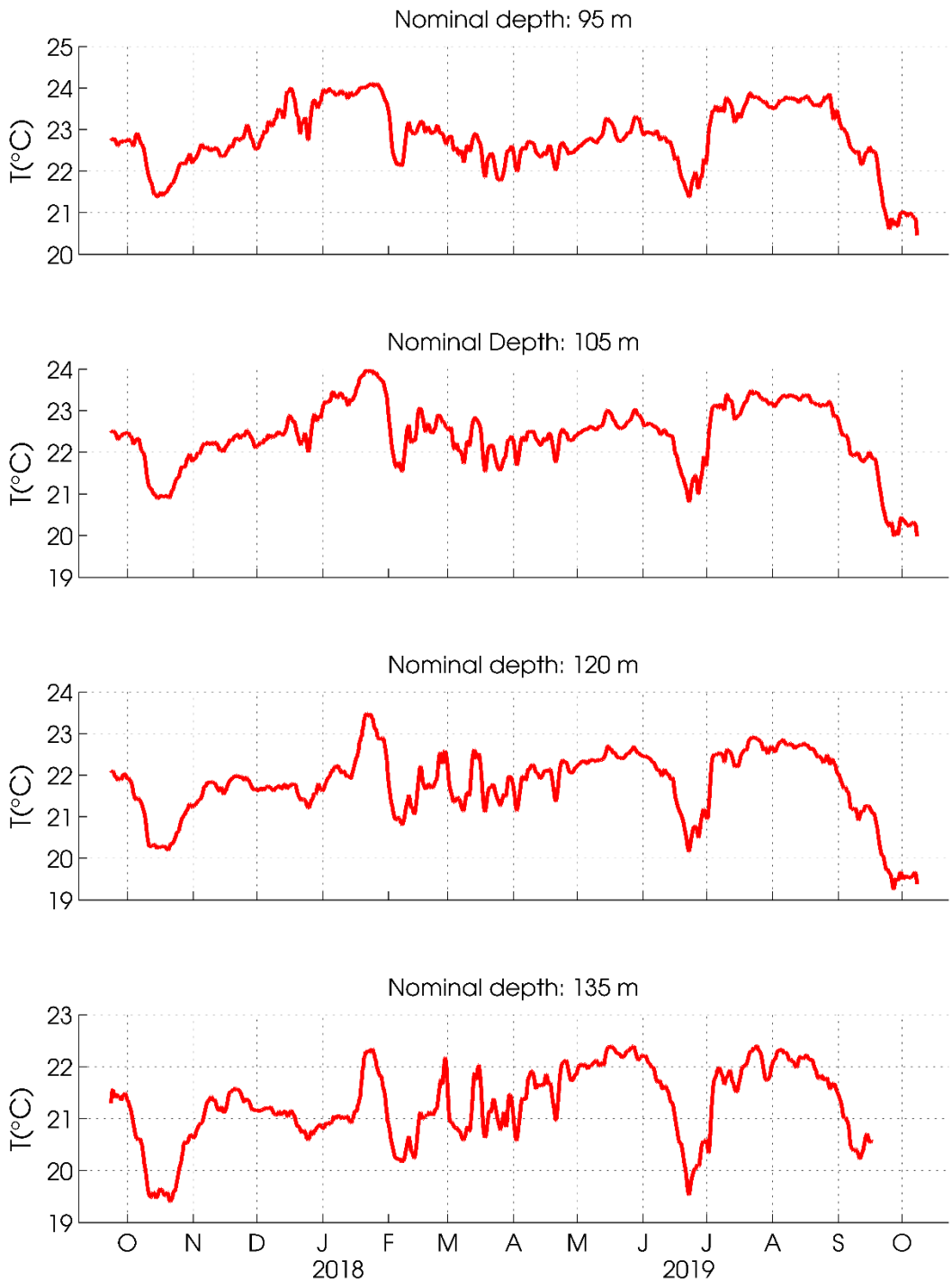

Figure VI-19. Same as in Figure VI-16, but at 95, 105, 120, and 135 m.

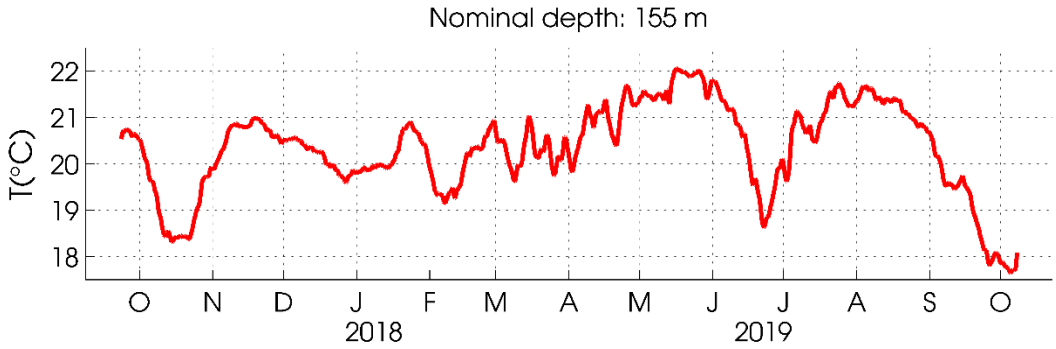

Figure VI-20. Same as inFigure VI-16, but at 155 m.

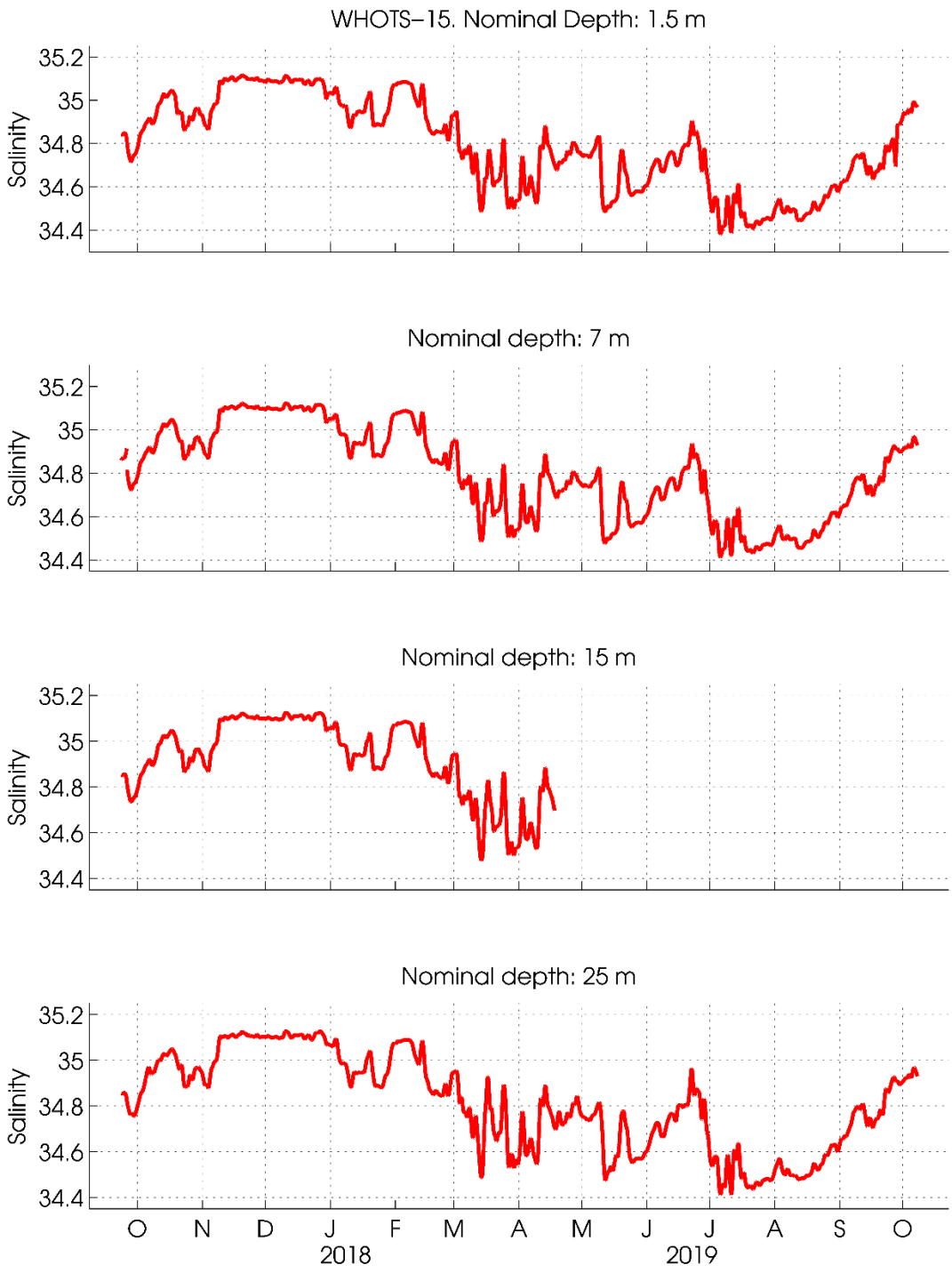

Figure VI-21. Salinities from MicroCATs during WHOTS-15 deployment at 1.5, 7, 15, and 25 m

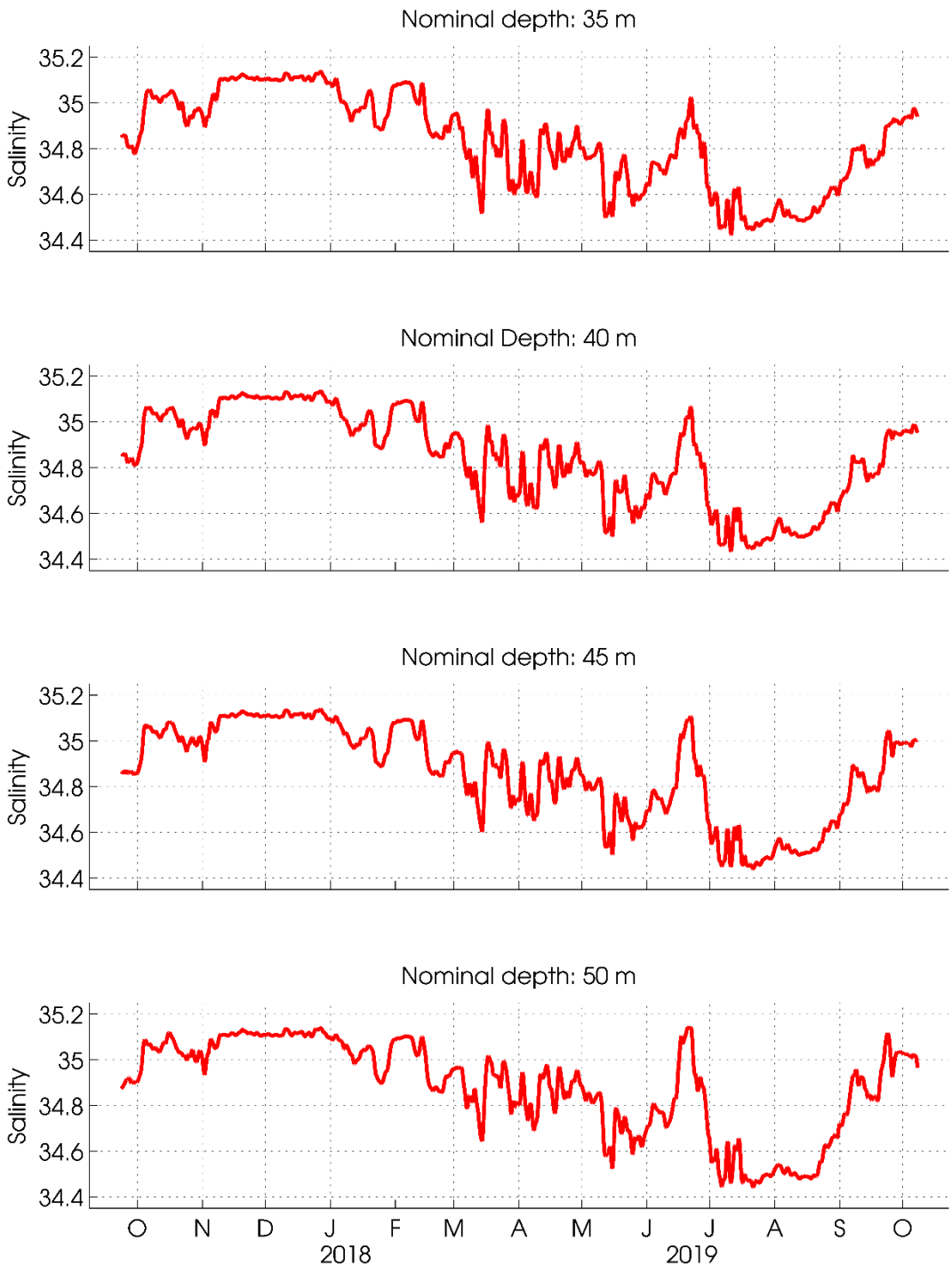

Figure VI-22. Same as in Figure VI-21, but at 35, 40, 45, and 50 m.

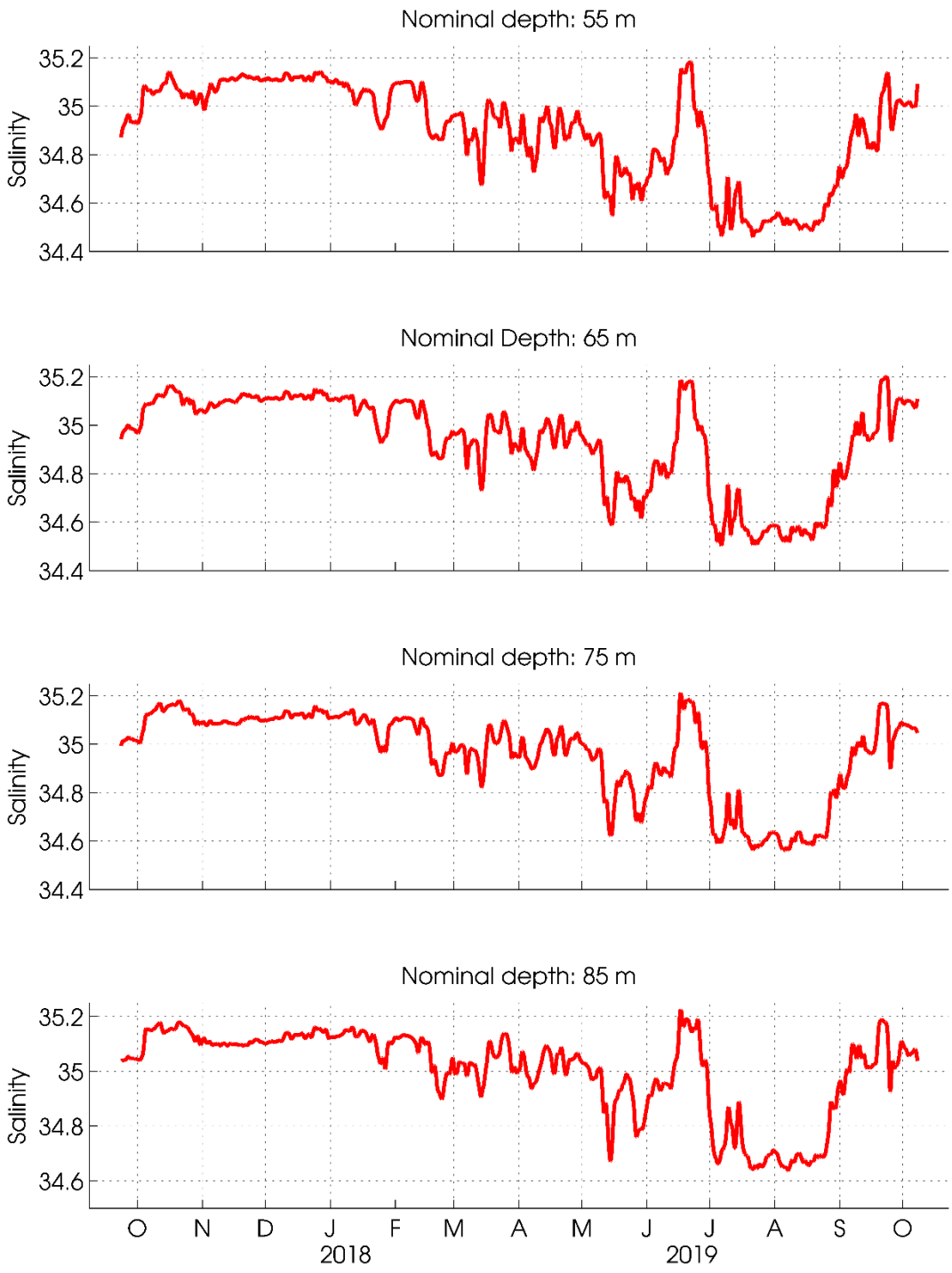

Figure VI-23. Same as in Figure VI-21, but at 55, 65, 75, and 85 m

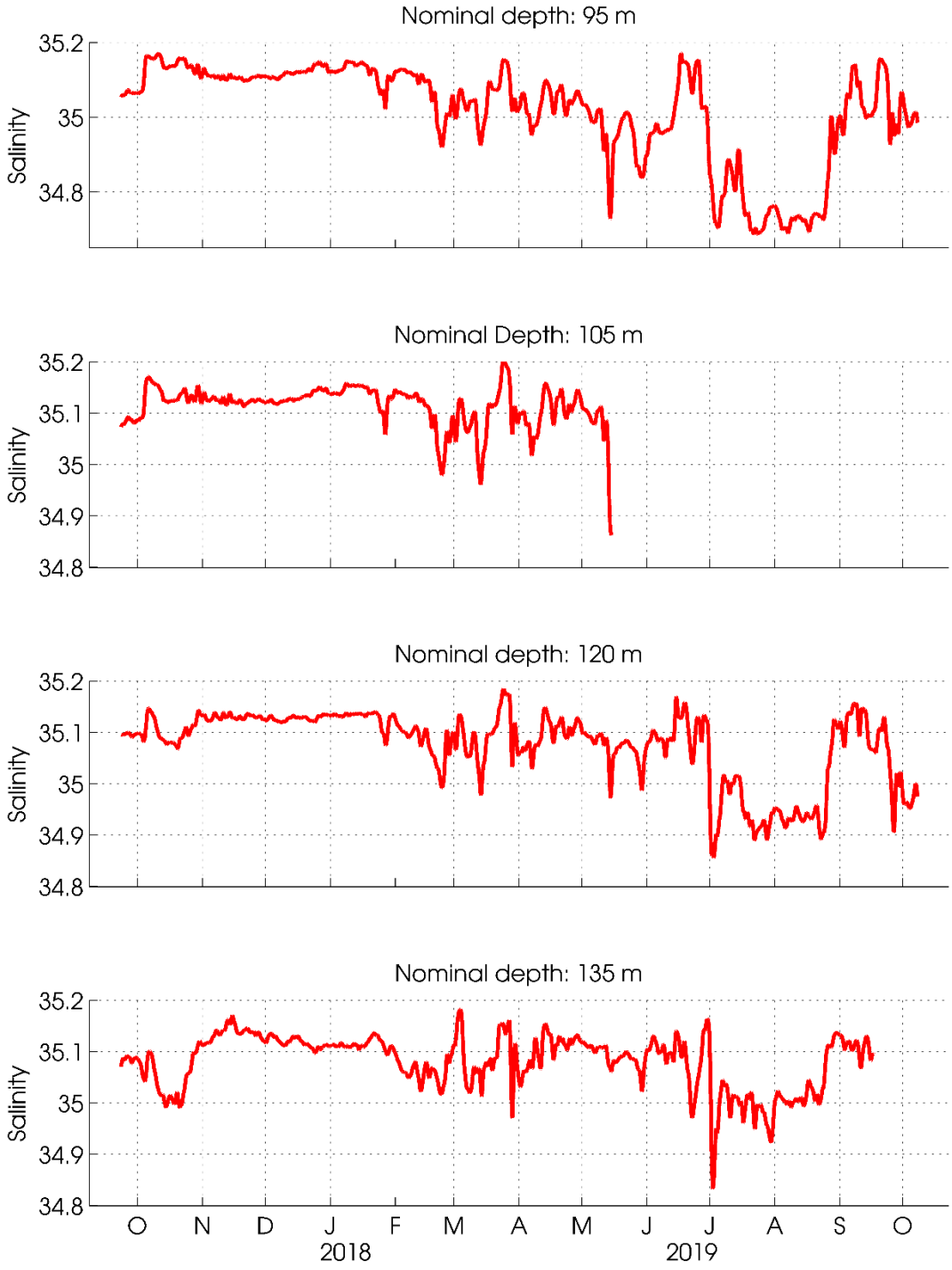

Figure VI-24. Same as in Figure VI-21, but at 95, 105, 120, and 135 m.

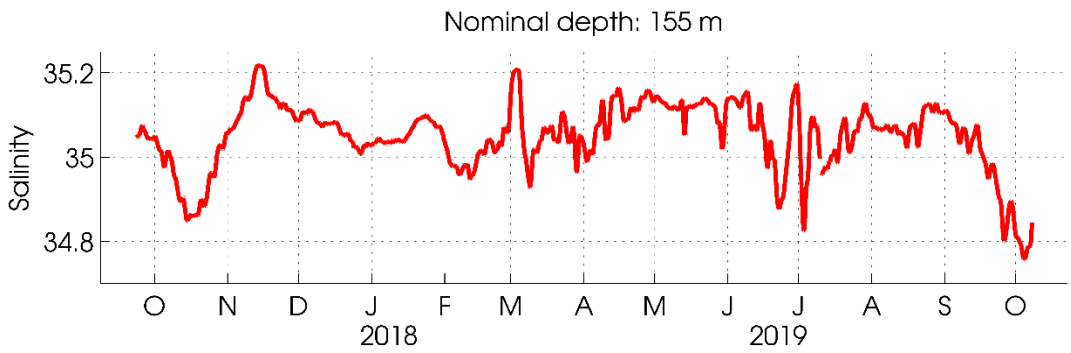

Figure VI-25. Same as in Figure VI-21, but at 155 m.

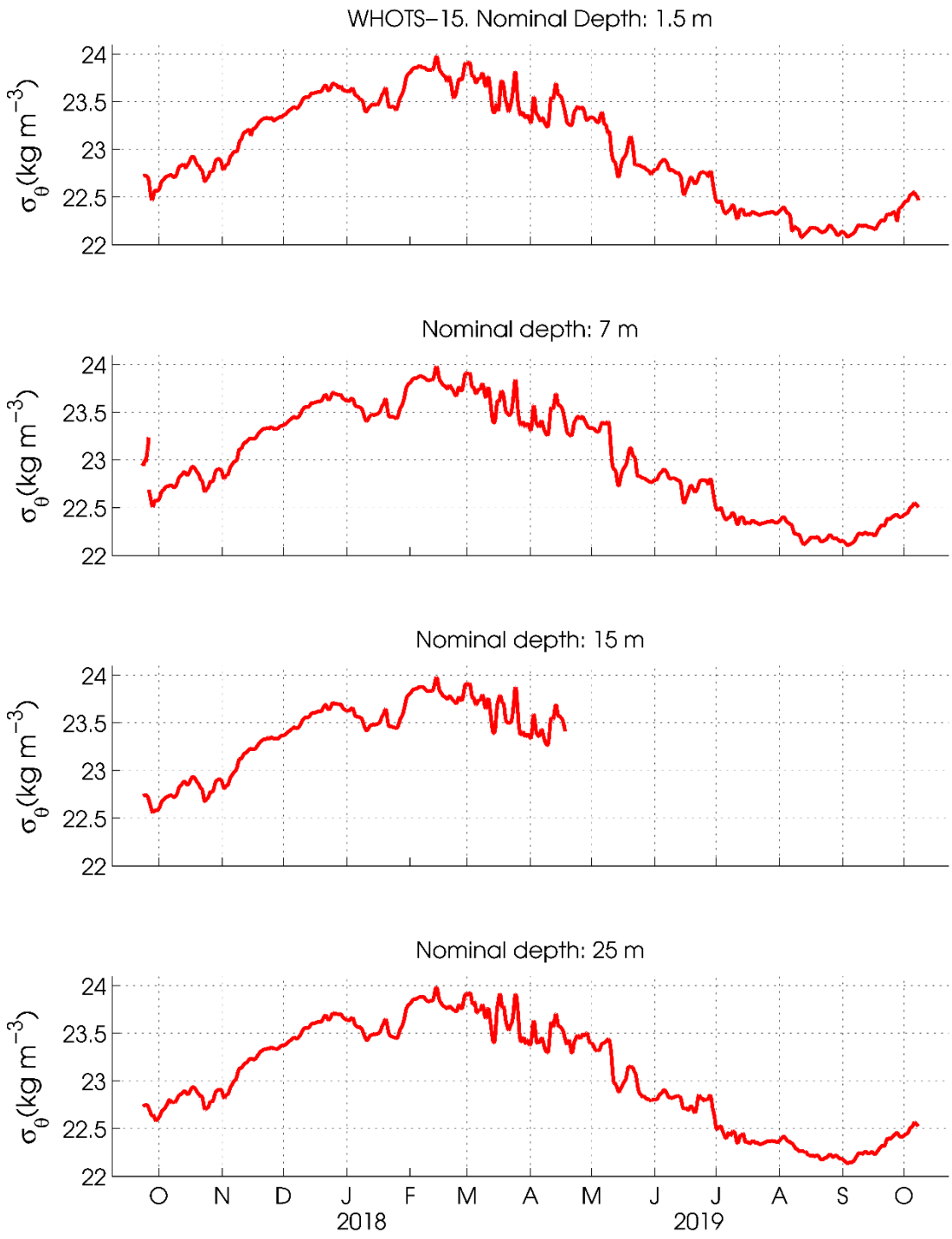

Figure VI-26. Potential densities (σθ) from MicroCATs during WHOTS-15 deployment at 1.5, 7, 15, and 25 m.

Figure VI-27. Same as in Figure VI-26, but at 35, 40, 45, and 50 m.

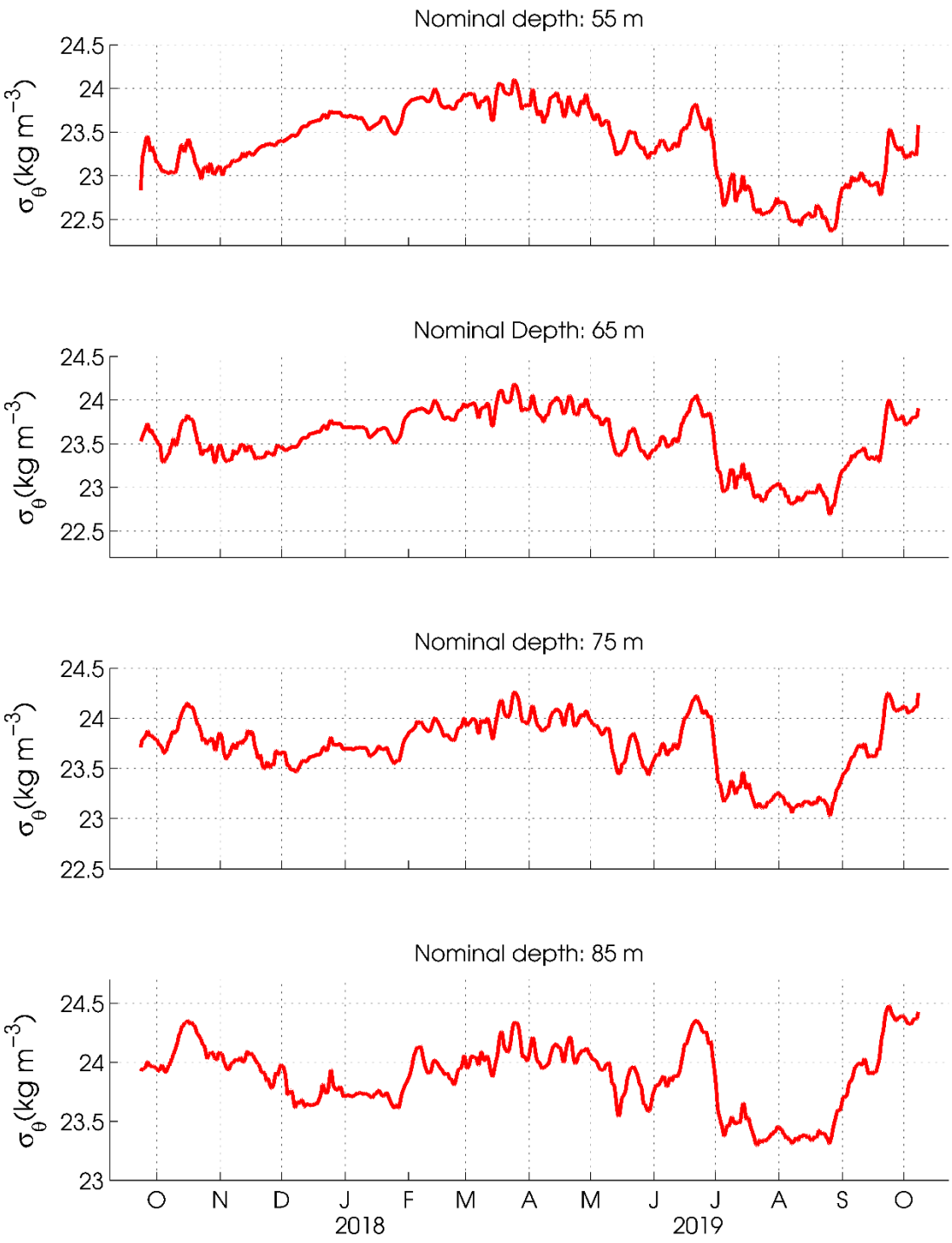

Figure VI-28. Same as in Figure VI-26, but at 55, 65, 75, and 85 m.

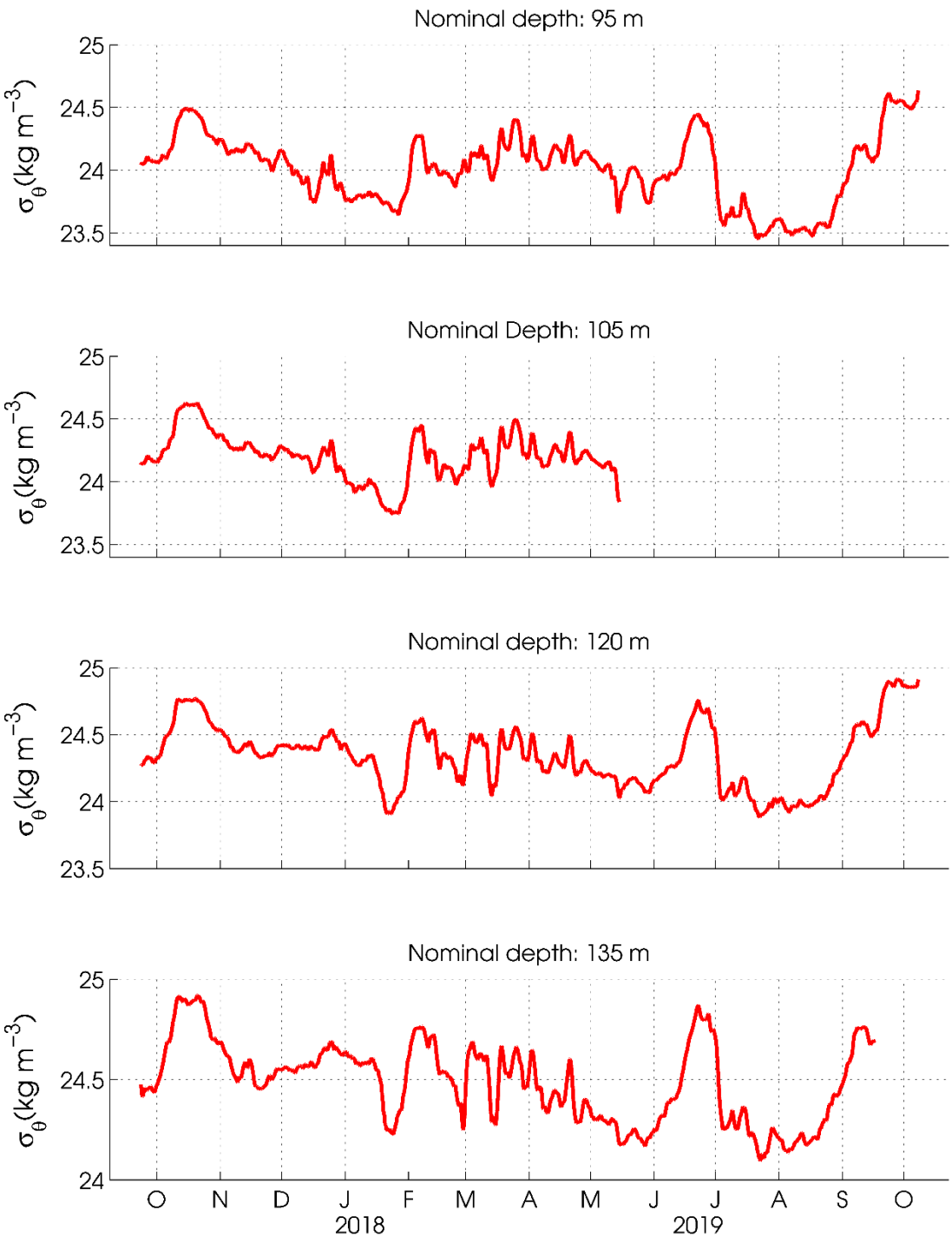

Figure VI-29. Same as in Figure VI-26, but at 95, 105, 120, and 135 m.

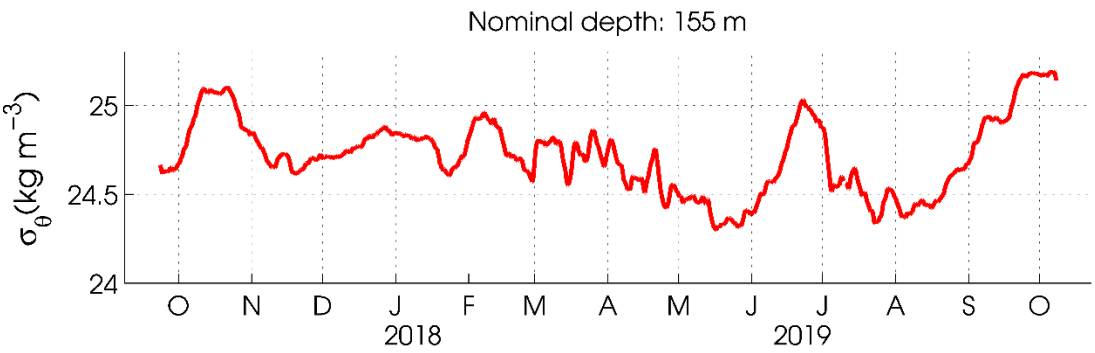

Figure VI-30. Same as in Figure VI-26, but at 155 m.

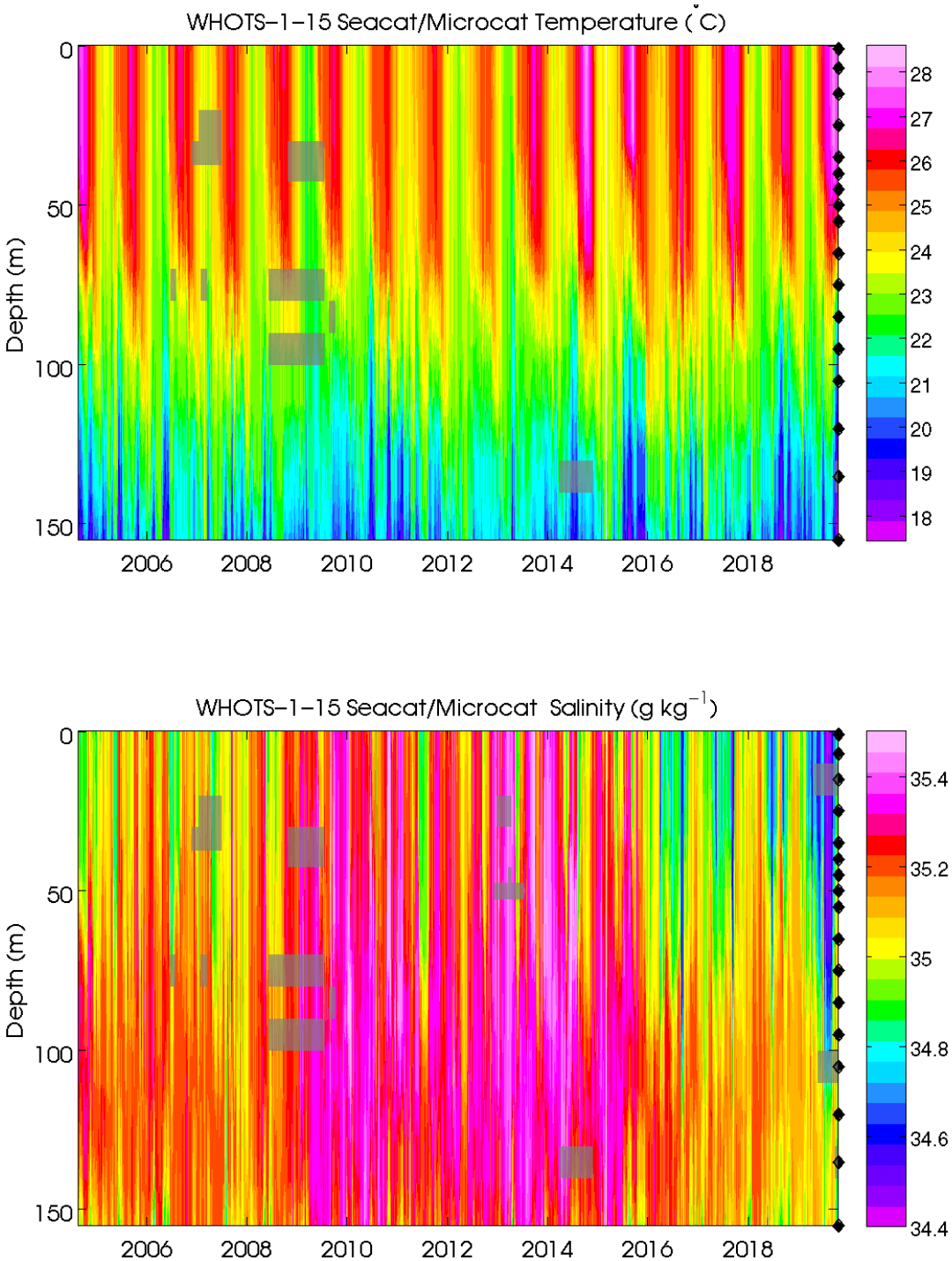

Figure VI-31. Contour plots of temperature (upper panel) and salinity (lower panel) versus depth from SeaCATs/ MicroCATs during WHOTS-1 through WHOTS-15 deployments. The shaded areas indicate missing data. The diamonds along the right axis indicate the depths of the instrument.

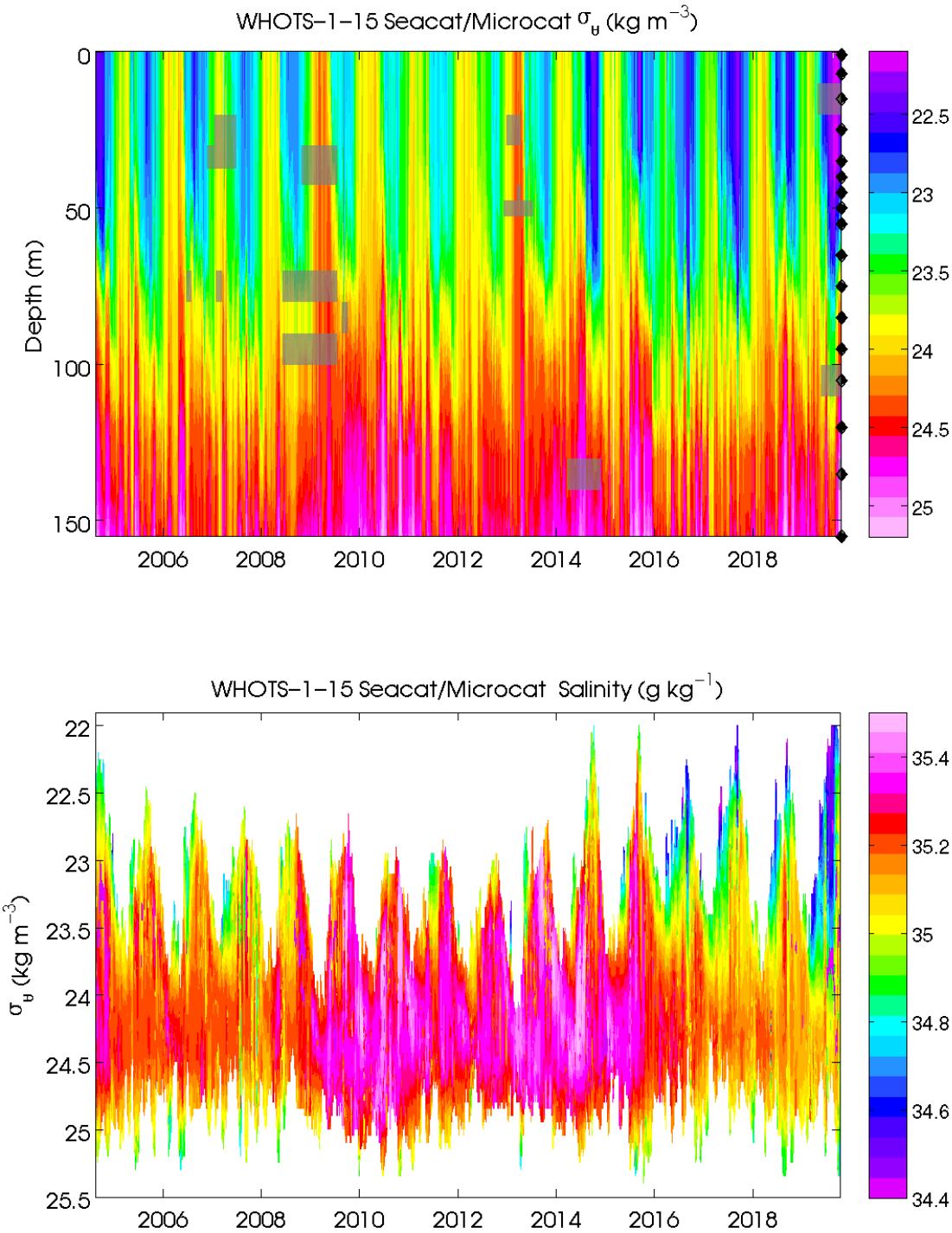

Figure VI-32. Contour plots of potential density (σ_θ, upper panel), versus depth, and of salinity versus σ_θ (lower panel) from SeaCATs/MicroCATs during WHOTS-1 through WHOTS-15 deployments. The shaded areas indicate missing data. The diamonds along the right axis in the upper figure indicate the depths of the instrument.

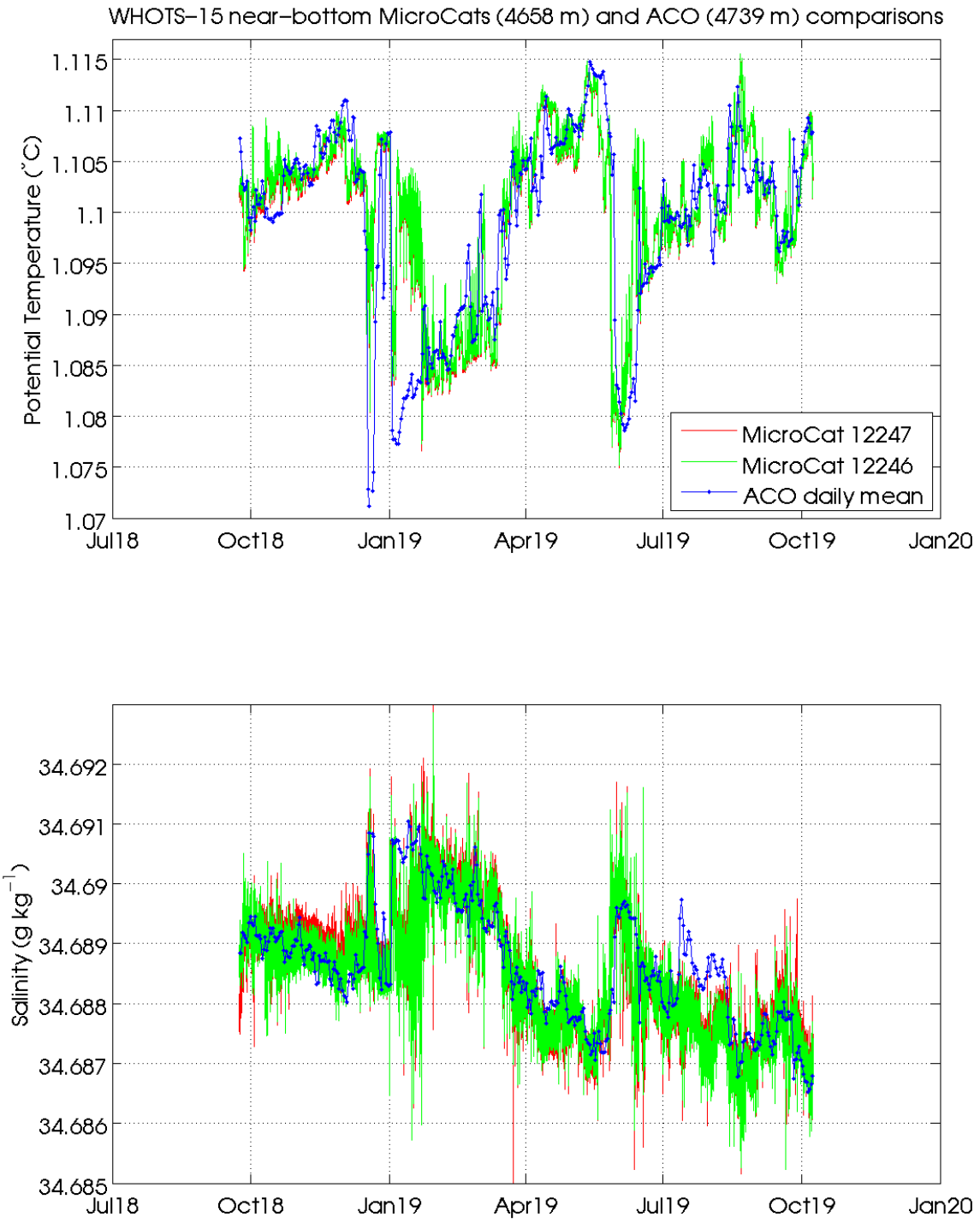

Figure VI-33. Potential temperature (upper panel) and salinity (lower panel) time-series from the ALOHA Cabled Observatory (ACO) sensors and the WHOTS-15 MicroCATs 12247 and 12246.

D. Moored ADCP data

Contoured plots of smoothed horizontal (east and north component) and vertical velocity as a function of depth during the mooring deployments 1 through 15 are presented in Figure VI-34 through Figure VI-36. A staggered time-series of smoothed horizontal and vertical velocities are shown in Figure VI-37 through Figure VI-39. Smoothing was performed by applying a daily running mean to the data and then interpolating it on an hourly grid.

Contours of east and north velocity components from the Ship *Oscar Sette* Ocean Surveyor broadband 75 kHz shipboard ADCP, and the moored 300 kHz ADCP from the WHOTS-15 deployment as a function of time and depth, during the WHOTS-15 cruise, are shown in Figure VI-40 and Figure VI-41.

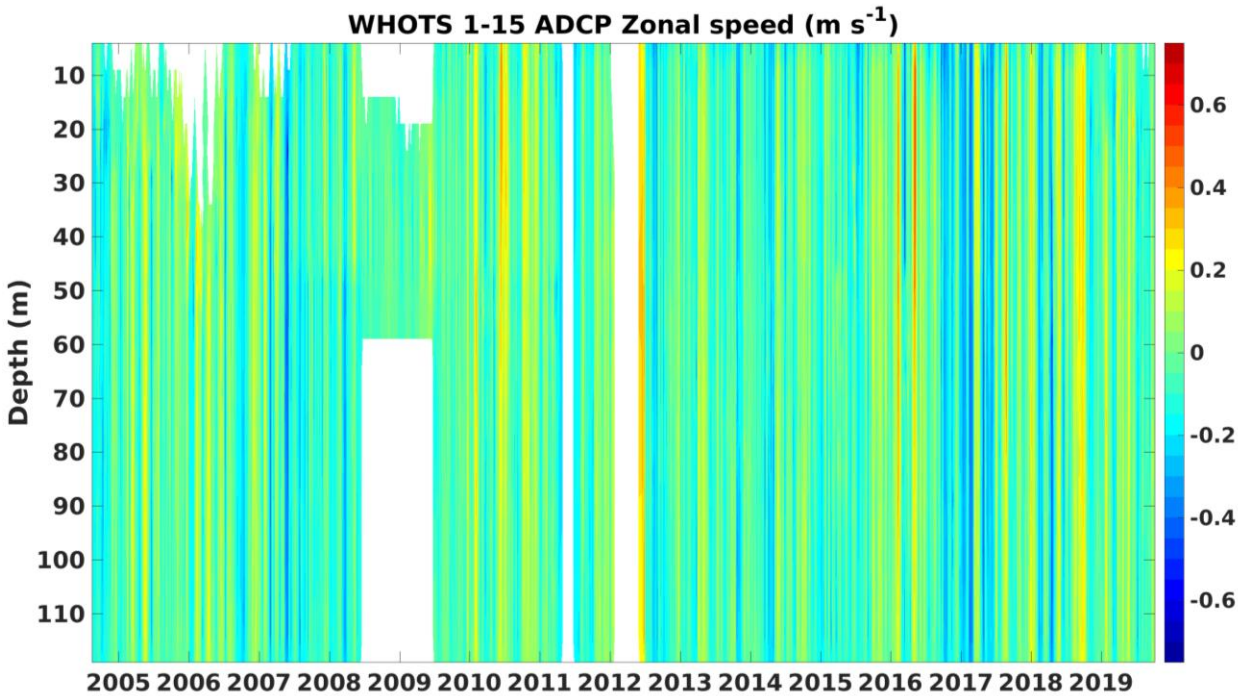

Figure VI-34. Contour plot of east velocity component (m s-1) versus depth and time from the moored ADCPs from the WHOTS-1 through -15 deployments.

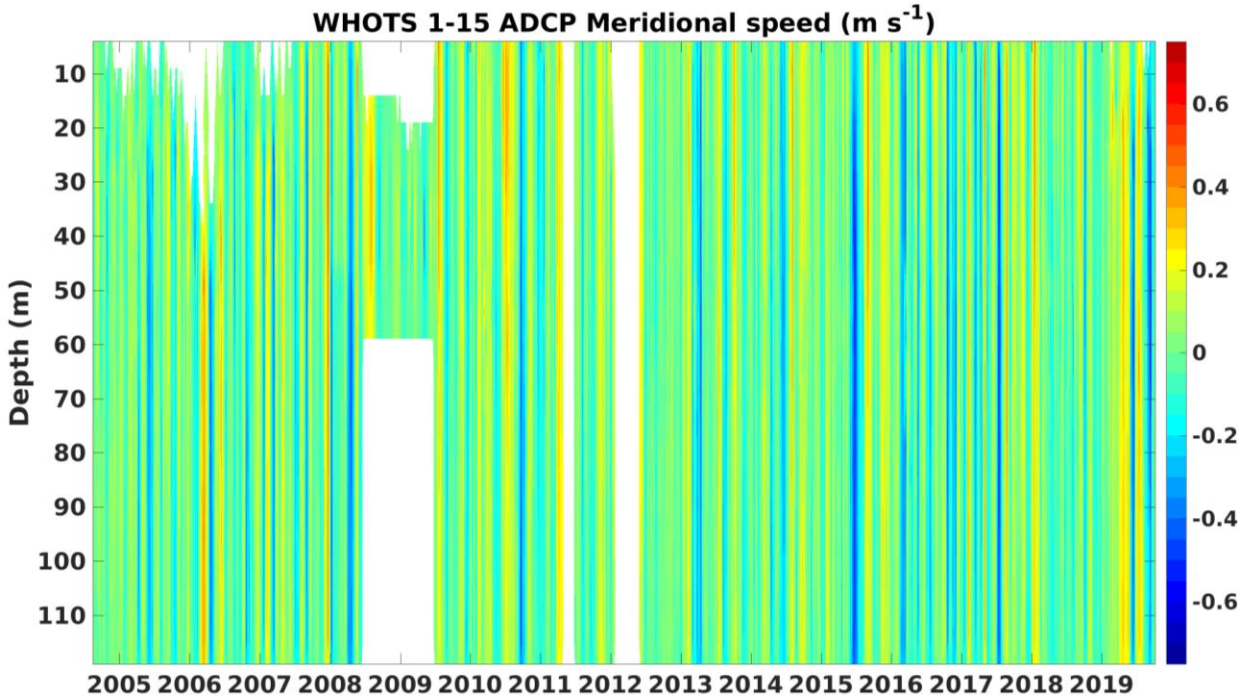

Figure VI-35. Contour plot of north velocity component (m s-1) versus depth and time from the moored ADCPs from the WHOTS-1 through -15 deployments.

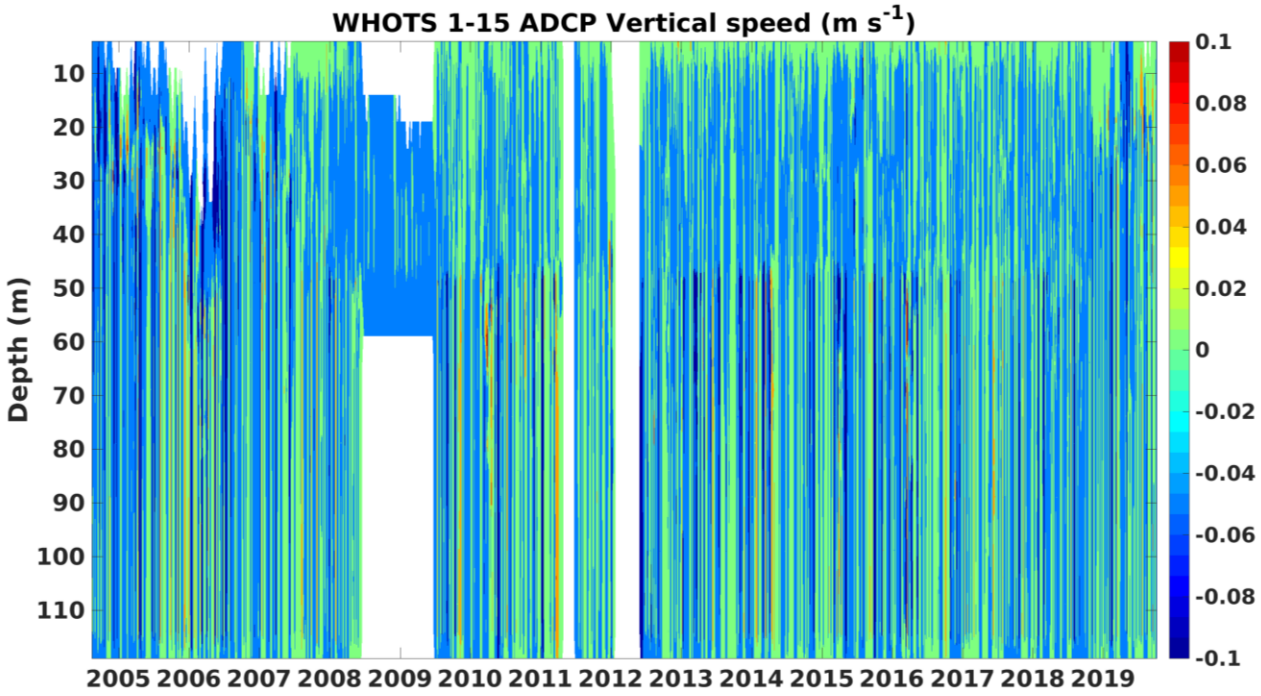

Figure VI-36. Contour plot of vertical velocity component (m s-1) versus depth and time from the moored ADCPs from the WHOTS-1 through -15 deployments.

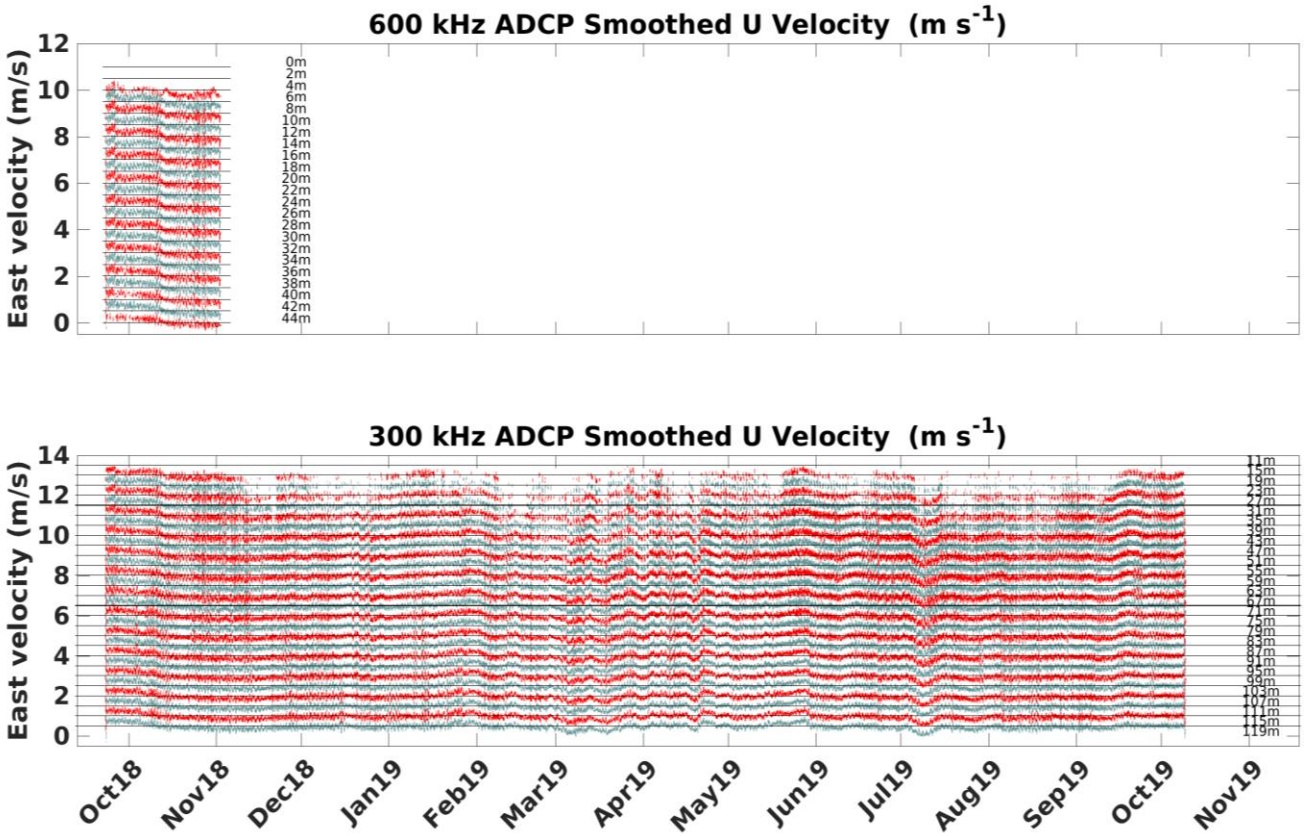

Figure VI-37. Staggered time-series of east velocity component (m s-1) for each bin of the 600 kHz (upper panel) and 300 kHz (lower panel) moored ADCPs during WHOTS-15. The time-series are offset upwards by 0.5 m s-1; each bin's depth is on the right.

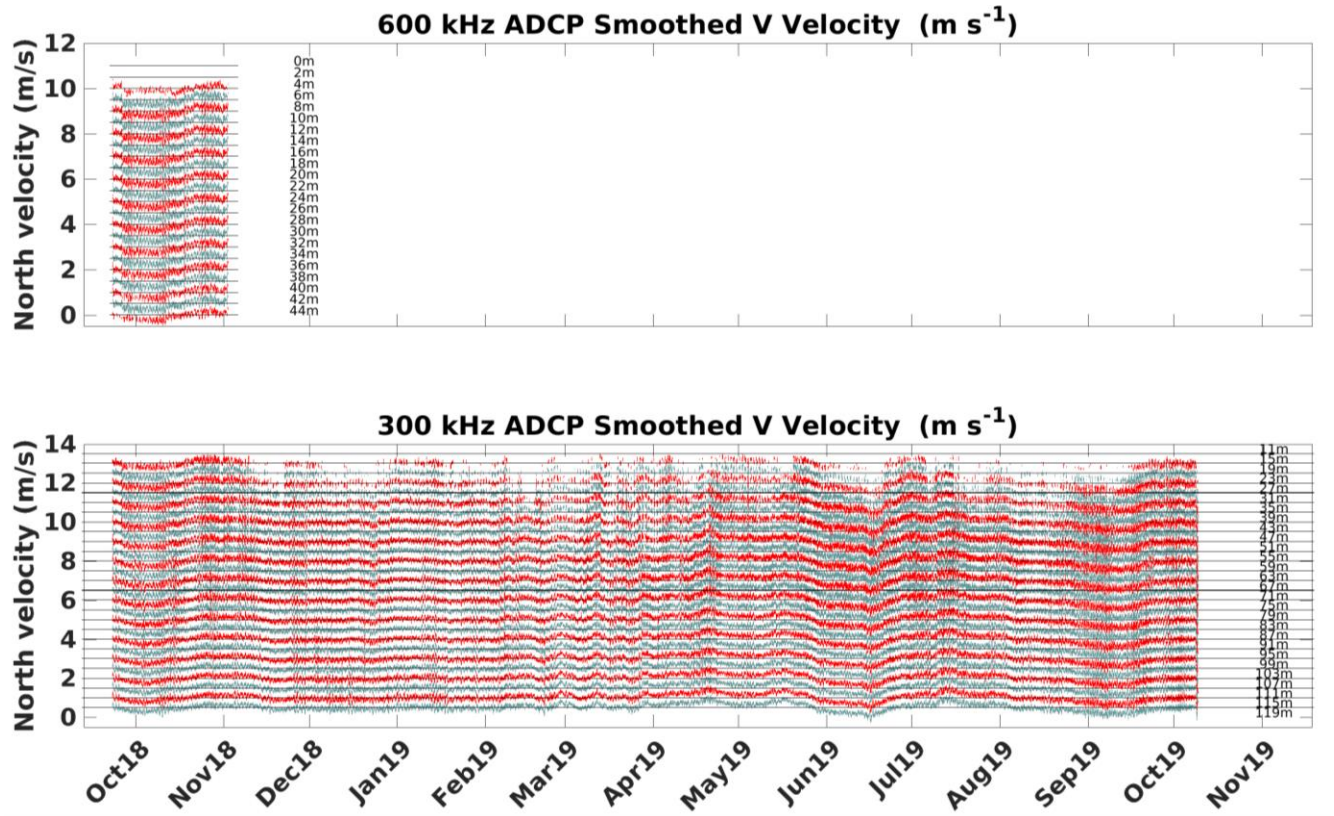

Figure VI-38. Same as Figure VI 38 but for north velocity component

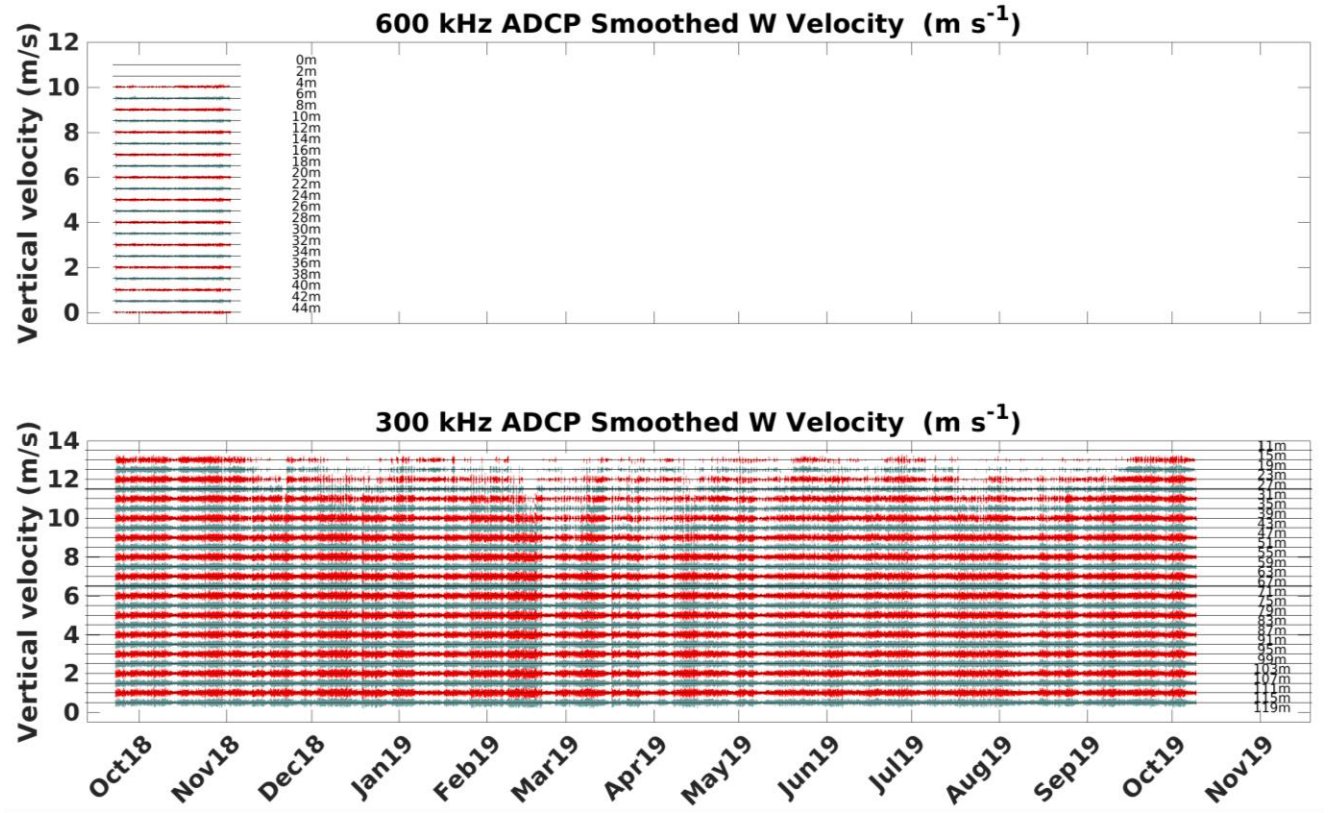

Figure VI-39. Same as Figure VI 38, but for vertical velocity component.

E. Moored and Shipboard ADCP comparisons

Contours of zonal and meridional current components from the Ship *Hi'ialakai's* and *Oscar Sette's* Ocean Surveyor broadband 75 kHz shipboard ADCP, and the moored 300 kHz ADCP from the WHOTS-15 deployment as a function of time and depth, during the WHOTS-15 cruise, are shown in Figure VI-40 and Figure VI-41. Similar comparisons during the WHOTS-16 cruise are in Figure VI-42 and Figure VI-43.

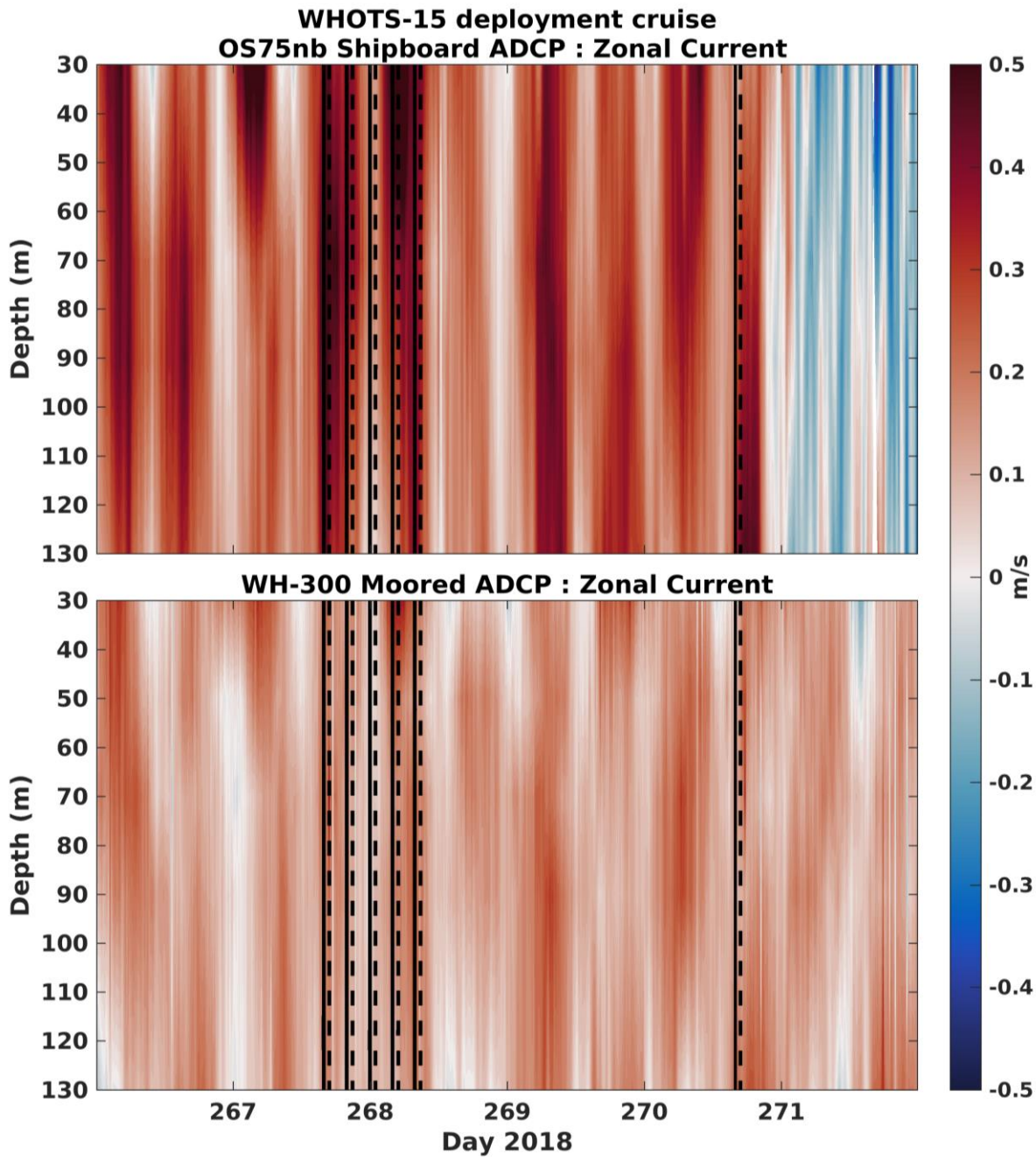

Figure VI-40. The contour of zonal currents (m s-1) from the Ship Hi'ialakai's Ocean Surveyor narrowband 75 kHz shipboard ADCP (upper panel), and the moored 300 kHz ADCP from the WHOTS-15 mooring (bottom panel) as a function of time and depth, during the WHOTS-15cruise. Times when the CTD rosette was in the water are identified between solid and dashed black lines.

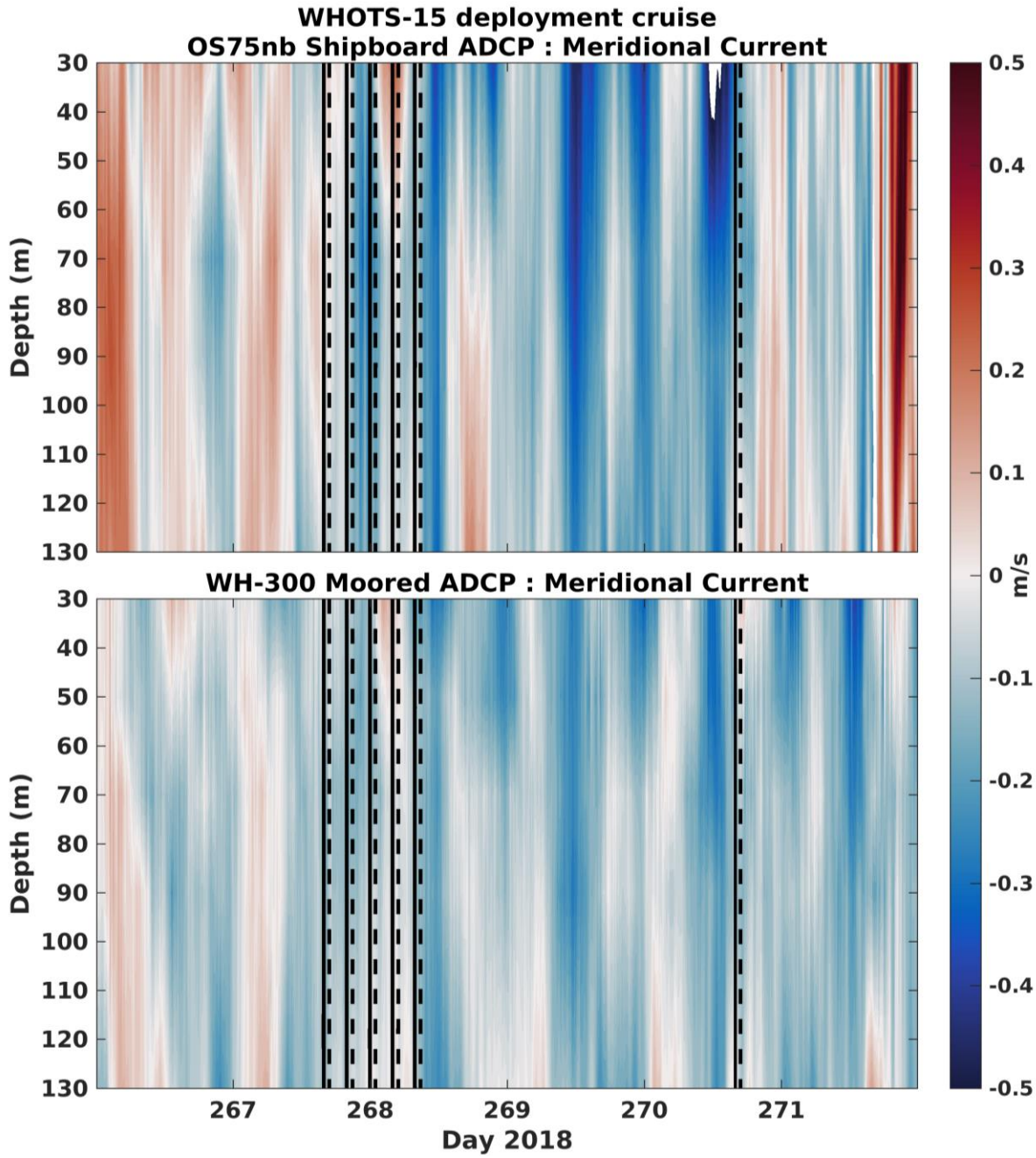

Figure VI-41. The contour of meridional currents (m s-1) from the Ship Hi'ialakai's Ocean Surveyor narrowband 75 kHz shipboard ADCP (upper panel), and the moored 300 kHz ADCP from the WHOTS-15 mooring (bottom panel) as a function of time and depth, during the WHOTS-15 cruise. Times when the CTD rosette was in the water are identified between solid and dashed black lines.

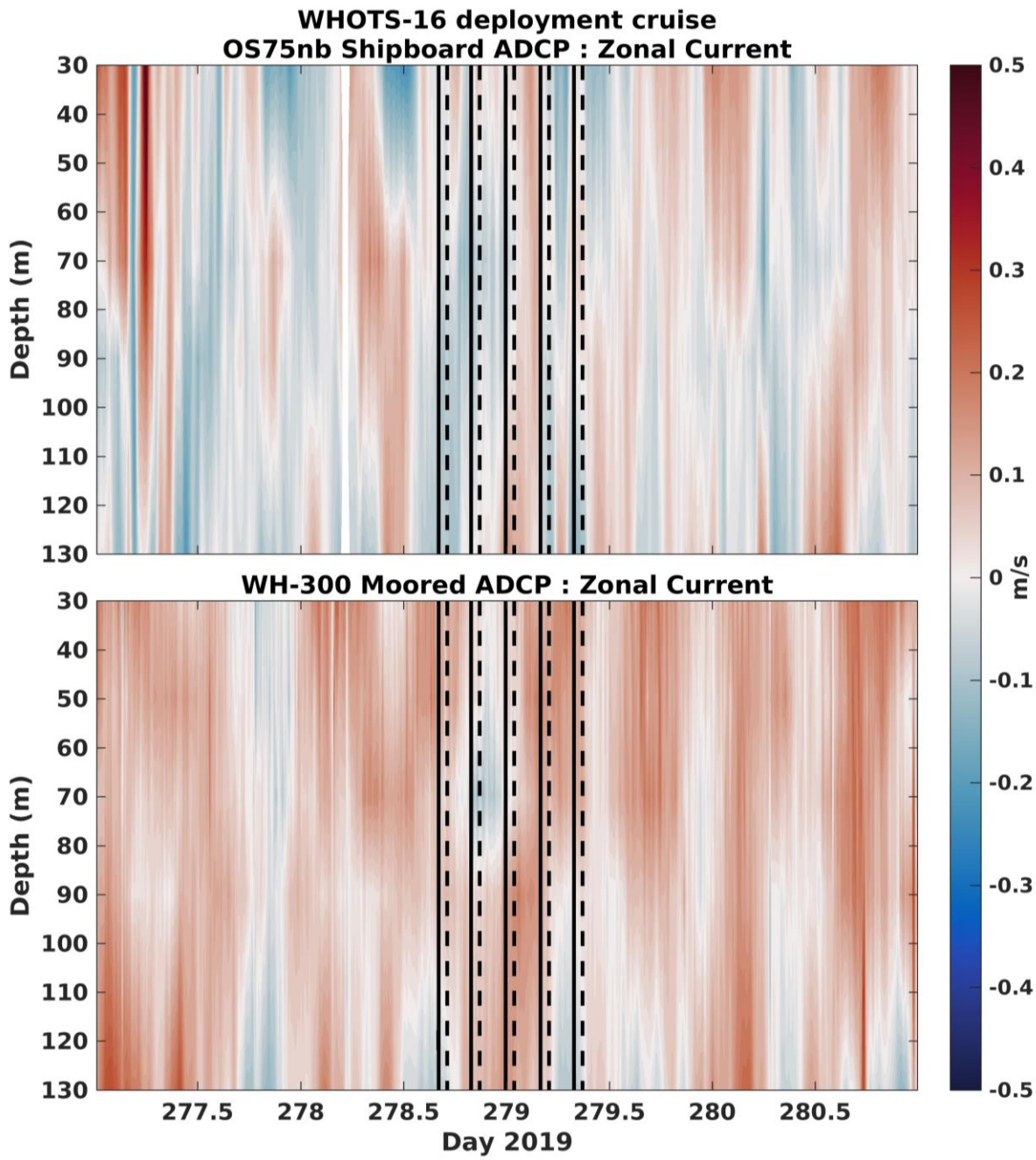

Figure VI-42. The contour of zonal currents (m s-1) from the Ship Oscar Sette Ocean Surveyor narrowband 75 kHz shipboard ADCP (upper panel), and the moored 300 kHz ADCP from the WHOTS-15 mooring (bottom panel) as a function of time and depth, during the WHOTS-16 cruise. Times when the CTD rosette was in the water are identified between solid and dashed black lines.

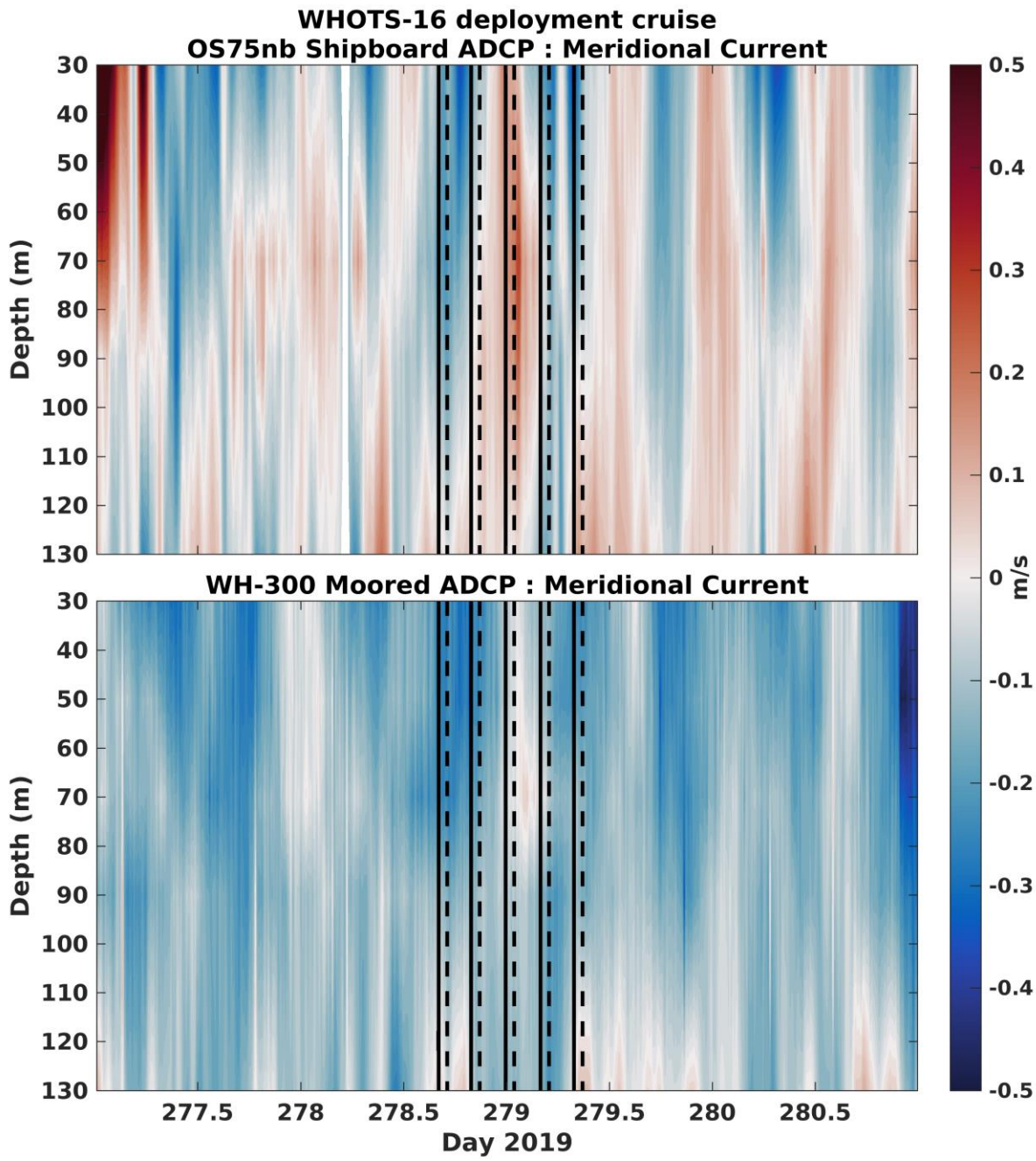

Figure VI-43. Contours of meridional currents (m s-1) from the Ship Oscar Sette Ocean Surveyor narrowband 75 kHz shipboard ADCP (upper panel), and the moored 300 kHz ADCP from the WHOTS-15 mooring (lower panel) as a function of time and depth, during the WHOTS-16 cruise. Times when the CTD/rosette was in the water are identified between the solid and dashed black lines.

Comparisons between quality-controlled moored ADCPs during the WHOTS-15 deployment and available shipboard ADCP obtained during regular HOT cruises 306 to 315, and during the mooring deployment (WHOTS-15) and recovery (WHOTS-16) cruises are shown in Figure VI-44 for the 300 kHz ADCP, and Figure VI-45 for the 600 kHz ADCP. Median and mean velocity profiles were computed when HOT CTD casts were being conducted near the WHOTS mooring specifically intended to calibrate moored instrumentation (see Conductivity Calibration section). The HOT shipboard profiles were taken when the ship was stationary, within 1 km of the mooring, and within 4 hours before the start and 4 hours after the end of the CTD cast conducted near the WHOTS mooring.

HOT cruises conducted on the R/V *Kilo Moana* (HOT-306 to HOT-315) used data from a TRDI Workhorse 300 kHz ADCP (wh300) with 2 m bin size, reaching 100 m, and averaging ensembles every 2 minutes, except for HOT-306 with 5-minute ensembles; and from a TRDI Ocean Surveyor 38 kHz operating in broadband mode (os38bb) with 12 m bin size, reaching 1200 m, with 5-minute ensemble interpolated to the profile resolution of the shipboard ADCP, and ensemble mean, and median profiles were obtained for each data set to compute differences and correlation coefficients between them. Bins with less than 50% of data were excluded.

Comparisons between the 300 kHz and the shipboard ADCP were available for HOT-306, HOT-309 to HOT-315; data from all other HOT cruises were excluded due to a lack of comparable data. Comparison between the moored 600 kHz and the shipboard ADCP was only available for HOT-306 due to a mechanical issue with 600 kHz ADCP in November 2018.

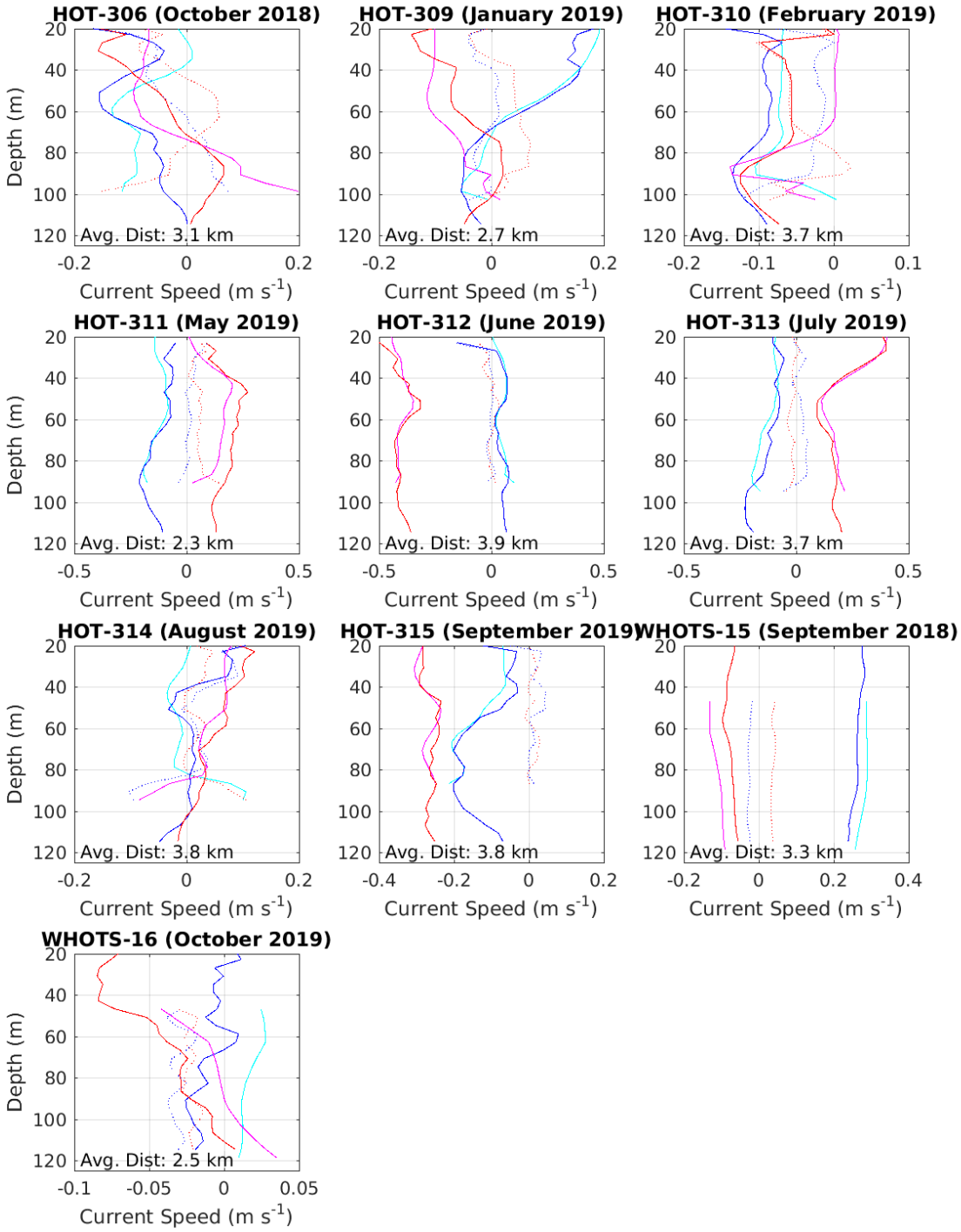

Figure VI-44. Mean current profiles during shipboard ADCP (cyan: zonal, magenta: meridional) versus moored 300 kHz ADCP (blue: zonal, red: meridional) intercomparisons from HOT-306 through HOT-315 and from WHOTS-15 and WHOTS-16 cruises. Moored minus shipboard ADCP differences shown in dotted lines (blue: zonal, red: meridional)

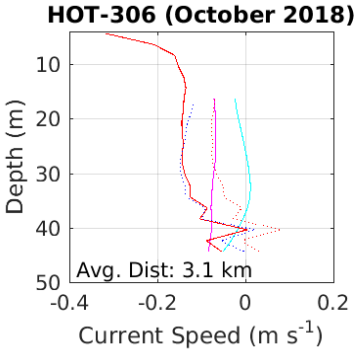

Figure VI-45. Mean current profiles during shipboard ADCP (cyan: zonal, magenta: meridional) versus moored 600 kHz ADCP (blue: zonal, red: meridional) intercomparisons from HOT-306. Moored minus shipboard ADCP differences shown in dotted lines (blue: zonal, red: meridional). WHOTS-15 600 kHz failed in November 2018.

F. Next Generation Vector Measuring Current Meter data (VMCM)

Time-series of daily mean horizontal velocity components for the VMCM current meters deployed during WHOTS-15 at 10 m and 30 m are presented in Figure VI-46.

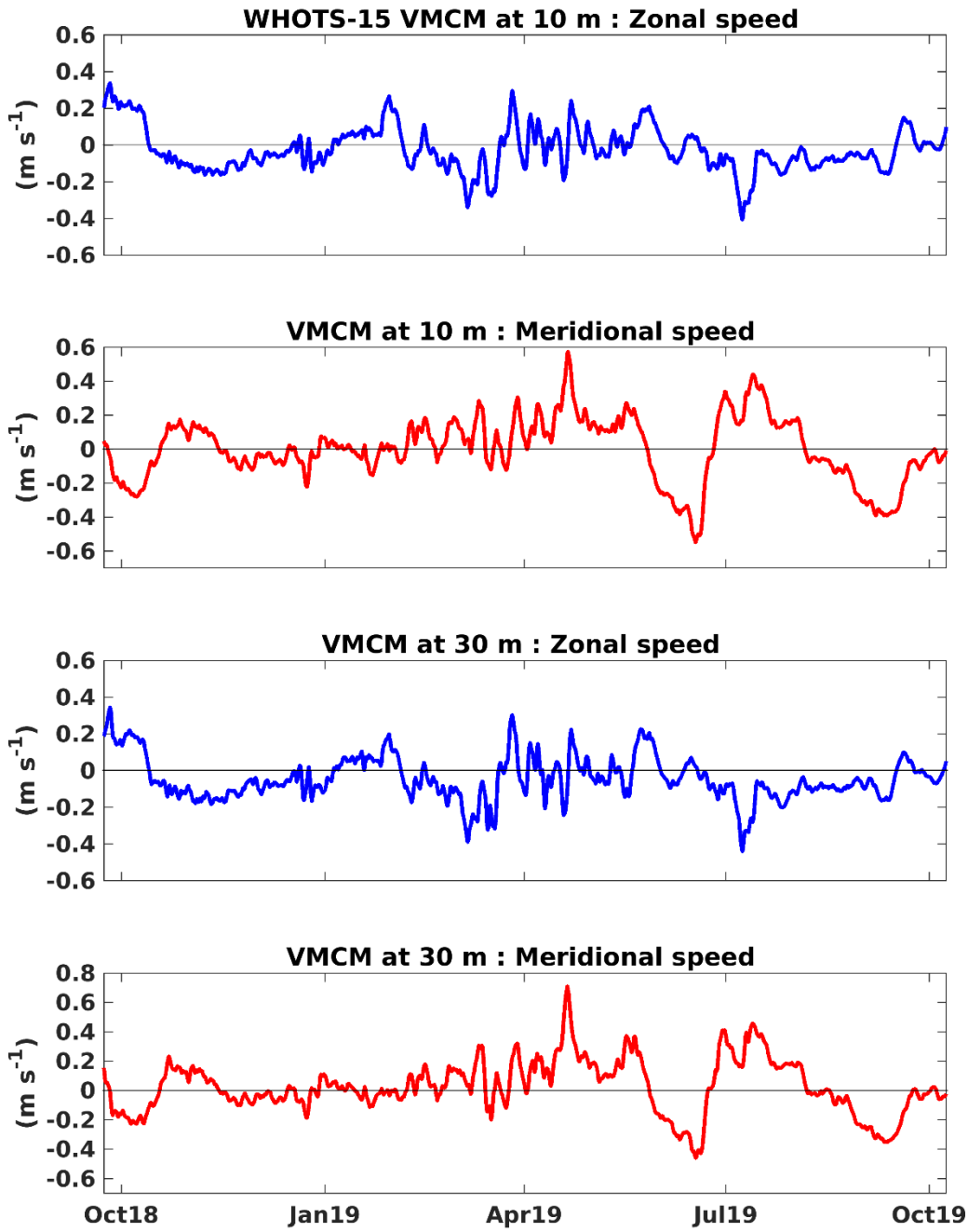

Figure VI-46. Horizontal velocity data (m/s) during WHOTS-15 from the VMCMs at 10 m depth (first and second panel) and at 30 m depth (third and fourth panel)

G. GPS data

Time-series of latitude and longitude of the WHOTS-15 buoy from GPS data are presented in Figure VI-47, and spectra of the time-series are shown in Figure VI-48.

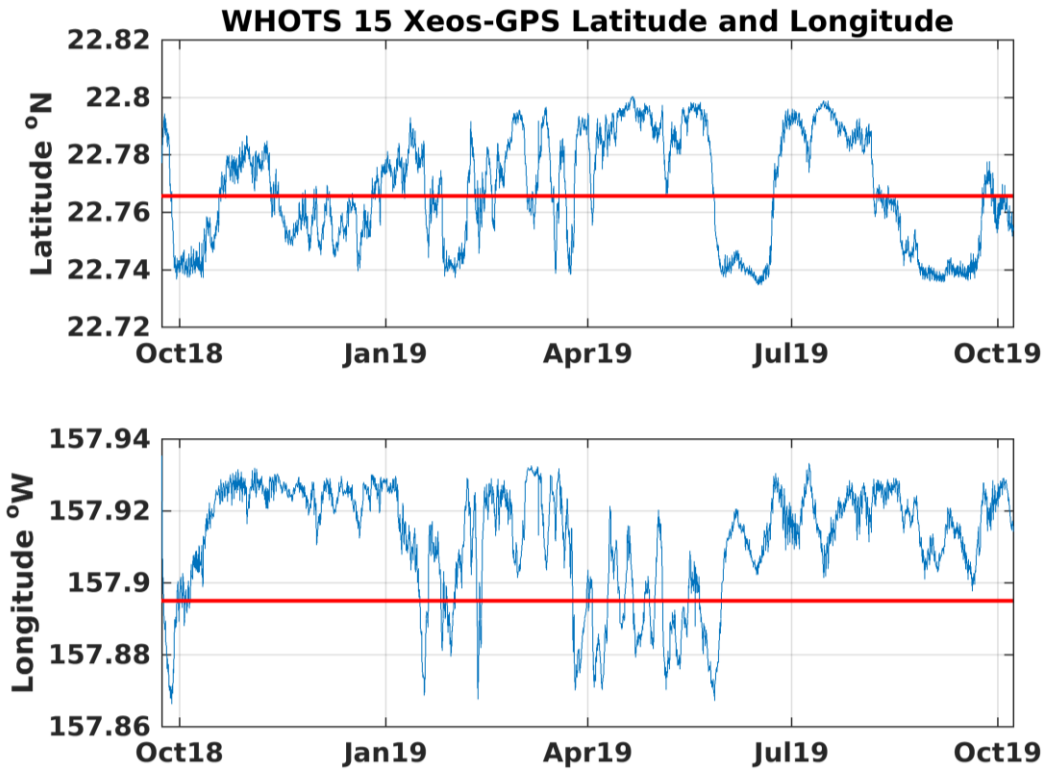

Figure VI-47. GPS Latitude (upper panel) and longitude (lower panel) time series from the WHOTS-15 deployment.

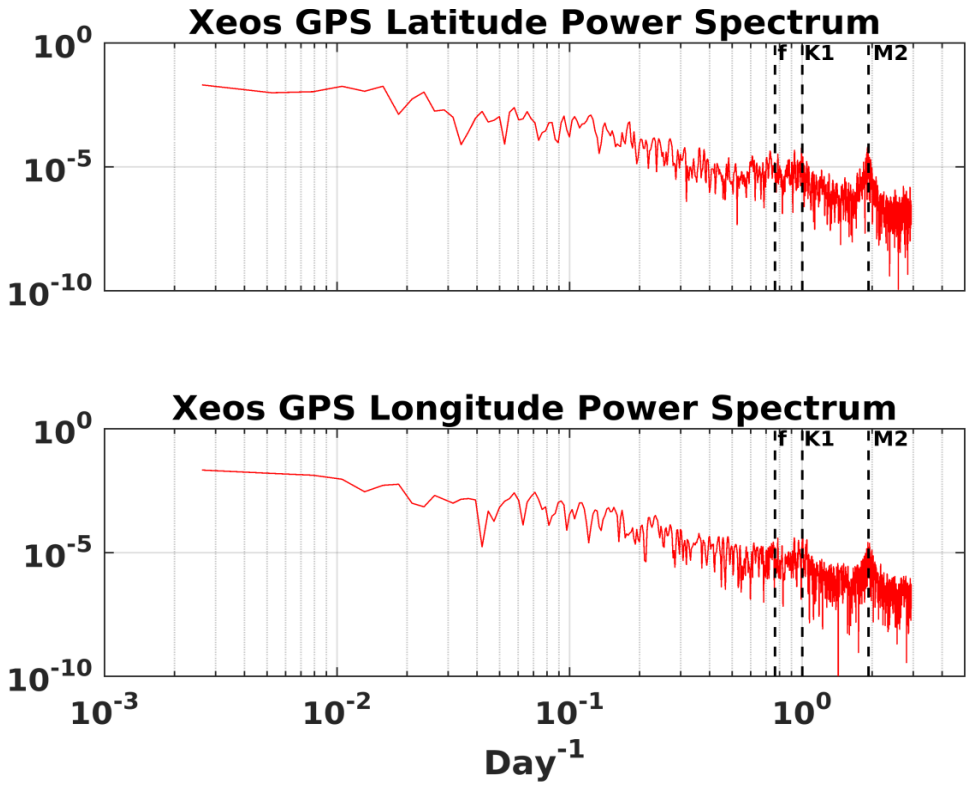

Figure VI-48. The power spectrum of latitude (upper panel) and longitude (lower panel) for the WHOTS-15. The variables f, K1, and K2 represent the inertial period, solar-diurnal and solar-semidiurnal constituents.

H. Mooring Motion

The position of the mooring with respect to its anchor was determined from the GPS positions. Additional information on the mooring motion was provided by the ADCP data of pitch, roll, and heading, shown in this section.

Figure VI-49 shows the ADCP data of the instrument's tilt (a combination of the pitch and roll), plotted against the buoy's distance from its anchor (derived from GPS positions), for both WHOTS-15 ADCP's. The plot's red line is a quadratic fit to the median tilt calculated every 0.2 km distance bins. The figure shows that during both deployments, the ADCP tilt increased as the anchor's distance increased. This tilting was caused by the mooring line's deviation from its vertical position as the anchor pulled it. The tilting of the line also caused the rising of the instruments attached to the line. The 600 kHz ADCP failed in November 2018.

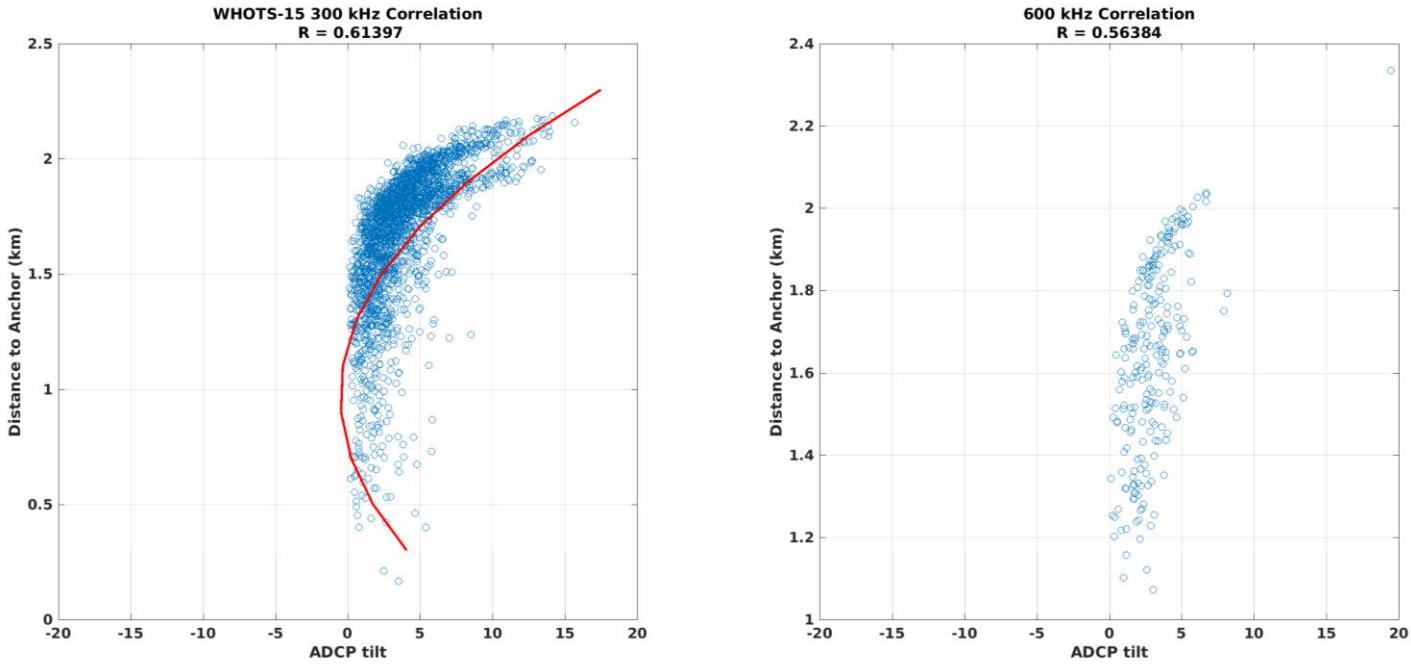

Figure VI-49. Scatter plots of ADCP tilt and distance of the buoy to its anchor for the 300 kHz (left panel) and the 600 kHz ADCP deployments (right panel, blue circles). The red line is a quadratic fit to the median tilt calculated every 0.2 km distance bins.

VII. References

Colbo, K., and Weller, R. A. 2009. Accuracy of the IMET sensor package in the subtropics. Journal of Atmospheric and Oceanic Technology, 26: 1867–1890.

Firing, E. 1991. Acoustic Doppler current profiling measurements and navigation. *In* WOCE Hydrographic Operations and Methods. WOCE Operations Manual, WHP Office Report WHPO 91-1, WOCE Report No. 68/91, p. 24.

Freitag, H. P., McCarty, M. E., Nosse, C., Lukas, R., McPhaden, M. J., and Cronin, M. F. 1999. COARE Seacat data: Calibrations and quality control procedures. NOAA Tech. Memo. ERL PMEL-115: 93.

Fukieki, L., Santiago-Mandujano, F., Pacheco, F. C., Trifonova, K., Fitzgerald, D., Potemra, J., and White, A. 2020. Hawaii Ocean Time-series Data Report 30: 2018. https://hahana.soest.hawaii.edu/hot/reports/rep_y30.pdf.

Hosom, D. S., Weller, R. A., Payne, R. E., and Prada, K. E. 1995. The IMET (Improved Meteorology) ship and buoy systems. Journal of Atmospheric and Oceanic Technology, 12: 527–540.

Kara, A. B., Rochford, P. A., and Hurlburt, H. E. 2000. Mixed layer depth variability and barrier layer formation over the North Pacific Ocean. Journal of Geophysical Research: Oceans, 105: 16783–16801. Wiley Online Library.

Owens, W. B., and Millard Jr, R. C. 1985. A new algorithm for CTD oxygen calibration. Journal of Physical Oceanography, 15: 621–631.

Plueddemann, A. J., Weller, R. A., Lukas, R., Lord, J., Bouchard, P. R., and Walsh, M. A. 2006. WHOI Hawaii Ocean Timeseries Station (WHOTS) : WHOTS-2 mooring turnaround cruise report. https://hdl.handle.net/1912/1074.

Santiago-Mandujano, F., Lethaby, P., Lukas, R., Snyder, J., Weller, R., Plueddemann, A., Lord, J., *et al.* 2007. Hydrographic Observations at the Woods Hole Oceanographic Institution (WHOI) Hawaii Ocean Timeseries (HOT) Site (WHOTS): 2004-2006. http://uop.whoi.edu/currentprojects/WHOTS/docs/UH_Whots_data_report_1.pdf.

Santiago-Mandujano, F., Snyder, J., Natarov, S., Maloney, K., Howins, N., Hebert, G., and Lukas, R. 2019. UH Contributions to WHOTS-15 Cruise Report. http://www.soest.hawaii.edu/whots/proc_reports/WHOTS-15_CruiseRpt.pdf.

Santiago-Mandujano, F., Fitzgerald, D., Maloney, K., Rohrer, T., Howins, N., Tabata, R., and Potemra, J. 2020. UH Contributions to WHOTS-16 Cruise Report. http://www.soest.hawaii.edu/whots/proc_reports/WHOTS-16_CruiseRpt.pdf.

Tupas, L., Santiago-Mandujano, F., Hebel, D., Lukas, R., Karl, D., and Firing, E. 1993. Hawaii Ocean Time-series Data Report 4, 1992. *In* SOEST Technical Report 93-14, p. 248. Citeseer.

Tupas, L., Bidigare, R., Firing, E., Fujieki, L., Hebel, D., Karl, D., Landry, M., *et al.* 1996. Hawaii Ocean Time-series Data Report 8, 1996. Citeseer. 289 pp.

Unesco. 1981. Tenth Report of the Joint Panel on Oceanographic Tables and Standards, Sidney, BC, Canada, 1-5 September 1980. Unesco.

Whelan, S. P., Weller, R. A., Lukas, R., Bradley, F., Lord, J., Smith, J., Bahr, F., *et al.* 2007. WHOI Hawaii Ocean Timeseries Station (WHOTS) : WHOTS-3 mooring turnaround cruise report. 103 pp. https://hdl.handle.net/1912/1825.

VIII. Appendices

A. Appendix 1: WHOTS-15 300 kHz - SERIAL 7637

Program Version 50.4
System Frequency 300 kHz
Convex
Sensor Configuration #1
Orientation UP
Beam Angle 20 Degrees
Transducer 4 Beam Janus

Serial Number: 31 00 00 00 126 107 252 9
False Target Threshold Maximum (WA) 70 counts
Blank After Transmit, cm (WF) 176 cm
Minimum Percent Good (WG) 0
No. of depth cells (bins) (WN) 30
Pings per ensemble (WP) 40
Depth Cell Size (bin length), cm (WS) 400 cm
Ambiguity Velocity, cm/s radial (WV) 175 cm/s

Heading Alignment, deg (EA) 0.00 degrees
Heading Bias, deg (EB) 9.34degrees
Coord Transform (EX) 00011111 Earth Coordinates
Sensor Source (EZ) 01111101 cdhprst
Sens Avail 00011101 cdhprst
Time per Ping, sec (TP) 00:04.00
Time per Ensemble, min (TE) 10:00.00

Hardware 4 Beams
Code Reps. 9
Xmt pulse 4.42 m
1st Bin 6.22 m

First Ensemble 00000001 2018 09 22 00:00:00
Last Ensemble 00055176 2019 10 10 03:49:59

B. Appendix 2: WHOTS-15 600 kHz ADCP Configuration (serial 13917)

Program Version 50.4
System Frequency 600 kHz
Convex
Sensor Configuration #1
Orientation UP
Beam Angle 20 Degrees
Transducer 4 Beam Janus

Serial Number: 211 00 00 6 7 204 136 9
False Target Threshold Maximum (WA) 70 counts
Blank After Transmit, cm (WF) 88 cm
Minimum Percent Good (WG) 0
No. of depth cells (bins) (WN) 25
Pings per ensemble (WP) 80
Depth Cell Size (bin length), cm (WS) 200 cm
Ambiguity Velocity, cm/s radial (WV) 175 cm/s

Heading Alignment, deg (EA) 0.00 degrees
Heading Bias, deg (EB) 9.34degrees
Coord Transform (EX) 00011111 Earth Coordinates
Sensor Source (EZ) 01111101 cdhprst
Sens Avail 00011101 cdhprst
Time per Ping, sec (TP) 00:02.00
Time per Ensemble, min (TE) 10:00.00

Hardware 4 Beams
Code Reps. 9
Xmt 2.21 m
1st Bin 3.11 m

First Ensemble 00000001 2018 09 22 00:00:00
Last Ensemble 0005987 2018 11 02 13:39:59